

NASA CR.

140267

SHUTTLE ACTIVE THERMAL CONTROL SYSTEM
DEVELOPMENT TESTING

VOLUME I

OVERALL SUMMARY

8 APRIL 1974

(NASA-CF-140267) SHUTTLE ACTIVE THERMAL
CONTROL SYSTEM DEVELOPMENT TESTING.
VOLUME 1: OVERALL SUMMARY (LTV
Aerospace Corp.) 108 p HC \$8.50

N74-34340

CSCL 22B G3/31 Jnc115
50981



VOUGHT SYSTEMS DIVISION
LTV AEROSPACE CORPORATION

SHUTTLE ACTIVE THERMAL CONTROL SYSTEM
DEVELOPMENT TESTING

VOLUME I

OVERALL SUMMARY

Report No. T169-28

8 April 1974

Submitted by

VOUGHT SYSTEMS DIVISION
LTV Aerospace Corporation
Dallas, Texas

To

The National Aeronautics and Space Administration
Lyndon B. Johnson Space Center
Houston, Texas

Prepared by:

H. R. Howell
H. R. Howell

Approved by:

R. J. French
R. J. French, Supervisor
EC/LS Group

F O R E W O R D

This volume is one of a series of reports describing the development tests conducted on a candidate Shuttle heat rejection system at the National Aeronautics and Space Administration - Johnson Space Center during the period from March to July 1973. The complete test series is reported in the following volumes:

- Volume I Overall Summary
- Volume II Modular Radiator System Tests
- Volume III Modular Radiator System Test Data
Co.relation With Thermal Model
- Volume IV Modular Radiator System Test Data
- Volume V Integrated Radiator/Expendable Cooling System
Tests
- Volume VI Water Ejector Plume Tests
- Volume VII Improved Radiator Coating Adhesives Tests
- Volume VIII Tube Anomaly Investigation

The tests were conducted jointly by NASA and the V. .t Systems Division of LTV Aerospace Corporation under Contract NAS9-10534. D. W. Morris of the NASA-JSC Crew Systems Division was the contract technical monitor. Mr. R. J. Tufte served as the VSD Project Engineer.

TABLE OF CONTENTS

		<u>PAGE</u>
1.0	SUMMARY	1
2.0	INTRODUCTION	2
3.0	TEST PROGRAM	4
	3.1 Phase 1 - MRS Tests	4
	3.1.1 Test Objectives	5
	3.1.2 Test Description	6
	3.1.3 Test Results	9
	3.1.4 Data Correlation	12
	3.2 Phase 2 - Integrated Radiator Expendable Cooling System Tests	15
	3.2.1 Test Objectives	15
	3.2.2 Test Description	16
	3.2.3 Test Results	18
	3.3 Phase 3 - Improved Coatings Tests	22
	3.3.1 Adhesive Selection	23
	3.3.2 Thermal Vacuum Testing	25
	3.3.3 Coatings/Adhesives Evaluation	27
	3.4 Tube Anomaly Investigation	28
4.0	CONCLUSIONS	30
	4.1 Phase 1 - MRS Tests	30
	4.2 Phase 2 - Integrated System Tests	31
	4.3 Phase 3 - Improved Coatings Tests	32

TABLE OF CONTENTS (CONT'D)

	<u>PAGE</u>
4.4 Tube Anomaly Investigation	32
5.0 REFERENCES	34

LIST OF TABLES

	<u>PAGE</u>
1 Simulated Baseline System Test Summary	35
2 Extrapolation of Test Data to Baseline Configuration . . .	36
3 Two Sided Radiation Test Summary	37
4 Summary of Set Point Changes (Two-Sided Radiation)	38
5 Summary of Heat Load Transient Test Points	39
6 Summary of Simulated Low α/ϵ Coating Tests	40
7 Steady State Correlation Test Points	41
8 Heat Rejection Test Point α 1A	42
9 Heat Rejection Test Point γ 51	43
10 Heat Rejection Test Point α 17	44
11 Heat Rejection Test Point γ 53	45
12 Heat Rejection Test Point α 14	46
13 Calculated Heat Rejection	47
14 Peel Strengths of Silver/FEP Teflon Bonded to 6061-T6 Aluminum Adherend	49
15 Outgassing Data For Adhesives	50
16 Silver/FEP Teflon Adhesive Summary	51
17 Outlet Temperature Data	53
18 Condition of Silver/FEP Teflon Thermal Control Coating . .	54
19 Summary of Panel Freeze Thaw History	55

LIST OF FIGURES

	<u>PAGE</u>
1 Orbiter ATCS Components	56
2 Simplified ATCS Schematic	57
3 Modular Radiator Panel Tube Arrangement	58
4 Shuttle Configurations Simulated by Test Article	59
5 SESL Chamber "A" Showing 8 MRS Panels and LTV Test Personnel	60
6 Detail of Insulation on Panels and Environment Simulator .	61
7 Flow Loop α	62
8 Flow Loop β	63
9 Flow Loop α_3	64
10 Flow Loop γ	65
11 Flow Loop δ	66
12 Flow Loop ϵ	67
13 Influence of Environment on Performance	68
14 Test Group 2.8 - Response to Set Point Changes	69
15 Comparison of Plumbing Arrangements	70
16 Comparison of Plumbing Arrangements	71
17 Panel Thermal Model	72
18 Test Point 1A Correlation	73
19 Test Point 51 Correlation	74
20 Test Point 17 Correlation	75
21 Test Point 53 Correlation	76
22 Test Point 14 Correlation	77
23 Integrated Radiator/Expendable Cooling System Schematic . .	78
24 Cutaway Drawing of the Flash Evaporator	79
25 Duct and Nozzle Dimensions	80
26 Mixed Outlet Temp Response During Set Point Changes	81
27 Flash Evaporator Inlet and Outlet Freon Temperatures	82
28 Calculated Heat Rejection for Radiators & Flash Evaporator	83
29 Evaporator Performance During Duct and Nozzle Heater Tests	84
30 Sublimator Inlet and Outlet Temperatures.	85
31 Impact Pressure Data - Evaporator With No Nozzle	86

LIST OF FIGURES (CONT'D)

		<u>PAGE</u>
32	Impact Pressure Data - Sublimator with Supersonic Nozzle .	87
33	Mass Flux Data - Phase III Test - OCM #9	88
34	Mass Flux Data - Phase IIIA Test - OCM #9	89
35	Water Flow to Tank During Flash Evaporator Testing	90
36	Water Flow to Tank During Sublimator Testing	91
37	Water Quantity During Maximum Flux & Heat Load Test Point	92
38	Flash Evaporator Tank Overfill Test Point.	93
39	Flash Evaporator Outlet Temperature Response to Cyclic Set Point Changes	94
40	MRS Panel Installation for Coatings Test	95
41	Anomaly Description	96
43	Photomicrograph of Extruded Coolant Tube with Yielded Thin Wall Adjacent to Failure Site of Tube 5	97
42	SEM Fractograph Showing Dimple Tension Failure	98
44	Stress in Coolant Tube vs Temperature	99
45	Fluid Trapping During Thaw Transient	100

1.0 SUMMARY

This report summarizes a series of thermal vacuum tests conducted in the NASA-JSC Space Environment Simulation Laboratory from March through July 1973. The tests were designed to support the development of the Orbiter Active Thermal Control System (ATCS) and included testing of a wide heat load range modular radiator system (MRS) configured to the March 1973 Orbiter baseline system, a candidate weight reducing radiator/water cooling system, and a smaller radiator system with a high performance radiator coating.

The test system consisted of eight modular panels arranged in various plumbing configurations to represent the baseline and alternate systems. The integrated radiator/water test included the MRS and a flash evaporator or sublimator with exhaust duct and nozzle to reduce water vapor impingement on the vehicle. For the coatings test the MRS panels were coated with silver backed Teflon attached with eight candidate adhesives.

The tests verified the performance of the baseline system and obtained detailed design information for application of a wide heat load range modular radiator system to the Orbiter. The two candidate ATCS weight reducing designs have undergone extensive concept verification testing and their system operating characteristics have been determined in sufficient detail for application to the Orbiter. Design information has been obtained for an integrated radiator/water cooling system that provides for vehicle heat rejection as well as water management of the excess fuel cell water. Processing techniques have been developed and verified for the application of a high performance thermal control coating to large radiator areas subjected to a temperature range of -280°F to $+160^{\circ}\text{F}$.

2.0 INTRODUCTION

The Space Shuttle Orbiter Active Thermal Control System (ATCS) consists of a coolant loop that flows to various locations throughout the vehicle (Figure 1) absorbing heat through heat exchangers with sub-loops and removing heat in the heat rejection subsystem. Figure 2 shows a simplified schematic of the loop including the heat rejection subsystems used in the different mission phases. The subject of the test program discussed herein is the on-orbit heat rejection system which consists of a space radiator and expendable water system.

Although the radiator design conditions, configuration and location on the Orbiter were not firmly established at the time of the test program (March - July 1973), it was anticipated that the radiators would be mounted on the inside surface of the cargo bay door and would require all or a major portion of the available door area. This arrangement provides protection during launch and re-entry and for the most part combines the radiator "deployment" and door opening into one function. The forward 30 feet of the door has a greater opening angle than the aft segment. Deployment of this forward segment of the radiator away from the door allows radiation from both sides, increasing the heat rejection capability. Figure 1 also shows a typical cross-section illustrating the radiator configuration. One-half of the radiator is thus one-sided and the other half is a two-sided radiator.

The Space Shuttle mission objective of delivering and returning a variety of payloads to and from earth orbit results in a wide range of heat rejection requirements both between missions and within a particular mission. A proposed design to meet the wide heat rejection criterion consists of a modular radiator system with panels added or deleted as required. Each modular panel uses the wide heat load control technique developed by the Vought Systems Division (References 1 and 2).

The flow passages (tubes) on each panel are arranged in a "U" shaped pattern (Figure 3) with flow control orifices at the inlet of each tube to maintain the proper flow distribution among the tubes. The innermost tube is designated the prime tube and is plumbed separately from the remaining bank of main tubes. A flow control valve regulates the flow split between the main and prime tubes to maintain the desired outlet temperature. During low load conditions the majority of the flow is routed to the prime tube and the main tubes begin to stagnate due to reduced flow. The main tubes sequentially stagnate (outer-most tube first) as the load and flow are reduced. At the lowest load, approximately 99% of the panel flow is routed through the prime tube and all but the main tube adjacent to the prime tube may be stagnated. Transition to high heat rejection conditions is accomplished by sequentially thawing the tubes in the reverse order of stagnation as the flow control

valve routes more flow to the main tubes. At the high heat rejection conditions the majority of the flow is to the main tubes, all tubes are flowing, and full heat rejection capability of the panel is achieved. A high to low heat load ratio of 86:1 for two sided radiation and 50:1 for one sided radiation have been demonstrated for these panels (Reference 2).

3.0 TEST PROGRAM

Previous testing of the modular radiator system (MRS) had evolved from the basic element tests described in Reference 1 through the single and two panel tests reported in Reference 2. The test program described herein is final concept verification and provides the basis for detailed application of the MRS to the Orbiter.

The National Aeronautics and Space Administration sponsored and jointly conducted with Vought Systems Division a series of tests involving the MRS concept in support of development of the Orbiter Active Thermal Control System (ATCS). The test was conducted in the NASA-Houston Space Environment Simulation Laboratory thermal-vacuum Chamber A from March through July 1973. The test was divided into three major phases:

- (1) MRS Tests
- (2) Integrated Radiator/Expendable Cooling System Tests
- (3) Improved Radiator Coating Tests

The objectives of the first phase of testing were to: (1) evaluate the MRS design concept by demonstrating the panel flexibility and "build to stock" approach to system design, (2) demonstrate the MRS performance over the full range of Orbiter heat loads, environments and flow configurations, and (3) provide data to support the Orbiter radiator design/development. Phases 2 and 3 investigated possible ATCS weight reducing designs including the use of excess fuel cell water to supplement the radiator heat rejection and the use of improved radiator coatings to reduce the radiator size. The objectives of phase 2 were to: (1) obtain performance data on an integrated radiator/evaporator design concept which provides for the Orbiter heat rejection and management of the excess fuel cell water and (2) evaluate the water evaporator overboard vent to minimize water vapor contamination. The objective of phase 3 was to evaluate various adhesives for attaching a low solar absorptance/high emittance coating to the panels under thermal-vacuum conditions.

3.1 Phase 1 - MRS Tests

This section describes the Modular Radiator System Shuttle Configuration Tests conducted in the NASA-Johnson Space Center thermal vacuum facility (Chamber A) from 5 March 1973, through 23 March 1973. The tests were conducted under the supervision of the Crew Systems Division of JSC. Vought Systems Division of LTV Aerospace Corporation designed, manufactured, and instrumented the radiator panels

and flow bench used to supply the radiator system. The chamber facilities, environment simulation and data gathering and reduction were supplied by NASA-JSC.

3.1.1 Test Objectives

The general test objectives were:

1. Provide data which will support detail design of the Orbiter radiators by defining performance limitations with environments and fluid temperatures characteristic of Orbiter operation.
2. Demonstrate performance of eight modular radiator panels in a variety of series and parallel flow arrangements with balanced and unbalanced panel environments.
3. Demonstrate that a modular radiator system performance range capabilities satisfy Orbiter requirements.
4. Demonstrate general modular radiator system operational capability in a thermal-vacuum environment.
5. Investigate test performance of various candidate Orbiter radiator panel arrangements to support analytical predictions.
6. Provide data for verification/correlation of math model predictions.

The test was divided into three major groups with specific objectives as follows:

- GROUP 1 - SIMULATED BASELINE SYSTEM - One-Sided Radiators
 - o Demonstrate performance of the March 1973 Rockwell International Corporation baseline Orbiter configuration with a variety of heat loads and thermal environments.
- GROUP 2 - ALTERNATE SYSTEM - Two-Sided Radiators
 - o Demonstrate performance of radiator portion of an alternate radiator-water heat rejection system.
 - o Investigate radiator system response to step changes in outlet temperature control point to support the Phase 2 testing.
- GROUP 3 - DESIGN DATA
 - o Compare performance of radiator systems plumbed in various alternative arrangements.
 - o Evaluate engineering design adequacy of the panels.
 - o Evaluate simulated low α/ϵ coatings.

- o Demonstrate system parallel flow stability with skewed environments.
- o Demonstrate system performance during transition between high and low heat loads (freezing and thawing) in various parallel/series flow arrangements with balanced and unbalanced environments.

Four basic Orbiter configurations were approximated during the test. The four configurations were based on a radiator design optimization study which permitted the use of water evaporation to supplement radiator heat rejection when needed. The four configurations and corresponding flow loops are illustrated in Figure 4.

The baseline configuration (3) with 1436 ft² of effective area can reject the Orbiter heat loads without supplemental water evaporation. For each cargo bay door, two panels are permanently attached to the aft door segments and four more panels are mounted back-to-back and separately deployed from the forward door segment. The 12 panels are identified as A through L on Figure 4.

Configurations 1 and 2 require supplemental water evaporation to satisfy heat rejection requirements, but all panels are permanently attached to (and supported by) cargo bay door segments. Configurations 1 and 2 differ only in the deployment angle of the forward doors. The eight panels are identified ABCD, GHIF and the environments are similar to those of Panels ABCD, GHIF of Configuration 3.

Configuration 4 consists of four panels which are separately deployed from the forward cargo bay door segments. The panels are uninsulated so that they radiate from both sides. The analytical trade study indicated that, with supplemental water evaporation, this concept yielded a weight optimum design. The four panels are identified as M, N, O and P since the two-sided configuration does not correspond to any panels in the other three configurations.

3.1.2 Test Description

The Modular Radiator System (MRS) for this test consisted of eight 6 ft x 12 ft flat panels arranged in flow patterns similar to those being considered for the Orbiter. Each panel consists of extruded tubes welded to 0.02 inch aluminum sheet on 6.0 inch centers in a U-shaped pattern as shown in Figure 3. The over/under tube arrangement (Figure 3) provides for completely redundant flow passages, but only the "under" passage was used in this test. Thorough thermal vacuum testing of two of the panels has previously been performed (Ref. 2) and all eight panels and the flow bench were checked out in the VSD thermal vacuum chamber prior to the Chamber A tests

to insure satisfactory operation of all equipment and verify all operational procedures. (Reference 3)

The eight panels were installed on the floor of Chamber A as shown in Figure 5. Numerous remote control on-off valves and panel interconnecting lines inside the chamber allowed for a wide variety of series/parallel flow arrangements to be tested without chamber repressurization and replumbing. Two different mixing valves were used during the test to control the prime and main mixed temperature. A thermally actuated valve supplied by Pyrodyne was used during some portions of the test (mostly during transients). This valve has a fixed set point of 47-49°F.

The second valve was an electro-mechanical valve and control unit originally designed for use in the Skylab Apollo Telescope Mount (ATM) coolant loop. The valve control unit was modified by VSD to provide outlet temperature control points of 40°, 50°, and 70°. The Skylab requirement for leakage through the ATM valve "closed" side is much higher than that required for MRS testing. Thus, additional restriction was added manually during various phases of the test, such that the leak rate was reduced to approximately 1% of full flow.

Instrumentation

A total of 39 fluid temperatures were measured for the flow system. The measurements included prime and main inlet and outlet temperatures for each panel, the main and prime system inlets, two mixed outlets, two mixed prime outlets and main/prime mixed outlet. In order to obtain good accuracy over the full range of expected temperatures two ranges of thermocouples were used for each fluid temperature measurement. The low range is from -300°F to -40°F and the high range is -60°F to +200°F. In addition to the fluid temperatures there were 37 thermocouples on each of the 8 panels for detailed evaluation of individual panel performance.

A total of 11 flow measurements were made, including total system, main system, prime system, and 4 panel or parallel leg flows in both the prime and main system. This flowmeter arrangement (total flow plus flow in each leg) is such that with the loss of any one flowmeter all flows are still known. The main and prime system and panel flows were measured with 3 different ranges of flowmeters to improve the accuracy over the relatively wide range of expected flows (0-2200 lb/hr). In addition to the flow measurements the pressure drop of each panel was measured with a pressure transducer.

Numerous other temperature, flow and pressure measurements were taken to monitor the test equipment and chamber facilities.

Environment Simulation

The environment was simulated by a temperature controlled panel located immediately below the radiator panels as indicated in the sketch of Figure 6. A freon 11 loop and a liquid nitrogen loop flowing in separate tubes were used to control the panel temperatures. The radiator panel absorbed heat was based on the simulator and radiator temperatures including the effect of reflected energy.

The top side of the radiator panels were insulated for the one-sided tests so that the chamber LN₂ cold walls were not required. For the two-sided tests a simulated cargo bay door replaced the top side insulation and the chamber cold walls used.

Test Configurations

During the first week the panels were insulated on one side and two flow loop arrangements tested to investigate the performance of segments of configurations 1, 2 and 3. Flow loop α (Figure 7) is used to simulate the two panels on one cargo bay door for configurations 1 and 2; all of the panels of configuration 2 with a low α/ϵ coating; and 1/4 of the upward facing panels combined with all of the downward facing panels of configuration 3.

Flow loop β (Figure 8) simulates the parallel to series flow setup of the baseline system for one cargo bay door. One half of the upward panel area and all of the downward facing area are simulated for this test arrangement. Since the flow loop of Figure 7 simulates all upward facing panels of configuration 3, the outlet temperature at point X (after one half of the upward facing panels) is used at the inlet temperature for corresponding conditions with flow loop β (Figure 8). The temperature at point Y (after 3/4 of the upward facing panels) is used as the inlet temperature for corresponding conditions with the arrangement of Figure 9 which simulates the outlet leg of both cargo bay doors.

The second week of testing investigated three more flow loops (Figures 10, 11 and 12) to demonstrate versatility of flow arrangements, the effect of panel isolation, panel shadowing, and limitations on performance. Freeze-thaw characteristics of panels connected in various parallel/series flow arrangements were also obtained during these tests.

For the third week of testing the insulation was configured to simulate the cargo bay door and the performance of configuration 4, (two-sided radiation) investigated with flow loop γ (Figure 10). This flow loop simulates the radiators on both sides of the forward 30 ft. of the cargo bay and represents the full radiator system where expendable water is used to supplement the radiator heat rejection.

3.1.3 Test Results

The sixty-four test points run during the three-week test series have been divided into three major groups as follows:

GROUP 1 - SIMULATED BASELINE SYSTEM	
o Nominal $\beta = 78^\circ$ environment	8
o Skewed environments	10
o Cold soak and recovery	1
GROUP 2 - TWO-SIDED RADIATOR SYSTEM	
o Nominal $\beta = 78^\circ$ environment	5
o $\beta = 0^\circ$ environment	3
o Cold soak and recovery	1
GROUP 3 - DESIGN DATA	
o Low α/ϵ coating simulation	4
o Response to set point changes	16
o Alternative plumbing arrangements	11
o Heat load transients	<u>4</u>
	64

Each major group has been further subdivided to include test points which together form the baseline system or are directly comparable to each other.

Simulated Baseline Tests

Table 1 shows the test data heat rejection for the Group 1 simulated baseline system. For those test points which simulate half of the system the average heat rejection over the orbit is doubled to get the system heat rejection. It is assumed that as one side of the system is at the maximum heat rejection the other side is at the minimum so that the orbital average of one side is approximately the same as the total system. Table 1 indicates that test groups 1.1 through 1.5 do not reject the desired heat loads. The difference in heat rejected and heat load for test groups 1.6 and 1.7 is due to the outlet temperature control point and slight differences between the main and prime system flow splits between the test segments. The fact

that test groups 1.1 through 1.5 do not reject the heat load is attributed to two reasons. First, although the total test area agrees with the baseline area, the distribution between the top panels and the cavity panels is different. Second, the test environments are generally higher than desired resulting in a lower heat rejection.

The test and baseline areas are:

	<u>TEST</u>	<u>BASELINE</u>
Top Panels	1152	1030
Cavity Panels	<u>288</u>	<u>410</u>
TOTAL	1440 ft ²	1440 ft ²

The baseline heat rejection can be estimated by adjusting the test heat rejection on the top panels and cavities by the differences in areas. Table 2 presents the results of this analysis for test groups 1.1, 1.2 and 1.5. The extrapolated results are close to the desired heat rejection for test groups 1.1 and 1.2 indicating that with lower environments the heat load could be met. The results of test group 1.5 indicate that the baseline system as tested will not reject the system heat load with the sun in cavity orientation. A flow reversal valve which routes the flow through the hot cavity panels first then to the top panels or a flow porportioning valve to route the flow to the cold cavity would improve heat rejection for this orientation.

The low heat rejection for test groups 1.3 and 1.4 is attributed to higher than desired environments. For example, the comparison of test points 5 and 8 shown in Figure 13 indicates that the high environment on panels 1, 3, 5 and 7, test point 8, caused the inlet to the cavity panels (panels 8 and 6) to be the same for both test points and resulted in the same outlet temperatures.

Alternate System Tests

Test groups 2.1 through 2.4 examined the performance of the radiator portion of the analytically determined weight optimum radiator/water heat rejection system. Table 3 summarizes the test results of these test groups. Test point 22 examined the radiator performance in the expected design orbit. The results indicate a maximum evaporation heat load of 17,864 BTU/hr which is close to the nominal 16 lb/hr rate. It should also be noted that the maximum heat rejection occurred during TP-27 which represents a sun in cavity orientation. This is in direct contrast to the baseline system which indicated that the sun in cavity orbit is the worst case condition.

Test group 2.4 examined the alternate system performance in simulated 0° inclination orbits. These orbits have been analytically shown to be not as severe as the 78° inclination orbits tested in test group 2.1. A comparison of the results verifies that less water evaporation is required. However, the peak outlet temperature occurs during TP-61 indicating that the maximum instantaneous water evaporation rate is during this orbit. This is important in sizing the evaporation system. The test data indicates a maximum water evaporation device heat load of 19,048 BTU/hr. An examination of the transient test environments to insure that they are representative of the orbit and an analytical verification of the results is required before a definite design criteria is established. The maximum and minimum test environments were lower than requested (a maximum deviation of 5.0 BTU/hr) indicating that the actual peak outlet temperature could be higher than the test data.

Groups 2.5 through 2.8 are included in the two-sided radiation test subgroup, although these tests were primarily intended to test system outlet temperature set point change response. Table 4 summarizes the test results of test groups 2.5 through 2.8. Figure 14 shows a typical transient heat rejection resulting from the change in set point temperature. As indicated the changes in radiator heat rejection are accomplished in five minutes or less, indicating that the water evaporation device to be used with the radiator system should have a fast response time.

The maximum observed change in heat load was from approximately 45,000 to 70,000 BTU/hr (Test Points 53-54 and 56-59). This 25,000 BTU/hr change under the maximum load conditions is above the anticipated change in load when the excess fuel cell water is used to top off the radiator system (10,000 - 16,000 BTU/hr). Test point 52 had a lower than desired heat rejection because the simulated heat load was low due to limited test equipment heater power for the prime system.

There were no observed flow instabilities due to the rapid changes in flow rates for the cold and skewed environments.

Alternative Plumbing Arrangements

A comparison of the heat rejection per unit area (Q/A) is shown in Figure 15 for panels plumbed in 4, 5 and 8 parallel paths. This data indicates that with equal panel inlet/outlet temperatures (TP-32, 33 and 45), the Q/A variation is 51.0 to 55.4 BTU/hr-ft². TP-46 has a Q/A of 62.5 BTU/hr-ft², but also has a higher outlet temperature indicating a higher average radiating temperature. Therefore, a direct comparison between TP-46, and TP-32, 33 and 45 cannot be made. It is concluded that changing the panel plumbing from 4 to 8 parallel paths results in approximately an 8 percent decrease in heat rejection capability. This agrees with previous analytical studies (pre-test predictions which were made for an inlet temperature of 111°F instead of 165°F).

The effect of different plumbing configurations for the cavity panels of the baseline system is shown in Figure 16. TP-48 and 49 indicate no difference in system performance. The difference between TP-20 and TP-48 and 49 is attributed to differences in environments. The test results again indicate that the plumbing arrangement does not affect the system performance.

Heat Load Transients

A total of 6 heat load transients with five different flow configurations were conducted (Test Groups 3.4 and 3.5). A summary of the heat load transient test points is shown on Table 5. Minimum-maximum-minimum and maximum-minimum-maximum heat load transients were tested with different environments on parallel panels. A maximum of five parallel panels with a hot environment on one panel and cold environment on the other four have been tested. All flow arrangements operated satisfactorily, with no observed flow instabilities.

Simulated Low α/ϵ Coatings

The low α/ϵ coating performance was simulated by reducing the absorbed heats to the analytically determined values and ratioing the test panel areas by the ratio of emissivities ($\epsilon_{\text{white paint}}/\epsilon_{\text{desired}} = .9/.76$). Table 6 summarizes the results of this group of tests and the test panel and simulated areas.

3.1.4 Data Correlation

Accurate predictions of the Orbiter radiator system performance is of prime importance in the design and development of this heat rejection system. The proposed location of the radiators attached to and/or deployed from the cargo bay doors introduces many design variables such as radiation from one side only, two-sided radiation or back-to-back panels. The worst case orbit and vehicle attitude must be determined analytically for each of these configurations to optimize the radiator design. The use of flow reversal or flow proportioning valves introduces more variables which must be considered. An accurate model is needed to parametrically study all design variables and insure optimum radiator performance.

The uniqueness of the modular panel concept, the valve stagnation method of heat load control and the large size of the radiator system present several modeling criteria not encountered in previous radiator systems. The multi-panel configuration proposed for use on the Shuttle requires that the model predict interaction between the panels; thus, dictating a separate model for each panel. In order to maintain similarity between the models, accurate predictions are required over a wide range of inlet temperatures in addition to the usual environment and flow variations. The downstream panel performance predictions must be as good as the upstream panel pre-

ditions and the individual panel errors must not accumulate to compromise the total radiator system performance.

The developmental testing of the MRS provides approximately 300 hours of thermal vacuum test data for thermal model correlation. The test panels are of a different size (6' x 12') than the anticipated baseline panels (approximately 11' x 15') and the baseline panels will probably have a different number of tubes, tube spacing and fin thickness. However, the modeling techniques developed from the test panel correlation analyses can be used for the baseline system model, thus improving the confidence of baseline system performance predictions.

Model Description

The primary objective of the thermal model is to provide a tool for performance predictions of the radiator system under the design conditions of maximum and minimum heat rejection. The maximum heat rejection capability must be in the most severe environment and the minimum heat rejection must be in the most favorable environment for heat rejection. Predictions of intermediate heat loads and environments are desirable, but are of secondary importance.

These model objectives and the system operating characteristics have been used as the basis for the construction of the thermal model. A single tube is used to model the bank of eleven main tubes as depicted in Figure 17. The single tube fluid-to-tube heat transfer and pressure drop characteristics are based on tube number 6 of the main system with a factor of 11 applied so that the total area for heat transfer between the fluid and tube in the model matches the main bank of tubes. The model includes the prime tube for low load operation when the majority of the flow is in the prime system.

During the third week of testing the radiators were allowed to radiate from both sides with a simulated Shuttle cargo bay door on one side (see Figure 6). The test configuration was designed to yield an effective radiation area from the cavity, formed by the panel and simulated door of 0.67 times the panel area. This factor is based on analysis of the Shuttle configuration considering reflection between the curved radiator and door. The thermal model also used this factor. Verification of the model under the test conditions does not verify the model for flight use because the test configuration is based on analysis only.

Correlation Analyses

Pretest analyses were conducted for the originally planned 56 test points. This data was used for real time evaluation of the test conditions and results during the test. For most of the test points, deviations from the planned test flow rates, inlet temperatures and environments prevent the use of the pre-test analysis for

correlation purposes. Table 3 shows a comparison of test results and predictions for several test points for which the test conditions were close to those planned. As indicated, the model predictions agree well with the data with differences attributed to different test conditions.

The test points used for post test correlation were chosen to give comparisons over a wide range of operating conditions. It is not practical to run the entire test sequence; however, proper selection of the test points for correlation will yield a model of known accuracy for any anticipated operating condition. The most important operating condition is at the maximum heat load and maximum design environment. Accurate performance predictions for this condition are required to insure that the radiator system capacity is sufficient to meet the load. A high heat load with a cold environment condition is best to determine model adequacy and highlight possible sources of error. Table 7 lists the test points chosen for correlation and the range of variables covered. As indicated low and high heat loads, low and high environments, skewed environments, various plumbing configurations, and one and two sided radiation conditions are considered in the correlation analyses.

The correlation analysis concentrated on steady state performance predictions. Transient predictions have been made for the two-sided radiation set point change test points to show the effect of transient inlet temperatures and panel flow rates. No correlation was done for the transient environment test points because only steady state environment data is available at this time. Recovery transients (minimum-maximum) heat load transients were also not correlated since the model does not predict tube freezing.

Results

Figures 18 through 22 present representative temperature maps comparing the correlation analysis and the test data for each of the five major conditions chosen for correlation. Tables 8 through 12 shows the comparison of heat rejection computed from the model predictions and test data corresponding to the temperature maps.

The model predictions show excellent agreement with the test data for the maximum design conditions of high load and hot environment. Predictions under minimum design conditions of low load-cold environments indicate good agreement with the measured data, but evaluation of low load predictions should consider the possibility of parallel flow instabilities due to main system freezing. Performance predictions under intermediate conditions in which the majority of the flow is not in either the main or prime system are adequate although model improvements in this area may be

desired. The primary modeling objective of providing an analytical technique for performance predictions of a multi-panel radiator system under the design conditions has been met.

A survey of the predicted and measured pressure drops (typical results are also shown on the temperature maps of Figures 18 through 22) indicates good correlation with the exception of Panel 1. This panel had a different tube restrictor design than the other panels and is not included in the pressure drop correlation analysis. The predicted pressure drops for those points which the model predicts a main system freeze-up are in considerable error as expected.

3.2 Phase 2 - Integrated Radiator Expendable Cooling System Tests

The concept of using both radiators and expendable cooling to provide a minimum weight ATCS derived from a study performed by VSD for the Crew Systems Division (CSD) of JSC. This study explored the possibility that by adding expendable cooling to the radiator system, the reduction in required radiator area would provide a decrease in overall weight which would more than offset the extra weight of the expendable cooling device. The results of the study indicated that this integrated system concept did provide a smaller launch weight for the Orbiter.

The attractiveness of expendable cooling is due to the substantial amount of excess water that is produced by the fuel cells. This excess water must be expelled from the vehicle to reduce the launch weight of the storage tankage, but if it is expelled through an expendable cooling device such as a flash evaporator, the radiator area requirement is lessened.

Thus, the integrated ATCS involves launch with sufficient water to assist a "smaller" radiator during the peak load period early in the mission, followed by use of the expendable device in a "water management" mode to maintain onboard water at an optimum level to accommodate peak loads toward the end of the mission.

3.2.1 Test Objectives

The key objectives of the integrated system test can be summarized as follows:

- o System verification and sensitivity
- o Component performance data gathering
- o Plume definition and nozzle verification
- o Mechanical, manufacturing suitability

Since it has been demonstrated analytically that a weight savings could result from an integrated concept, it was desired to test the suitability, sensitivity, and limits of the control system designed to "allocate" heat rejection between the radiator and the expendable device while maintaining desired water levels. To this end, a limit condition series of tests were run to attempt to deplete and overflow the tank and to cause the control system to chatter. Also, typical mission profiles were run to gather response data on orbital transient situations.

The comparison of the flash evaporator and the sublimator as potential candidates for selection as Shuttle flight hardware was another major objective of the test.

The supersonic nozzles on each expendable cooling device are intended to direct the effluent vapor plume away from the Shuttle in such a way that the vapor does not scatter back onto surfaces that might be contaminated. Nozzles were designed to minimize this backscatter, and the chamber was instrumented to measure the extent of the vapor plume. The actual plume definition and nozzle effectiveness was determined from subsequent nozzle component tests. However, the nozzles were included in the Integrated System Tests to verify system operation.

The general mechanical and manufacturing suitability of the various components of the ATCS was also an objective of the testing. This also includes verification of procedures such as startup and shutdown of devices and stagnation and destagnation of radiator panels.

3.2.2 Test Description

Figure 23 is a simplified schematic of the integrated ATCS. The system is made up of the following components.

- o Modular Radiator System
- o Expendable Cooling Device with Nozzle
- o Water Storage System

The radiator system used in this phase of the test was the previously described MRS. The eight panels were arranged to represent configuration 4 (Figure 10) with radiation from both sides including the simulated cargo bay door.

Two different expendable cooling devices were used: a flash evaporator (FE) and a sublimator.

The flash evaporator is a heat transfer device in which water evaporates in contact with the inside surface of a heat exchanger while Freon circulates on the

outside surface. Figure 24 is a cutaway drawing of the device that was used for integrated testing.

The water is sprayed into the chamber on command from a sensing thermocouple located adjacent to one of the freon tubes. For this test, the control temperature was 40°F, which caused water spray (and heat rejection) whenever the Freon temperature was greater than 40°F. The spraying nozzle is designed to flow 16 lb/hr for a full open evaporant valve, and for heat loads less than 16,000 BTU/hr, the action of the thermocouple causes a rapid pulsation of spray. Only at a 70°F or greater inlet freon temperature will the FE spray water continuously at 16 lb/hr.

The sublimator is a device which depends for operation on the formation of an ice layer between the feedwater supply and the chamber vacuum. With the addition of heat from the Freon system, the ice layer is continuously sublimated to space while new ice is formed beneath. The action of the ice layer is such that "automatic" water demand is created in proportion to the heat rejected.

The sublimator package was designed to reduce Freon temperature from a maximum of 70°F to 40°F, at high load conditions. For inlet temperatures above 70°F, ice is sublimated faster than it can be formed, a condition which will eventually lead to a "breakthrough," in which water is boiling into the vacuum. When this occurs, the heat load must be removed and a "dryout" period commenced, followed by the re-establishment of the ice layer.

Each expendable cooling device was fitted with a six-foot duct with two 45° bends to simulate a typical routing problem aboard the Orbiter. In addition, a supersonic nozzle was mated to each duct in order to assess the degree of backscatter onto the orbiter surface. The nozzles were designed by personnel of the Propulsion and Power Division (PPD) of JSC, and these PPD engineers also had primary responsibility for defining the vapor plume via particle counters located at various points in the chamber.

Both ducts and both nozzles were heated to prevent ice buildup. The ducts were heated by routing Freon flow around them, as shown in Figure 25. The nozzles were fitted with electrical heaters. Figure 25 also shows a comparison of the size requirements of the two nozzles. The difference in size between sublimator and FE ducts is due to the different pressure ranges required for operation of these devices.

The water storage system controls the amount of water stored by sensing the current level in the water tank and modifying the MRS set point temperature, which in turn modifies the water demanded by the FE or sublimator. The purpose of this arrangement is to efficiently manage the excess fuel cell water by using it as

a heat sink in an optimally weight-effective manner. Use of this water provides a reduction in the radiator area requirements.

In effect, at peak heat rejection loads, both radiator and evaporative heat sink are needed to reject the load, and the system design point is to provide just enough radiator area such that at the worst environmental extreme, the peak load can be rejected. At lower loads, the evaporative device is used to maintain tank water level between 85 and 95% full, and the MRS is used as required.

The interaction between MRS and evaporative device is provided by the tank quantity meter and its effect on set point. As an example of this interaction, if the tank is only 85% full, the radiators are asked to provide a low (40°) set point, which, in turn, causes the evaporative device to turn off (i.e., use no water). Thus the tank begins to fill. Conversely, if the tank is at its high-water mark, a high MRS set point is signalled and water is used by the evaporator, thus rejecting heat and lowering the tank level.

The water tank was filled with a fuel cell simulator which simulated fuel cell water flow consistent with anticipated vehicle heat loads.

3.2.3 Test Results

This section summarizes the test data in terms of the key objectives of the test program. For purposes of discussion, these results are grouped to include (1) modular radiator performance, (2) evaporator performance and response (including nozzle heating tests), (3) sublimator performance and response (including nozzle heating tests), (4) nozzle performance, and (5) system-wide aspects of performance, including interaction between MRS, expendable cooling device, and water management system.

Modular Radiator System

The MRS performance is evaluated by observation of the following parameters; (1) steady state heat rejection and (2) rapid response to change in outlet temperature set point. Both of these attributes were demonstrated in the MRS testing, and were reverified in these tests.

Table 13 is a display of heat rejection by the radiator main and bank circuits for each test point. The total radiator heat rejection can be seen to be adjustable between essentially zero and 67,500 BTU/hr for total Freon flow rates of 2200 lb/hr. The ability of the MRS to reject typical shuttle heat loads was demonstrated again as it had been in previous testing.

The quick response to set point changes can be seen in Figure 26 for several test points. No more than a three minute delay was observed between a set

point change and the establishment of the desired outlet temperature.

Flash Evaporator

The performance of the FE is summarized in Figures 27 and 28. Figure 27 shows the inlet temperature to the evaporator (downstream of the duct) and the outlet temperature. This data indicates that the FE provides adequate outlet temperature control for sudden changes in inlet temperature from 40 to 50°F, 50 to 70°F, 70 to 50° and 50 to 40°F as well as for rapid cycles between 40 and 50°F (day 121, 1500 to 1700 hrs.). The calculated heat rejection across the FE is shown in Figure 28. This data demonstrates the ability of the FE to supply any heat rejection between 0 and the design value of 16,000 BTU/hr.

Estimates of flash evaporator efficiency were made throughout the test by comparing the rejected heat to the amount of water consumed. The parameter h_{fg} represents the ratio of these two quantities, and for perfect efficiency would equal the latent heat of vaporization of water. Typical average h_{fg} values are shown below, for one-hour periods of relatively stable test conditions:

From	To	Rejected Heat (BTU)	Change In Tank Level (lb)	Fuel Cell H ₂ O (lb)	Calc. Usage (lb)	h_{fg} (BTU/lb)
121/2030	2130	5020	3.2	8.0	4.9	1045.8
122/0300	0400	5350	1.5	7.0	5.5	972.7
0700	0800	15,477	-2.4	12.1	14.5	1067

The FE was shown to be operating with its normal efficiency for the majority of the test.

Figure 29 is a composite plot of pressure and temperature data taken during the nozzle and duct heating test. The falling nozzle throat and duct temperature was observed for approximately 2-1/2 hours following the turning off of the duct heater. As the duct and/or nozzle became ice-clogged, the FE chamber pressure began a rapid rise until all vapor flow stopped, a condition that was observed by the duct temperatures starting upwards again. When the Freon was routed back to the duct, the clogged duct/nozzle condition was alleviated and restart of the flash evaporator was accomplished.

Sublimator

Facility problems encountered during the sublimator portion of the integrated test caused substantial reduction in the time available for sublimator testing. Furthermore, even during the reduced time available, many test profile

changes were made on a realtime basis to maintain sublimator operation. Thus, component data taken was not as complete as that taken on the MRS/flash evaporator system.

Figure 30 is a recording of the sublimator inlet and outlet temperatures. The many inlet temperature spikes which can be seen are realtime manual increases which were undertaken to restore sublimator water flow and prevent long test delays. The reason that the flow stopped intermittently during low load operation could be related to facility problems (localized freezing of the water line in the unheated section). However, this characteristic is typical of low load sublimator operation. The excursions in the outlet temperature above 40°F are representative of breakthrough phenomenon and show the sublimator's sensitivity to higher-than-spec-limit heat loads. In cases such as this, the ice layer must be reformed after a complete sublimator dryout period. Considerable design margin (excess capacity) will be required to insure against complete loss of heat rejection for higher than anticipated heat loads.

Due to facility problems the performance of the sublimator under cyclic and step changes in inlet temperature was not obtained. Further testing will be required to verify this design requirement.

Nozzle Performance

No plume data were obtained from the integrated system test. A supersonic nozzle was included on each expendable cooling device to demonstrate total system performance. Subsequent nozzle tests were conducted without the MRS with the expendable cooling device operated in the same manner as observed in the system tests. Three different nozzle configurations were tested: supersonic, sonic (orifice) and plugged.

Typical impact pressure data taken within the water vapor plume are shown in Figures 31 and 32. The specific test conditions correspond to the flash evaporator with no nozzle (sonic nozzle) and the sublimator with supersonic nozzle. The measurements are seen to be in general agreement with the predictions. It is apparent from this data that the supersonic nozzle configuration resulted (as predicted) in generally higher impact pressure readings than for the configurations with no nozzle, reflecting its tendency to concentrate mass flow near the centerline.

Quartz crystal microbalances (QCM's) were used to measure mass flux in the nozzle exit plane in order to determine the nozzle "back-flow". Summary data for the "back-flow" measurements are shown in Figures 33 and 34. The data of Figure 33 are scattered, particularly for the no nozzle case, but the general trends are as expected: the supersonic nozzle configuration resulted in less backflow than with no nozzle and the backflow tended to increase with increasing flow rate. The estimated

means for the data from the two configurations shows a reduction of approximately a factor of 3 with the supersonic nozzle, compared with a predicted value of 3.7.

The data of Figure 34 indicates a backflow reduction of approximately 3 to 4, which compares with the supersonic nozzle over the no nozzle configuration. The plugged nozzle data also correlates quite well with predictions.

A more significant nozzle effectiveness is the total mass flow at angles greater than 90° . This parameter must be determined analytically. Correlation of the test data and analysis indicates that the expansion angle of the plugged nozzle is in the range of 110° to 118° , resulting in an effectiveness ratio of 25 to 100. A similar analysis indicates that the supersonic nozzle will reduce backflow by a factor of 3 to 10 for the sublimator, with a slightly higher value possible for the flash evaporator because of reduced boundary layer effects with the shorter nozzle.

System Performance

The performance of the integrated systems has two aspects: (1) the adequacy of water level control system to prevent overflowing or depletion of the water tank, and (2) the sensitivity of the MRS/expendable cooling device to changes in set point. The latter performance criterion should demonstrate that total heat rejection is acceptable even though the "allocation" of this rejection may change rapidly. These two aspects of system performance will be discussed separately.

The water supply to the storage tank is displayed in Figures 35 and 36 for FE and sublimator. This flow rate was keyed to the heat load during the mission profile test points. Figure 37 shows the water level in the tank during a high load, high flow test point. It can be seen that the tank quantity can be controlled at these conditions. The maximum tank quantity that was observed during the test was 98 lb.

During the design limit cases, worst case conditions were set up in an attempt to overflow the tank. The system was allowed to drop to a cold-soaked condition by running for several hours at a low inlet temperature. Then the tank was manually filled to 94.7 lbs, or just below the point at which a 70°F set point switch would occur. At this point a high heat load was applied, but a lag was assumed to exist between the high water flow rate and the increase in radiator inlet temperature. Thus the tank began filling at a rapid rate, the set point was changed to 70°F , but, due to the inlet temperature to the radiators coming up slowly from 50°F , the evaporator could not operate to remove tanked water.

Figure 38 shows that tank quantity peaked at approximately 98 lbs before the radiator outlet temperature got high enough to require expendable cooling.

Another key test objective was to observe system performance under cyclic conditions. These conditions were generated in two ways. In the design limit runs,

the water flow to the tank and the heat load were set at just such a point that the 85 lb tank quantity indicator would be set into continual cycling. That is, at a 50°F set point the tank would be depleted below 85 lb, at which time a 40°F set point would cause filling again to raise the tank level above 85 lb. The resulting valve swings occurred approximately every 11 minutes, and as can be seen from Figure 39, resulted in no loss of control for the evaporator.

In a related mission simulation, the cycling environment caused inlet temperatures to the evaporator to cycle. This was due to the inability of the radiator to maintain 40°F set point for a 150 BTU/hr-ft² imposed environment. Again, the evaporator was able to maintain a constant outlet temperature despite the variation in inlet temperature.

3.3 Phase 3 - Improved Coatings Tests

The use of silver/FEP Teflon* film as a thermal control surface for space radiators is based on a favorable solar absorptance/emittance ratio in the 0.08 to 0.01 range, a stable solar absorptance varying between 0.06 and 0.08, high transparency, and minimal degradation in the charged particle-ultraviolet radiation environment of near-space(Ref.4). The combination of properties available in the silver/FEP film could result in both area and weight reductions for the Orbiter radiator system which has baselined the use of Z93 white paint as the thermal control surface. The silver/FEP thermal control material consists of FEP teflon film, Type A, with a layer of silver deposited on one side by vacuum evaporation to a thickness of 1000-2000 A.U. The silver is protected by an evaporated overlay of Inconel 600** to a thickness in the 1000-2000 A.U. range. The Inconel serves to retard chemical attack on the silver, aids the handleability of the film, prevents mechanical damage to the silver, and furnishes a bondable surface for the film. The silver/FEP functions as a second surface mirror since the attachment from the radiator panel is to the metallized surface of the FEP; this leaves the bare FEP exposed as the radiating surface. The favorable hemispherical emittance, $\epsilon = 0.8$ typically of the FEP is thus retained. The FEP absorbs relatively little in the solar wavelength region, meaning that the solar absorptance, $\alpha = 0.08$ typically of the silver/FEP film will be essentially that of the silver. Alternate thermal control materials include paint systems, fused silica sheets with evaporated metal coatings, and dielectric coated metals. Paint systems are limited by relatively high solar absorption and deterioration of properties (primarily increased absorption) with exposure to the charged particle ultraviolet radiation environment. The optical properties of the

* DuPont Trademark

** International Nickel Co. Trademark

metallized silica sheets are excellent, but their application to large, irregular surfaces poses a severe economic and technological problem. The dielectric coated metals, typically silicon monoxide coated aluminum, do not have optimum optical properties, and are difficult to apply to contoured areas of the design likely to be required by the radiator panels of the Shuttle Orbiter vehicle(Ref.4). Technical problems with silver/FEP in previous work on flight hardware scale radiator panels in thermal-vacuum tests extending into the cryogenic temperature regime have been numerous(Ref.2). These include (a) thermal expansion mismatch between the aluminum radiator and the silver/FEP film, (b) adhesive bond failure between the aluminum and the silver/FEP film, and (c) delamination of the metallized layer(s) from the FEP film.

The key objectives of the present investigation are to (a) establish bonding materials and processes for the silver/FEP thermal control material to Orbiter radiator panels and (b) subject the selected adhesives to a thermal vacuum test on full scale MRS panels under the thermal cycles and environments anticipated for the Orbiter vehicle.

3.3.1 Adhesive Selection

Prior work on silver/FEP as a thermal control material for radiator panels of the type required by the Orbiter vehicle was disappointing. Even though supplier experience and recommendations regarding adhesive and application process were positive, an off-the-shelf silver/Teflon film separated from the radiator skin during a full scale thermal-vacuum test(Ref.2). With this experience in mind, a concerted push was needed toward solution of the attachment problem of the silver/FEP film to the aluminum radiator panel. A multiple effort, with both industry and NASA laboratories contributing to attachment method screening and selection, was undertaken. LTV Aerospace Corp., Vought Systems Division (VSD) was selected to have overall responsibility for evaluation of screening test results, applying candidate silver/FEP-adhesives to the modular radiator panel test articles, thermal-vacuum test conduct, and analysis of test data.

Organizations contributing to the program include:

- (1) NASA Langley Research Center
- (2) NASA Goddard Spaceflight Center
- (3) NASA Johnson Space Center
- (4) G.T. Schjeldahl Corp.
- (5) McDonnell Douglas Co. - East
- (6) LTV Aerospace Corp., Vought Systems Division

Each of these organizations recommended several adhesives and bonding concepts and performed the initial screening tests on their selections. The screening tests consisted of immersion of bonded panels in liquid nitrogen followed by a thaw cycle to ambient temperature. The test panels consisted of 0.020 inch 6061-T6 aluminum sheet, 2 by 10 inches as the adherend. Silver/FEP strips, 1 by 4 or 1 by 8 by 0.005 inches were bonded to these adherend sheets to form the element test panels.

Final selection of adhesives to be included in the thermal vacuum test of 6' x 12' modular radiator panels was based on peel tests at cryogenic, ambient, and elevated temperatures as well as cryogenic soak tests. Outgassing data were also taken on the selected candidates, but due to the lack of absolute standards and specific requirements for the Orbiter Vehicle, this data was not used for disqualification of a promising adhesive. The peel strength and outgassing data were taken on the adhesives that the individual laboratories felt were most promising from their internal screening tests. Each organization prepared peel test and outgassing specimens to NASA-JSC-SMD specifications using adherend substrates prepared by VSD. Results of the peel tests run at NASA-JSC-SMD are given in Table 14. Only the following adhesives of those listed in Table 14 had measurable peel strengths at -300°F; Adiprene L-100 urethane, RTV 560 silicone, and Permace1 6962 double backed Kapton/silicone.

The outgassing data on the various adhesives are included in Table 15 for reference purposes only; absolute outgassing limits for the Orbiter and its payload are yet to be established.

Representatives from NASA/JSC-Crew Systems Division and Structures and Mechanics Division, NASA/Langley, NASA/Goddard, VSD, McDAC, and Rockwell International participated in the final selection of adhesives. A prime consideration in choosing adhesives was to get the widest variety of chemical types which might function in the anticipated -280°F to +175°F thermal environment. The following adhesives were selected for evaluation on the modular radiator panels:

IDENTIFICATION	TYPE/APPLICATION	INVESTIGATOR
RTV560	silicone/2 part brush	VSD
Mystic A117	silicone/contact	Langley
SR585	silicone/transfer laminate	McDAC
Permace1 6962	silicone-Kapton/transfer laminate	VSD
Crest 7343	urethane-aluminum/2 part hot mix	Langley
Adiprene L-100	urethane/2 part hot mix	Goddard
Adiprene L-167	urethane/2 part ambient mix	VSD
G401903	polyester/transfer laminate	Schjeldahl

Variations in the size of the silver/FEP film as it influenced handling and coating operations were also investigated. For this reason silver/FEP film was specified from the supplier, G. T. Schjeldahl, in various widths from 1" to 48". Three of the adhesives, Permacel 6962, SR585, and G4501903 were applied to the silver/FEP by Schjeldahl on a laminating machine to form a tape. The resulting laminates could be handled as tape with tack varying from nil (G401903) to moderate (Permacel 6962) to very high (SR585). Each of the adhesives was applied by VSD per instructions from and under the direct supervision of the contributing laboratory. Table 16 summarizes the application and cure technique used for each adhesive.

3.3.2 Thermal Vacuum Testing

The objective of the modular radiator coating evaluation was to determine the ability of the coating to adhere to the panels over a wide range of MRS operational conditions. The test included both one-sided and two-sided radiation. The one-sided tests consisted of maximum and minimum heat load operation under environments simulating:

1. Typical orbital cyclic environments (0 degree inclination solar oriented, 270 N.M.)
2. Maximum orbital flux expected for steady state
3. Minimum orbital flux expected for steady state
4. Deep space simulation with LN₂ temperature environment

The worst combinations of maximum and minimum heat load and the four simulated environments were tested to provide as wide a range of panel temperatures as possible with these conditions. The panels were mounted for the thermal-vacuum tests with the silver/Teflon coated surface down facing the IR simulator panels as illustrated in Figure 40.

The two-sided tests were designed to obtain the coldest expected panel temperatures (-250°F range) and most severe thermal shock. Both sides of the panels were exposed to the LN₂ environment and the heat load was cycled between the maximum and minimum.

The philosophy of the test was to as nearly as possible subject all seven panels to the same conditions in order to provide an equitable test for each adhesive. For this reason the seven panels were flow connected in parallel. In order to evaluate the coating condition throughout the test, a baseline performance point with LN₂ environment and 163°F inlet temperature was established at the start of the test and repeated at regular intervals. A comparison of the heat rejection of the panels at these points along with video monitor observations gave an indication of any change in the state of the coating. The test conditions began with nominal panel temperature variations and proceeded to more severe temperature conditions to determine limits on

the adhesives.

The test panel outlet temperatures for the baseline performance points are compared in Table 17. The panel outlet temperature is a function of the heat rejected by the panel and will therefore indicate changes in the condition of the coating. Should the coating dislodge from the aluminum panel or should the Teflon delaminate from the silver, the thermal emissivity of the panel would be reduced from the 0.08 value for the silver/FEP Teflon, to about 0.25 for bare aluminum or silver. The dislodged/delaminated portion would act as a radiation shield. This would reduce panel heat rejection significantly and result in an increase in panel outlet temperature. The test data indicates a degradation in performance of panels 4 and 6 between baseline points 2 and 3 and 7 and 8. The second point was just prior to the first cold soak and the third was just after. Between points 7 and 8 a longer cold soak with the rapid recovery was conducted. The thermal performance of the other five panels did not degrade during the one-sided test. The data of panel 4 correlated with visual observation via TV which indicated some of the coating dislodged between the second and third baseline points. The TV observations of panel 6, however, did not clearly indicate a change in the coating. Some dislodgement of corners of coating strips were noted on panel 7; however, this was never apparent from the thermal performance during the one-sided test. In comparing the outlet temperatures of the seven panels, it is noted that there was a range of 30°F variation in the first baseline point prior to any degradation of coatings. This difference was due to flow rate differences between panels caused by asymmetrical plumbing and flow control valves in the test equipment.

An analysis of the panel pressure drop and outlet temperature data indicated that the flow distribution among the seven panels changed throughout the test due to performance degradation in some panels. Thus, the observed change in outlet temperature of panels 4 and 6 between baseline points include the effect of panel flow changes and it would be expected that the other panel outlets would change due to flow changes. A detailed system analysis indicated good correlation of flow and outlet temperature for the first baseline point except for panel 2. The analysis indicated that this panel started with a degraded coating. Between the time of coating application and delivery of panel 2 to JSC, delaminated areas between the FEP and silver, 3-6 inches in diameter, were observed. Panel 2 was field refurbished with approximately 75% of the silver/FEP replaced, indicating the possibility of a degraded coating at the start of the test. The analysis showed agreement with the observed outlet temperatures indicating that panels 4 and 6 performance began degrading after the number two baseline point and continued to degrade during the test. Another definite step downward in performance between points seven and eight was noted. As well as indicating that panel 2 began

with an inferior coating, indication that this condition degraded somewhat during the test with the outlet temperature increasing from an average of 5 degrees above the analytical value for the first four baseline points to an average of 10 degrees for the last four. In the last baseline point all the panel outlet temperatures were above the analytical prediction. The trend of the data, however, at the end of the one-sided test indicates panel 4 performance had degraded significantly, panel 6 somewhat, and panels 2 and 7 indicated the possibility of some damage. This correlated well with the post test examination of the coatings which indicated the only undamaged panel coatings were panels 3, 5 and 8.

The outlet temperature data for the two-sided tests are also given in Table 17. The second baseline point appeared to have some differences in flow rates from the first points. The outlet temperature increased about 10°F for panel 2 from the first to the second baseline point, by 12°F for panel 5 and 13°F for panel 7. Panel 6 outlet temperature, however, decreased by 24°F, panel 8 by 5°F and panel 3 by 3°F. This combination of increases and decreases in panel outlet temperature precludes drawing conclusions regarding the state of the coating from the outlet temperature data except for panel 2. No pressure drop data were obtained in the second baseline point due to instrumentation problems; therefore, no flow rate data were available to resolve the outlet temperature changes between the first and second baseline points. The panel 4 coating, which suffered some loss of adhesion in the one-sided test, was restuck to the panel by hand prior to the two-sided testing, thus explaining the improved performance of this panel. The third baseline point for panel 2 indicates a possibility of some further degradation of this coating. The two-sided testing was not completed due to leaks which developed in the Freon 21 cooling loop.

No degradation of the three undamaged panels was observed from the thermal data of the two-sided tests. Further degradation of the damaged panel coatings could not be determined from the thermal data except in the case of panel 2.

3.3.3 Coatings/Adhesives Evaluation

No change in the silver/FEP coating on any of the radiator panels occurred during the normal cyclic conditions of on-orbit simulation. This result is supported by (a) video monitor sweep over the panels in real time during the thermal-vacuum test, (b) limited direct visual observation of the panels, (c) stable thermal performance thru the normal cyclic portion of the test. Coating failures, evidenced by video or thermal indications, occurred during the initial cold soak/recovery cycle. Limited data available indicates the failed area on certain panels progressed with subsequent cold soak/recovery cycles.

Failures were apparent in four of the adhesives (560, A117, 7343, G401903) at the conclusion of the eight 6 hour cold soak/recovery cycles (one sided). No failures in the remaining four adhesives (585, 6962, L-100, L-167) during the two subsequent two-sided 12 hour cold soak/recovery cycles were noted. The extent of the failed areas increased during the 12 hour cold soak/recovery cycle on the panels with 560, A117 and 7343 adhesives as determined by visual observations. The condition of the silver/FEP coating on each radiator panel before and after the thermal-vacuum test is summarized in Table 18. The width of the FEP film did not influence or induce coating failure with any of the adhesives investigated. The handleability and ease of application with a particular adhesive can be used as major criteria for film width selection.

3.4 Tube Anomaly Investigation

During the concluding phase of the coating adhesive tests and the complete six-month series of thermal-vacuum tests, ruptures occurred in the coolant tubes on three MRS panels. Four tube ruptures on three panels (out of a total of seven panels and 89 tubes in test) were noted during a thaw cycle following a two sided radiation condition (prime tube bypassed) to a liquid nitrogen sink temperature. After a cold soak of some twelve hours with temperatures as low as -270°F measured, a recovery transient was started. The MRS inlet temperature up-ramp was 60°F/hour maximum. Approximately 24 minutes into the thaw, tube 5 on panel 6 developed a leak. Tube 7 and possibly tube 9 of panel 5 began to leak some 34 minutes later. The thermal up-ramp was halted, but the thaw continued, causing tube 10 of panel 3 to rupture about 46 minutes after the initial leak was detected. The failure locations are diagrammed on the sketch in Figure 41. Note that all fractures occurred between the tube bends.

An analysis of the test anomaly indicates that the tube rupture was caused by non-uniform thawing of frozen tubes. The tubes were not attached to the radiator fin at the tube bends (corners) causing the corners to remain frozen, due to a poor conduction path to the adjacent hot tube, after the rest of the tube had thawed. The fluid trapped between the frozen corners underwent thermal expansion, causing high pressures and tube deformation to occur. After repeated thaw cycles and deformation the tube failed.

Metallurgical analyses of the tubes were conducted to determine the mode of failure and condition of the 6063 extruded aluminum tubing. Electron fractography coupled with macroscopic examination was used to determine that the mode of failure was ductile tension. Considerable deformation was found at each failure site indicating that failure was preceded by considerable yielding. The primary topographic feature

observed from the scanning electron microscope examination was elongated dimples, illustrated by Figure 42, which indicates a tensile/shear mode of crack propagation.

Chemical analysis and mechanical property measurements including Rockwell hardness and strength tests indicated that the tubing material was 6063-T42 aluminum.

A typical transverse section of the tube is shown in Figure 43. The lower tube was typically off center as-manufactured. The fracture followed the thin walled area of the tube at each failure location. Physical tube outside diameter measurements on all panels indicated that the majority of tubes had deformed between the tube corners and in some instances between the inlet and outlet and the corners.

The data plotted in Figure 44 show that concentric walls in the coolant tubes cause considerably lower stress levels to be developed at a given temperature of Freon 21. In addition the heat treatment of 6063 to the -T6 condition raises the yield strength to the 33 - 36 ksi range at cryogenic temperatures. Maximum temperature differences of 35°F were measured between frozen corners and thawed tubes at mid-points. Assuming a concentric tube and a delta of 35°F from -211°F to -176°F, a stress of 26 ksi would be induced in the coolant tube by expansion of the F-21. This is below the yield strength of ca.33 ksi for 6063-T6, allowing a thaw under these conditions to leave the tube undamaged.

Figure 45 presents measured temperature data during the last freeze-thaw cycle in which the tube failed. This data indicates that the section between the tube corners thawed approximately 3 minutes before the corners. The fluid in this section thus underwent thermal expansion while constrained by the frozen corners. The trapped fluid was heated to approximately -180°F before the tube corners thawed and allowed the tube to flow. This demonstrates the postulated failure mechanism and indicates that thermally attaching the tube corners to the radiator fin to provide uniform heating of a frozen tube would prevent or reduce the trapping.

The radiator test panels have undergone extensive previous thermal vacuum testing including as many as 17 freeze/thaw cycles. Panels 1 and 2 were tested in February of 1972, all eight panels were included in a checkout test in the VSD simulator in December 1972, and all eight panels were tested in the present Orbiter ATCS (Active Thermal Control System) Development Tests. Panel 1 was not included in the final two phases of this test. Table 19 summarizes the number of freeze/thaw cycles and observed fluid trappings that each panel was exposed to. Since the panel thermocouples were not located such that all traps on all tubes could be recorded, an estimate of the number of traps based on the available measurements has been made. This estimation is also included in Table 19.

4.0 CONCLUSIONS

A series of thermal-vacuum tests have been conducted over a six month period from February through July 1973 in support of the Orbiter ATCS development. Performance data has been obtained for the March 1973 Rockwell baseline radiator configuration as well as detailed design information for application of a wide heat load range modular radiator system to the Orbiter. Two candidate ATCS weight reducing designs have undergone extensive concept verification testing and their system operating characteristics have been determined in sufficient detail for application to the Orbiter. Design information has been obtained for an integrated radiator/water cooling system that provides for vehicle heat rejection as well as water management of the excess fuel cell water. Processing techniques have been developed and verified for the application of a high performance thermal control coating to large radiator areas subjected to a temperature range of -280°F to $+160^{\circ}\text{F}$.

Specific conclusions for each test phase are given in the following paragraphs.

4.1 Phase 1 - MRS Tests

The Phase 1 MRS tests accumulated over 300 hours of panel operation in a thermal vacuum environment with no problems. Performance data has been obtained for Rockwell's baseline system and the alternate two-sided configuration for a variety of known environments and heat loads representative of the shuttle design conditions. Design data for alternate plumbing arrangements, heat load transient capabilities and simulated low α/ϵ coating operation have also been obtained. All test objectives have been met.

The maximum observed baseline system heat rejection was 76,600 BTU/hr obtained in segmented tests, and 52,931 BTU/hr for the alternate system. The minimum observed heat rejection was 8260 BTU/hr for the baseline system and 4163 BTU/hr for the alternate system. The test results indicate the applicability of the MRS to the Shuttle; however several differences between the test and baseline panels should be examined in future testing. These differences include: the panel size, the panel aspect ratio (length to width), and the reach (maximum distance between frozen and non-frozen tubes during low load). It is also recommended that future testing include the effect of backside and edge heat leaks.

The concept of modular radiator panels used to "build" a system to the required area was demonstrated by obtaining operating data for panels plumbed in eight

different series/parallel arrangements with skewed and balanced environments representing eight different situations. Each of the test panels provided the same performance under similar heat loads and environments.

A total of 17 test points were made to collect design data to support detail design of the shuttle radiators. The test data indicates that any convenient plumbing arrangement can be used (up to eight panels in parallel) with only a slight degradation in performance due to low panel flows (laminar flow heat transfer coefficients). The transition between the minimum and maximum heat rejection rates was demonstrated for a variety of series/parallel flow configurations with balanced and unbalanced environments. No unstable flow conditions were observed during any of the tests.

The simulated low α/ϵ coating tests indicates that the MRS should operate satisfactorily with a low α/ϵ coating and that the performance is in the range used in previous heat rejection system weight optimization studies.

Data for thermal model correlation has been obtained by recording total system and individual panel inlet and outlet and tube temperatures, flow rates and pressure drops for approximately 302 hours of testing. Correlation of the test data and thermal model predictions have verified the model use for design and performance studies. The model predictions show excellent agreement with the test data for the high heat load-hot environment conditions; thus indicating that one of the primary objectives of the model (providing good predictions under maximum load design conditions) has been met. The second primary objective of providing good performance predictions under the minimum load design conditions has also been met, although low load correlations were generally not as good as the high load. Careful evaluation of the low load predictions are required to insure that flow instability in parallel flow paths caused by erroneous panel freeze predictions do not cause large errors in system performance. As expected, predictions under conditions in which the majority of the flow is not routed to either the prime or main system are the least accurate, but are considered adequate.

Comparison of predicted and measured panel pressure drops over a wide range of flows and temperatures indicates accurate model predictions and should insure accurate panel flow rate predictions in any panel plumbing arrangement.

4.2 Phase 2 - Integrated System Tests

The integrated concept was tested and generally verified over a wide range of conditions. Although the test was subject to many problematical situations, none

was related to a failure related to the system aspect, i.e., the temperature control system or the water level indicators. The water tank level was maintained within acceptable limits, and heat rejection was in the amounts desired and predicted.

The system response to rapid changes in heat load, and to mission-type cyclic heat load was stable, with the flash evaporator maintaining desired outlet temperature within adequate limits. System operation with the sublimator was not verified. Due to the possibility that the operational problems encountered by the sublimator were caused by facility problems, further testing should be done.

The testing to determine necessity of duct and nozzle heaters resulted in a conclusion that the nozzle heater is not required, but the duct heater is required to prevent ice buildup although the ice buildup is probably in the nozzle throat.

Comparative data for FE and sublimator was acquired on a component level, although the system performance of the sublimator was confused due to facility problems. Again, further testing is indicated.

4.3 Phase 3 - Improved Coatings Tests

Four coatings/adhesives, two silicones and two urethanes, were carried through the test sequence successfully.

There was no damage to any of the panel coatings until the panels were exposed to temperatures below -200°F.

The heat rejection of the panels was nominal for an undamaged silver/FEP coating regardless of the adhesive used.

The most promising adhesives were the silicones, Permacel 6962, and G.E. SR585, which were applied to the silver/FEP Teflon film to form a laminate tape.

The urethanes have the disadvantages of a potentially carcinogenic curing agent and difficult application process.

The laminate adhesives in tape form required a vacuum bag/heat cure to adhere during the cryogenic temperature excursion.

Adhesives with attractive thermal performance properties may be impractical for application to hardware for reasons such as high tack or bubble formation during cure.

4.4 Tube Anomaly Investigation

The test anomaly is understood. Non-uniform thawing of frozen tubes due to unattached tube corners caused sections of the fluid undergoing thermal expansion to be constrained. Repeated thaw cycles and tube deformations resulted in eventual tube failures. The failure was fortuitous in that a new tube design criteria was found

(tube attachment to the radiator fin must be uniform). Analysis indicates that concentric extrusion holes and heat treatment of the tubes will prevent the anomaly even if non-uniform thawing does occur in future designs.

5.0 REFERENCES

1. Tufte, R. J., "Wide Heat Load Range Space Radiator Development", First Intersociety EC/LSS Conference, ASME Paper No. 71-AV-5, July 1971.
2. Dietz, J. B., et.al., "Modular Radiator System Development for Shuttle and Advanced Spacecraft", ASME Paper No. 72-ENAV-34, August 1972.
3. Howell, H. R., "Modular Radiator System Dallas Checkout Test Results", VSD Report No. T169-27, 9 October 1973.
4. James B. Heaney, "Suitability of Metallized FEP Teflon as A Spacecraft Thermal Control Surface", ASME publication 71-AV-35, 1971.

TABLE 1
SIMULATED BASELINE SYSTEM TEST SUMMARY

TEST GROUP	HEAT LOAD 1000 BTU/HR DESIRED	ACTUAL	SIMULATED ORBIT SUN ON	ENVIRONMENT, BTU/HR CAVITY	TOP	SYSTEM HEAT REJECTED 1000 BTU/HR
1.1	80	79.4	CB	0-60 (14.8-59)	130 (135.6)	72.5-68.4
1.2	70	70.5	CB	0-60 (14.8-59)	130 (137.5)	65.7-61.6
1.3	57.7	57.4	CB	3-42 ; 61-0 (31-51);(60-35)	130 (139.2)	50.5 - 48.2
1.4	42	41.6	CB	0-60 (15.6-57.3)	130 (135.8)	39.7 - 29.5
1.5	70	66.8	CAVITY	216-20 ; 20-216 (172-32);(29-153)	30 (35.6)	64.5 - 61.3
1.6	7	9.6	BELLY	70-20 ; 20-70 (56-29) ; (33-59)	20 (24.6)	8.3
1.7	70	72.1	BELLY	0-20 (7-28)	20 (35.6)	69.1

TABLE 2
 EXTRAPOLATION OF TEST DATA TO BASELINE CONFIGURATION

TEST GROUP	TEST POINT	TEST CONDITIONS				TEST RESULTS			SHUTTLE VEHICLE EXTRAPOLATED RESULTS		
		HEAT LOAD	PORTION OF SYS SIMULATED	ORBIT (SUN ON)	AVERAGE SYS. TOTAL HEAT REJ.	TOP OF CARGO BAY DOOR Q _{REJ}	CAVITY Q _{REJ}	TOP CBD Q _{REJ}	CAVITY Q _{REJ}	AVERAGE SYS TOTAL Q _{REJ}	
1.1	1A,5	79.4	1/2	CB	71.8	25.0	10.9	22.4	15.5	76.6	
1.2	1,5	70.5	1/2	CB	63.6	20.9	10.9	18.7	15.5	68.4	
1.5	10,11 & 10,12	55.0	1/2(Each ca- vity tested separately)	Cavity (Const Env.)	55.0	64.6	-13.6/ 4.3	57.8	-19.4/ 6.1	44.5	
	10,14	62.8	Full	Cavity (Const Env.)	58.5	66.6	-11.4/ 3.3	52.2	-16.2/ 4.7	40.7	
	10,14A	61.3*	Full	Cavity (Cyclic Env.)	61.3	67.4	-10.4/ 4.3	54.6	-14.8/ 6.1	45.9	

All Values In 1000 BTU/HR

* Outlet Control Point = 49°F

TABLE 3 TWO SIDED RADIATION TEST SUMMARY

Test Group	Test Point	AVERAGE ENVIRONMENTS				TEST CONDITIONS				TEST RESULTS			
		DESIRED PANELS 1-4	ACTUAL PANELS 1-4	DESIRED PANELS 5-8	ACTUAL PANELS 5-8	INLET TEMPERATURE °F	TOTAL FLOW LB/HR	IMMEDIATE HEAT LOAD BTU/HR	OUTLET TEMPERATURES °F	Actual	Predicted	Actual	Predicted
2.1	21	160	160.79	160.79	163.2	2200	2212	70K	74 78	74 78	51670	49426	
		133-158	171-130	170.3 161.6	162.7 162.3	2200	2201	70K	66.8 71 72	70.6 101.1	55570 53529	52931 51196	
2.2	23	133-158	171-130	169 159.4	141.3 128.3	2200	2212	57.7K	64.7 58.7	64.7 58.7	46473 44363	43289 41620	
		133-158	171-130	166 155.2	116.5 125.5	2200	2214	42K	57.2 72.7	57.2 72.7	33344 33135	33508 32339	
2.2	25	133-158	171-130	152.3 124.8	95.3 124.8	2200	2202	31K	47 60.1	51.2 61.7	27104 24850	25229 23552	
		174	70	168.8	67.3	2200	2201	42K	40.9 57.8	44.8 49	41910	39990	
2.3	27	174	70	171.5	67.2	2200	2227	70K	55.5 85.2	59.5 57.4	61736	61255	
		174	70	167	68.5	2200	2238	7K	0.2 51.1	8.7 46.9	7500	3375	
2.4	61	22-40	40-22	31.5-39.4 25.4	53 46.3	2200	2206	7K	-122.3 49.2	-126.5 48.2	6987 6837	4163 4754	
		59.5- 171.5	59.5- 171.5	57.0- 167.5	163.6	2200	2214	70K	70630	14.2 145	75 75	51782 70830	
2.4	63	23.3- 156.4	23.3- 156.3	31.9- 151.5	164.6 151.5	2200	2294	70K	70864	-4.9 150.6	73.0 111.0	53100 70864	
		51.4- 171.5	12.4- 73.2	49.7- 170.5	162.7 71.1	2200	2212	70K	70024	0.8 147.8	57.0 121.0	60678 70024	

TABLE 4

SUMMARY OF SET POINT CHANGES
(TWO-SIDED RADIATION)

TEST GROUP	TEST POINT	SET POINT (°F)	AVERAGE ENV. (BTU/HR FT ²)	INLET TEMP (°F)		FLOW RATE (LB/HR)		OUTLET TEMP (°F)		HEAT REFLECTED (1000 BTU/HR)	
				MAIN	PRIME	MAIN	PRIME	MAIN	PRIME		MIXED
2.5	57	40	3.8	59.3	53	134	1945	-137	50	40.6	7.56
	58	50	2.9	-18	52.3	5.7	2010	-125	50	50	12.78
2.6	60	40	3.7	59.3	53	136	1919	-132	50	40.6	7.48
	51	40	12.7	159	157.6	1379	884	-38	149	39.5	69.51
	52	50	7.6	113	113	647	1557	-109	109	50	35.67
2.7	52A	50	5.0	73	75	275	1881	-157	72	46.9	16.15
	52B	40	5.2	73	75	337	1881	-157	72	40.6	19.48
	52C	50	4.9	72.5	75.7	243	1984	-159	72	50	14.95
	52D	70	3.3	56	74	22.9	1958	-157	71	70	2.61
	52E	40	5.2	73	74.3	385	1868	-139	71	39.5	20.62
2.8	53	70	121.8/10.65	163.3	133.7	970	1273	-19	130	67.9	45.66
	54	40	126.6/14.1	163	155.5	1950	275	24	137	40.6	70.53
	55	50	126.4/14.2	164	162	1727	510	16	151	50	66.51
	56	70	122.7/10.5	163	134.3	957	1273	-20	130	68.9	45.44
	59	40	126.8/14.6	163.2	154	1975	266	26	135	39.5	70.50

TABLE 5
SUMMARY OF HEAT LOAD TRANSIENT TEST POINTS

TEST GROUP	TEST POINT	AVG. ENVIRONMENTS BTU/HR	INLET TEMP RANGE - °F	MAIN OUTLET TEMP. RANGE - °F	HEAT REJECTION RANGE-BTU/HR
3.4	47	125.4 (Panels 1-4) 7.3 (Panels 5-8)	51.6/160./50.5	-8.3/27.9/8.7	6248/67786/5654
	19	Variable (12.9-171)*	162.7/52.1/161.6	72/17.4/72	67860/6495/67596
	50	10.5 (Panels 2,3,5 & 6)	45.6/162.7	4.2/89.0	2789/43530
3.5	17A-18	26.2(Panels 1,3,5,7) 5.5(Panels 2 & 4)	47.9/154.3	-152.3/-64.2	1580/12412
	36-36A	13.5	47.9/164.6	-146.5/-22.2	2668/36049
	60 - 51	3.7/12.7	53/159	-130.5/-35.0	7178/69373

* Panels 2, 6, 7 and 8 environments not known exactly due to degraded insulation blanket configuration.

TABLE 6
SUMMARY OF SIMULATED LOW α/ϵ COATING TESTS

TEST GROUP	TEST POINT	FLOW CONFIGURATION	AVERAGE ENVIRONMENT (BTU/HR FT ²)	ACTUAL AREA FT ²	SIMULATED AREA FT ²	HEAT LOAD BTU/HR	HEAT REJECTED (BTU/HR)	CALCULATED WATER BOILING REQUIRED (LB/HR)
3.6	31	Y - 1,3	58.6	432	512 (half of system)	74,012	67,392	6.62
			2,4,5					
			6,7,8					
36	36	Y - 1,3	4.2	432	512	5,336	5,336	-
			2,4,5					
			6,7,8					
36A	36A	Y - 1,3	14.8	432	512	72,098	72,098	-
			2,4,5					
			6,7,8					
3.7	2	α	60.2-65.2	576	682	66,803	51,265 -	14.08
			2,3,4					
			6,7,8					

TABLE 7 STEADY STATE CORRELATION TEST POINTS

LOAD	CONDITIONS		NO. OF SIDES RADG.	TEST POINT	FLOW CONFIG.	INLET TEMP.		FLOW		PANEL ENVIRONMENT							
	ENVIRON.					MAIN	PRIME	MAIN	PRIME	1	2	3	4	5	6	7	8
High	Hot		1	1A	α	178.3	91.5	1094.	13.2	135.	136.6	133.6	135.6	136.4	136.6	135.4	135.5
			1	45	ε	160.8	128.7	2198.	16.	129.4	129.	130.1	128.9	128.3	127.2	129.3	128.1
			1	32	γ	165.25	111.5	2223.	47.1	130.5	129.3	130.8	130.2	129.1	128.5	130.8	129.6
			1	4	α	116.	86.	1106.	13.4	132.6	140.5	135.5	134.7	134.5	139.5	134.9	134.4
High	Cold		1	10	1/2 α	163.6	161.8	283.	268.	45.1	-	34.8	30.			32.6	
			1	51	γ	159.	158.5	1379.	884.	16.5	16.8	8.8	9.2	16.0	16.3	9.0	9.1
Low	Cold		1	17	1/2 α	55.3	53.2	17.1	549.	28.8		26.6	21.2			21.8	
			1	17A	β	51.6	52.6	11.6	1169.	26.4	5.1	25.1	3.4	22.0		21.7	
			1	36	γ	57.7	53.5	52.	1053.		4.8		2.9	4.8	4.6	3.0	3.1
High	Skewed		2	53	γ	164.1	134.25	974.	1268.9	126.5	125.7	120.7	114.2	14.	14.	7.4	7.2
			2	54	γ					130.2	128.6	124.1	123.4	17.5	17.6	10.7	10.6
			2	55	γ					129.9	128.2	123.7	123.8	17.6	18.2	10.5	10.5
			2	56	γ					124.8	124.8	119.8	121.5	13.9	13.7	7.3	7.0
			2	59	γ					130.2	128.6	124.1	123.4	17.5	17.6	10.7	10.6
			1	49	γ	100.	89.5	2161.	44.8	127.5	128.4	29.5	29.5	128.8	129.3	78.2	75.
Low	Skewed		2	27	γ	164.6	114.5	2200.	16.4	170.	170.	172.	174.	66.	67.	68.8	67.
			1	14	α	18.4	152.4	1615.	626.	30.	180.	30.	180.	30.	30.	30.	30.
Low	Skewed		1	47	α	49.5	51.5	111.	988.	126.2	126.6	125.	129.6	5.8	2.8	3.5	2.95

TABLE 8
HEAT REJECTION
TEST POINT α 1A

BTU/HR

<u>PANEL</u>		<u>PRIME</u>	<u>MAIN</u>	<u>TOTAL</u>
1	Predicted Test	4.4 -23.9	5540.3 6100.5	5544.7 6076.6
2	Predicted Test	0.8 5.3	1209.5 991.1	1210.3 996.4
3	Predicted Test	3.8 8.9	3492.7 3064.5	3496.5 3073.4
4	Predicted Test	2.0 1.8	1997.1 1863.5	1999.1 1865.3
5	Predicted Test	3.7 -26.7	5481. 5776.2	5484.7 5749.5
6	Predicted Test	1.2 9.7	1175.4 984.6	1176.6 994.3
7	Predicted Test	3.3 11.4	3337. 3241.2	3340.3 3252.6
8	Predicted Test	2.3 -1.6	1941.5 1996.	1943.8 1994.4
<u>SYSTEM</u>				
	Predicted Test	21.1 38.4	24126.4 24245.6	24147.5 24284.

TABLE 9
HEAT REJECTION
TEST POINT y 51

		BTU/HR		
<u>PANEL</u>		<u>PRIME</u>	<u>MAIN</u>	<u>TOTAL</u>
1	Predicted	535.0	11111.6	11646.6
	Test	264.6	11536.2	11800.8
2	Predicted	534.0	11102.8	11636.8
	Test	440.3	10802.5	11242.8
3	Predicted	518.5	5577.5	6096.
	Test	233.6	5431.9	5665.5
4	Predicted	519.4	5561.3	6080.7
	Test	58.2	5079.8	5138.
5	Predicted	537.9	11234.0	11771.9
	Test	231.8	11499.6	11731.4
6	Predicted	537.9	11225.1	11763.
	Test	166.2	11499.6	11665.8
7	Predicted	516.1	5578.9	6095.
	Test	229.7	5776.0	6005.7
8	Predicted	516.1	5653.	6169.1
	Test	303.8	5583.7	5887.5
<u>SYSTEM</u>				
	Predicted	4207.8	66791.0	70998.8
	Test	1969.4	66400.0	68369.4

TABLE 10
HEAT REJECTION

TEST POINT α 17

BTU/HR

<u>PANEL</u>		<u>PRIME</u>	<u>MAIN</u>	<u>TOTAL</u>
1	Predicted Test	135.3 0.0	571.4 551.	706.7 551.
2	Predicted Test			
3	Predicted Test	135.3 715.8	49.8 10.2	185.1 726.
4	Predicted Test	148.6 134.8	73.8 27.4	222.4 162.2
5	Predicted Test			
6	Predicted Test			
7	Predicted Test	135.1 0.0	-3.9 -7.4	131.2 -7.4
8	Predicted Test			
<u>SYSTEM</u>				
	Predicted Test	553.7 850.8	691. 424.4	1244.7 1275.2

TABLE 11
HEAT REJECTION

TEST POINT Y 53

BTU/HR

<u>PANEL</u>		<u>PRIME</u>	<u>MAIN</u>	<u>TOTAL</u>
1	Predicted	311.3	6316.2	6628.2
	Test	103.0	6593.7	6696.7
2	Predicted	311.3	6343.9	6655.2
	Test	53.6	6472.7	6526.3
3	Predicted	297.4	2193.6	2491.0
	Test	123.6	1898.5	2022.1
4	Predicted	314.5	2371.6	2686.1
	Test	90.7	2069.3	2160.0
5	Predicted	484.3	9517.8	10002.1
	Test	200.1	9257.2	9457.3
6	Predicted	484.3	9517.8	10002.1
	Test	111.2	9976.3	10087.5
7	Predicted	466.7	4002.3	4469.0
	Test	44.3	3761.1	3805.4
8	Predicted	466.7	4008.1	4474.8
	Test	-536.5	3996.4	3459.9
<u>SYSTEM</u>				
	Predicted	3157.3	44007.0	47164.3
	Test	945.9	43911.3	44857.2

TABLE 12
HEAT REJECTION
TEST POINT α 14
BTU/HR

<u>PANEL</u>		<u>PRIME</u>	<u>MAIN</u>	<u>TOTAL</u>
1	Predicted Test	307.5 234.3	2951.5 2245.7	3259. 2480.
2	Predicted Test	43.2 -170.8	-1982.9 -1910.	-1939.7 -2080.8
3	Predicted Test	296. 404.3	2394.6 2133.3	2690.6 2537.6
4	Predicted Test	52.1 170.8	-6393.5 -6189.8	-6341.4 -6019.
5	Predicted Test	306.5 159.9	2953.8 2347.5	3260.3 2507.4
6	Predicted Test	282.8 262.1	1428.2 1354.9	1711. 1617.
7	Predicted Test	296.2 415.2	2405.8 3787.	2702. 4202.2
8	Predicted Test	336.7 -8.8	3726. 1807.7	4062.7 1798.9
<u>SYSTEM</u>	Predicted Test	1910.9 2445.	4168.6 2054.3	6079.5 4499.3

TABLE 13
CALCULATED HEAT REJECTION

TEST POINT	HEAT REJECTION (BTU/hr)			TOTAL
	RADIATOR PRIME TUBES	RADIATOR BANK TUBES	EVAPORATOR/SUBLIMATOR	
1	1,022	50,330	14,630	65,982
2	229	52,600	14,680	67,509
3	49	48,620	14,400	63,069
4	111	32,570	9,817	42,498
5	-42	13,990	163	14,111
6	-29	9,005	- 324	8,650
7	746	13,470	594	23,813
8	690	13,310	2468	16,468
9	1,073	4,033	4,961	10,067
10	1,284	3,103	14,320	18,707
11	1,011	26,850	719	28,580
12	420	41,110	6,539	48,069
13	1,145	48,380	15,260	64,785
14	-1,232	681	6,410	5,859
15	207	40,810	12,470	60,570
16	913	33,710	5,238	39,862
17	212	29,890	6,210	36,312
18	61	40,090	6,494	46,645
19	564	28,310	4,743	33,617
20	-15	48,710	7,577	56,272
21	418	44,620	15,150	60,188

TABLE 13 (cont'd)

CALCULATED HEAT REJECTION

TEST POINT	HEAT REJECTION (BTU/hr)			TOTAL
	RADIATOR PRIME TUBES	RADIATOR BANK TUBES	EVAPORATOR/ SUBLIMATOR	
22	1,579	29,910	14,120	45,609
23	- 71	15,980	15,110	31,019
24	306	28,770	15,640	44,716
25	- 189	31,070	11,820	42,701
26	- 260	16,310	6,931	22,981
27	1,494		17,840	
28	5,903	27,030	9,313	42,246
29	553	39,690	10,640	50,883
30	210	37,460	12,660	50,330
31	1,461	66,080	10,160	77,701
32				
33				
34	545	23,910	14,190	38,545
35	988	41,490	15,430	57,908
36				

TABLE 14 PEEL STRENGTHS OF SILVER/FEP
TEFLON BONDED TO 6061-T6 ALUMINUM ADHEREND
VSD DATA

ADHESIVE IDENTIFICATION	PEEL STRENGTH lb/in*	PEEL STRENGTH lb/in(avg. of 4)
RTV560, surface prep: wet sand/ 180 grit Al ₂ O ₃ , MEK wet wipe, wipe dry	1.65	1.81
	1.90	
	2.00	
	1.70	
RTV560, surface prep: Penn Walt841	1.70	1.76
	1.85	
	1.90	
	1.60	
Emerson & Cuming #6 surface prep: wet sand/180 grit Al ₂ O ₃ , MEK wet wipe, wipe dry	2.35	2.35
	2.30	
	2.40	
	2.35	
Permacel 6962 surface prep: wet sand/180 grit Al ₂ O ₃ , MEK wet wipe, wipe dry; overlay removed before cure	0.76	0.76
	0.76	
	0.78	
	0.74	
Permacel 6962, surface prep: wet sand/180 grit Al ₂ O ₃ , MEK wet wipe, wipe dry; cured with overlay on FEP	0.8	0.8
	0.8	
	0.8	
	0.8	

Test Temperature: 75°F

*Federal Test Method Std. #175, Method 1041.1

TABLE 15 OUTGASSING DATA FOR ADHESIVES

TML : TOTAL MASS LOSS
 VCM : VOLATILE CONDENSABLE MATERIAL
 CONDITIONS : TML @125°C, 24 hrs, 1 x 10⁻⁶TORR
 VCM @125°C, 25°C CONDENSING SURFACE

MATERIAL	TYPE	SUPPLIER	CURE INFORMATION	SILVER/FEP TEFLON/ADHESIVE/ALUMINUM			ADHESIVE ONLY					
				Original Adhesive Weight (g)	WE (g)	Original Adhesive Weight (g)	VCM %	CURE INFORMATION	TML %	VCM %		
1. Mystic A117 with AP-134	Silicone	NASA-LaRC		0.1383	4.31(a)	0.1626	0.00583	0.1626	0.23(b)			
2. RTV 560	Silicone	VSD		0.2010	3.94	0.1567	.00791	0.1567	2.12(c)			
3. Permacel 6962	DBL Backed Tape Silicone/Kapton	VSD		0.1133	1.64	0.2221	.00186	0.2221	0.56(d)			
4. 6-401903	Polyester	Schjeldahl		0.040863	1.60	0.040863		0.040863	0.25(e)			
5. DC 282	Silicone	Schjeldahl		0.102159	0.57	0.102159	.00058	0.102159	1.24(f)			
6. Solithane 113 50% Resin 113 50% C113-300	Urethane	NASA-LaRC	Resin Deg. @60°C, In Vac							0.29	0.03	
7. Crest 7343/7139	Urethane	NASA-LaRC(g)								-0.39	-0.09	
8. RTV 566	Silicone	LaRC/VSD(h)								1.41	0.17	
9. E/C CPC-6	Urethane	VSD(i)								0.23	.030	
10. Adiprene L-167	Urethane	VSD								5.78	2.01	
11. Adiprene L-100 /MOCA 100/10 by weight	Urethane	NASA-6SFC								3.23	0.97	
12. SR 537	Silicone	MDAC(k)								7 da @ RT	1.15	0.15
13. SR 585	Silicone	MDAC(l)								3 hr @ 100°C	1.06	0.06
Mystic 7366	DBL Backed Tape Silicone/Kapton	--								+50%Toluene	10.37	5.09
Stycast 2651	Epoxy	JSC								72 hrs @55°C in vacuo	1.3	0.94
Epon 828	Epoxy	JSC								8 hr @ 25°C	0.37	0.03
Crest 7344/7119	Urethane	--								3 da @ 25°C	0.505	0.012
										21 da @ RT	2.78	0.66

NOTES: (a) TML ok, run after bearing surf clean; (b) VCM Quest. (Run L); (c) Sample delaminated; (d) Good data; (e) Good data; (f) below inst-capab; (g) Unrec; (h) Contingency-unrec; (i) In Test; (j) Questionable; (k) Unreceived; (l) Unreceived

TABLE 16 SILVER/FEP TEFLON ADHESIVE SUMMARY

MR PANEL NO.	ADHESIVE NAME (VENDOR)	ADHESIVE TYPE	SIZE OF COATING STRIPS	ADHESIVE APPLICATION TECHNIQUE	ADHESIVE CURE TECHNIQUE
2	RTV 560 (G.E.)	Silicone	48" 15" 4" 1"	2 part mix; trowel/ brush	ambient temp./pressure for 16 hours minimum
3	SR 585 (G.E.)	Silicone	3"	transfer laminate (tape)	275°F for 0.5 hours in vacuum bag
4	6401903 (Schjeldahl)	Polyester	4"	transfer laminate; heat gun for initial adhesion	250°F for one hour in vacuum bag
5	6962 (Permacel)	Silicone Double-backed Kapton	4-1/2"	transfer laminate (tape)	290°F for 1 hour in vacuum bag
6	7343 (Crest)	Urethane	12" 48"	2 part mix; hot melt catalyst/hot resin	ambient temp/pressure, plus 150°F for 8 hours
7	A117 (Mystic)	Silicone	12"	1 part contact cement; both surfaces coated	225°F for four hours in vacuum bag

TABLE 16 SILVER/FEP TEFLON ADHESIVE SUMMARY (CONTINUED)

NR PANEL NO.	ADHESIVE NAME (VENDOR)	ADHESIVE TYPE	SIZE OF COATING STRIPS	ADHESIVE APPLICATION TECHNIQUE	ADHESIVE CURE TECHNIQUE
8	Adiprene L-100 (DuPont)	Urethane	48"	2 part mix; hot melt catalyst/hot resin	ambient temperature for 16 hours
	Adiprene L-167 (DuPont)	Urethane	15"	2 part mix; ambient catalyst/resin	ambient temperature/ pressure for 16 hours

NOTE: Subsequent to adhesive cure, each panel subjected to outgassing cycle consisting of 150°F for 8 hours in a circulating air oven.

TABLE 17

OUTLET TEMPERATURE DATA

MIXED OUTLET TEMPERATURE FROM EACH PANEL, °F
 FOLLOWING EACH HEAT LOAD TRANSIENT

PANEL	Phase 4 Baseline Performance Point No.								Phase 3A Baseline Performance Point No.		
	1	2	3	4	5	6	7	8	1	2	3
2 RTV 560 (VSD)	68	68	68	69	67	67	68	71	17.4	26.9	30.1
3 SR585 (MDAC)	82	82	82	84	82	82	83	84	42.7	39.5	-
4 G401903 (Schjel)	57	57	89	90	89	88	91	109	32.2	33.2	-
5 Permace1 6962 (VSD)	65	65	65	66	64	64	65	68	33.2	44.8	-
6 Crest 7343 (LaRC)	63	62	76	77	78	77	78	86	25.8	1.9	-
7 Mystic A117 (LaRC)	57	57	57	58	57	56	58	60	8.7	21.6	-
8 Adiprene (VSD/GSFC)	51	51	51	52	50	50	51	53.2	5.3	-	.3

TABLE 18 CONDITION OF SILVER/FEP TEFLON THERMAL CONTROL COATING

Solar absorptance of as-received silver/FEP teflon = 0.050-0.085

MR PANEL NO.	ADHESIVE NAME (VENDOR-TYPE)	CONDITION OF COATING AS-BONDED	CONDITION OF COATING POST-TEST (SOLAR ABSORPTANCE)
2	RTV560 (G.E.-silicone)	Spotty delamination in both original bond and refurbished areas	75% delaminated between silver and FEP. 4 square feet of FEP separated completely from panel ($\alpha = 0.06-0.22$)
3	SR585 (G.I.-silicone)	Excellent	no apparent change ($\alpha = 0.06-0.07$)
4	G-401903 (Schjeldahl-polyester)	Excellent	98% of FEP separated completely from silver which remained bonded to the panel ($\alpha = 0.06-0.07$)
5	6962 (Permacel-silicone)	Excellent	no apparent change except 3 square inches lost adhesion to aluminum ($\alpha = 0.06-0.08$)
6	7343 (Crest-urethane)	Many bubbles in adhesive	complete separation of FEP from silver in mid-region of panel. No apparent separation in inlet and outlet regions. Possible batch mixing variation ($\alpha = 0.06-0.08$)
7	A117 (Mystic-urethane)	Many folds, wrinkles, creases in FEP film	90% failure at aluminum-adhesive bond line. 7 square feet of silver/FEP intact along "warm" inlet manifold. ($\alpha = 0.05-0.06$)
8	L-100, L-167 (DuPont-urethane)	Many bubbles in adhesive; ripples in L-100 bond area	no apparent change ($\alpha = 0.06-0.07$)

TABLE 19 SUMMARY OF PANEL FREEZE THAN HISTORY

PANEL	NO. FREEZES	NO. TRAPS OBSERVED	NO. TRAPS ESTIMATED
1 Upper	7	4	6
1 Lower	5	2	3
2 Upper	2	1	1
2 Lower	17	2	4
3	13	3	3
4	14	1	3
5	15	5	6
6	15	3	4
7	14	4	4
8	14	3	3

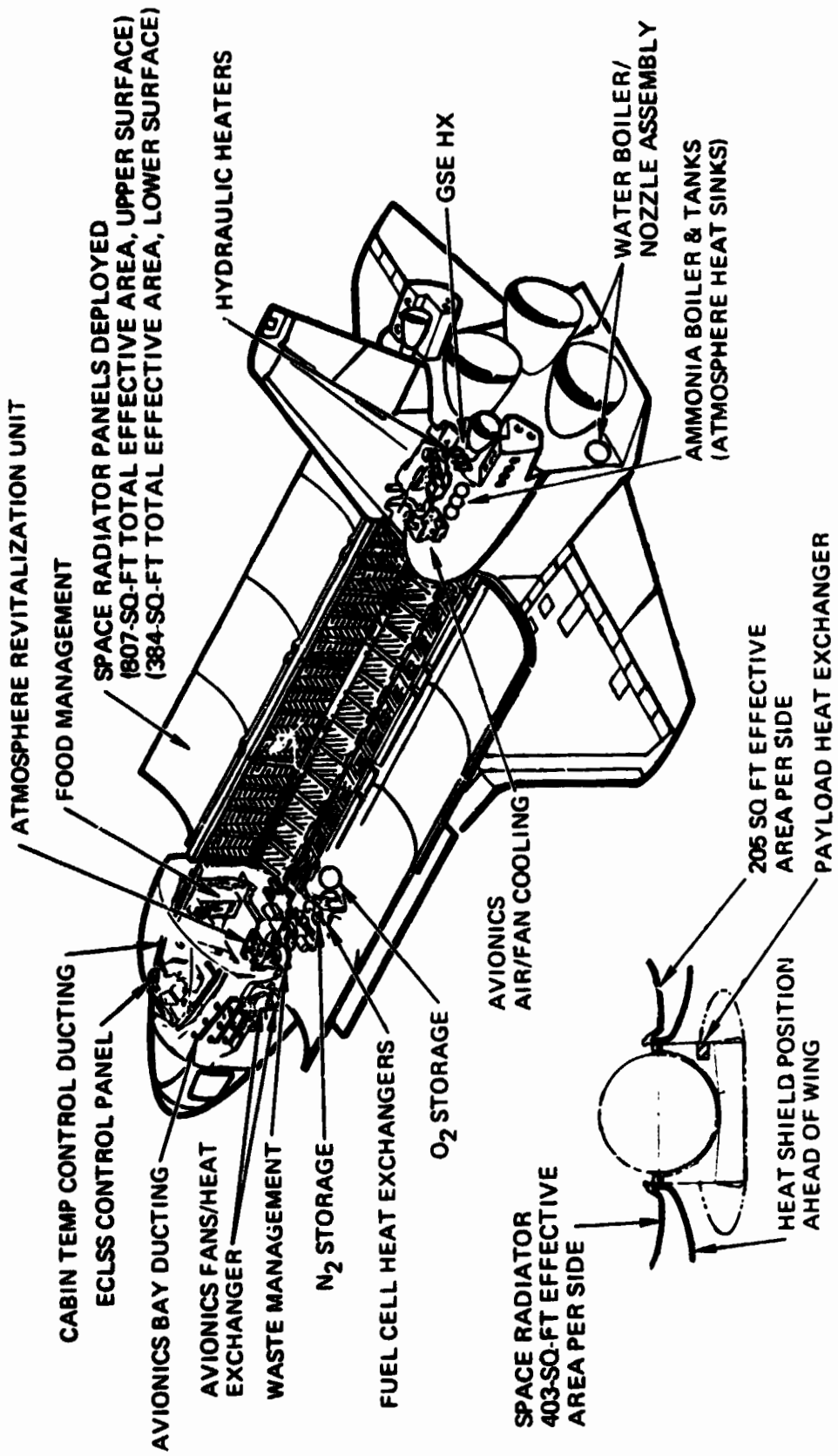


FIGURE 1 ORBITER ATCS COMPONENTS

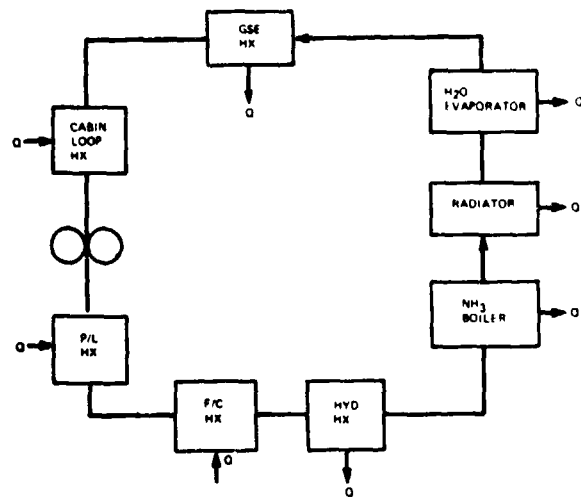


FIGURE 2 SIMPLIFIED ATCS SCHEMATIC

REPRODUCIBILITY OF THE ORIGINAL PAGE IS POOR

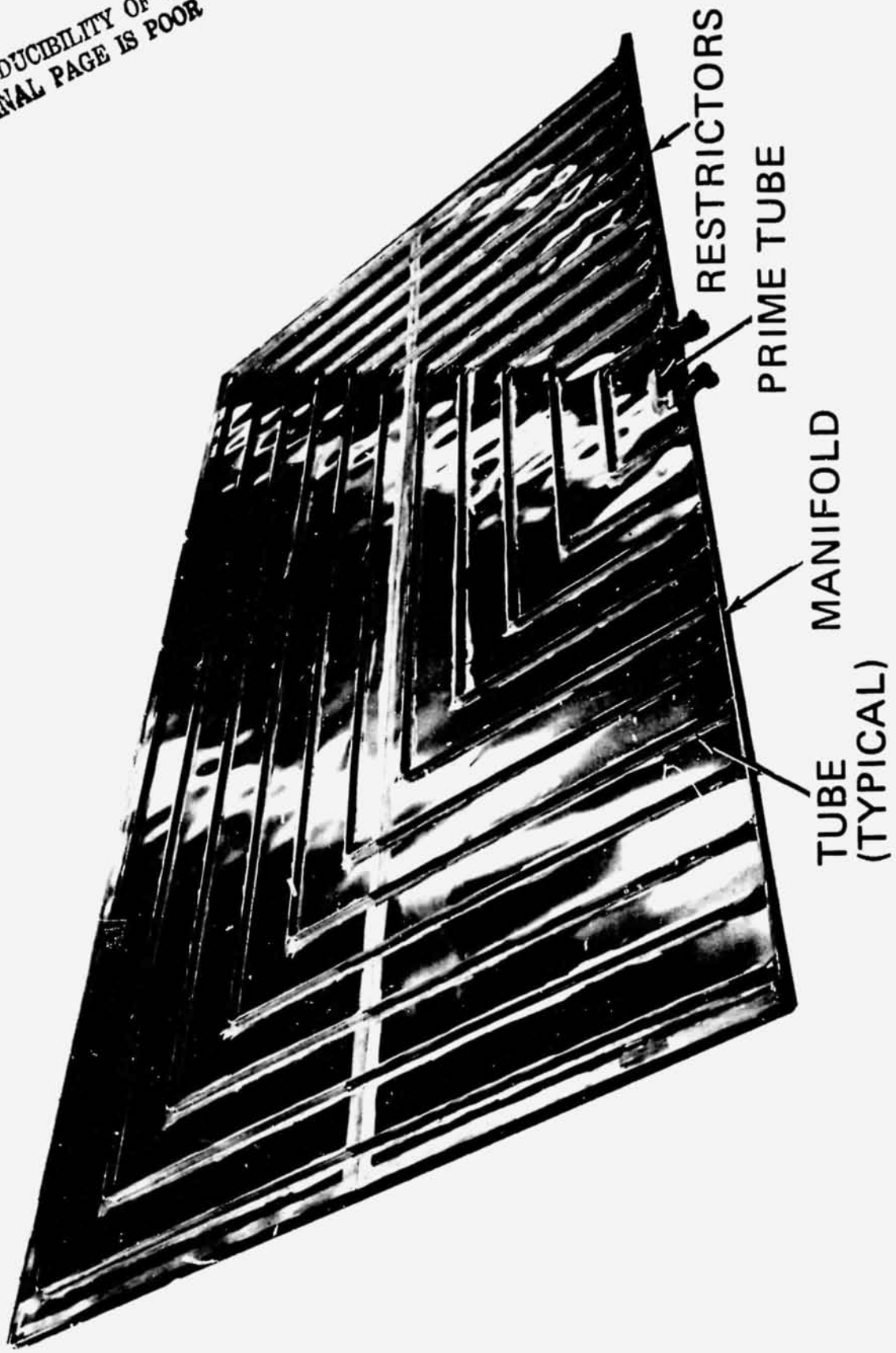
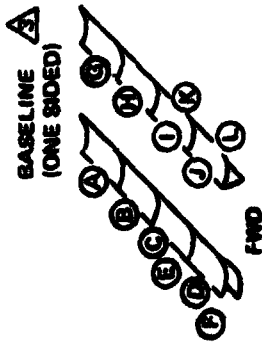
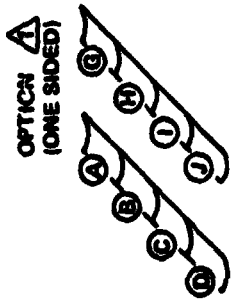
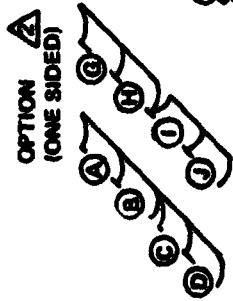
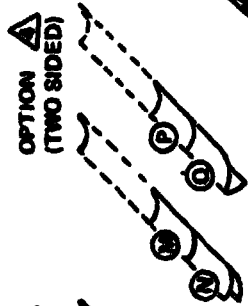
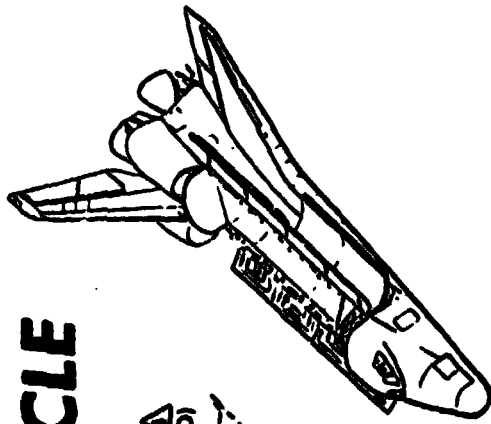


FIGURE 3 MODULAR RADIATOR PANEL TUBE ARRANGEMENT

FIGURE 4 SHUTTLE CONFIGURATIONS SIMULATED BY TEST ARTICLE



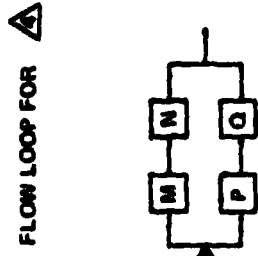
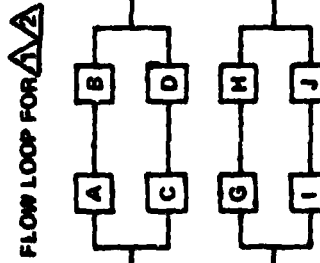
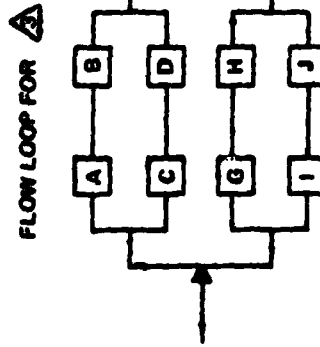
EFFECTIVE AREA FT²

1064 UP
372 DOWN
1436 TOTAL

1064 UP

1064 UP

532 UP
372 DOWN
904 TOTAL



NOTES:
 Δ ANALYSIS CONFIGURATION
 ⊗ SHUTTLE PANEL (LETTER)
 EFFECTIVE PANEL AREAS FT²
 ABCDGHJ 133 UP
 EFKL 93 DOWN
 MNPO 228 (133 UP, 93 DOWN)

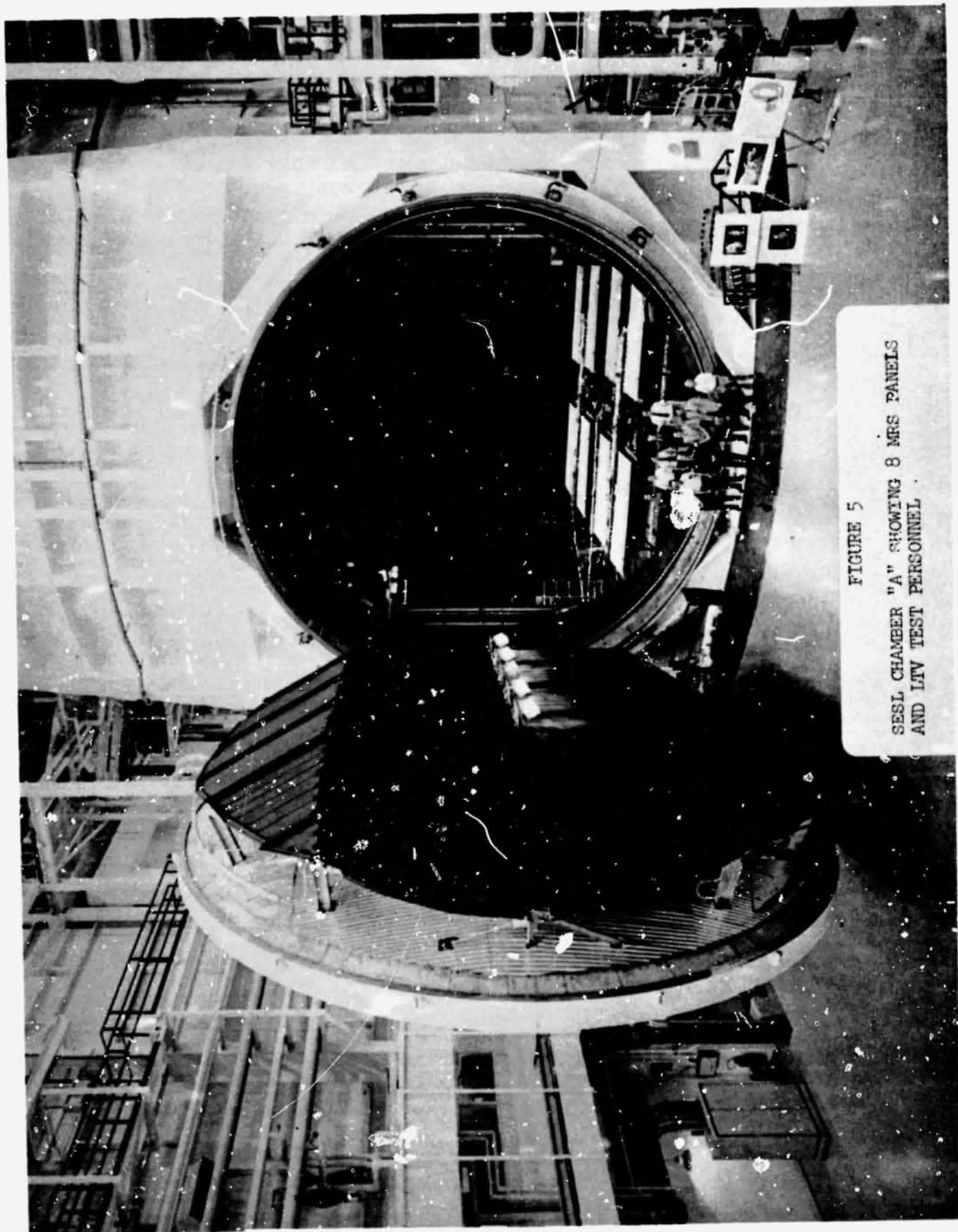


FIGURE 5
STEEL CHAMBER "A" SHOWING 8 MRS PANELS
AND LTV TEST PERSONNEL

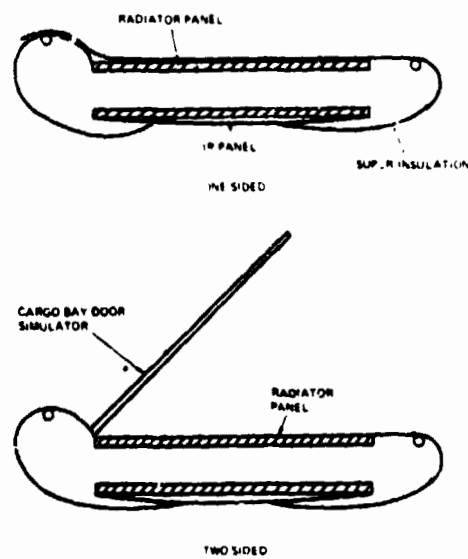
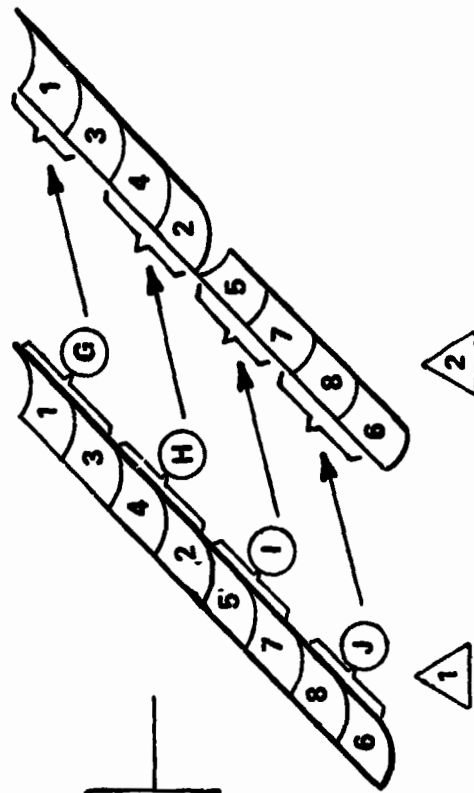


FIGURE 6 DETAIL OF INSULATION ON PANELS AND ENVIRONMENT SIMULATOR

FIGURE 7
FLOW LOOP α



EFFECTIVE AREAS

TEST

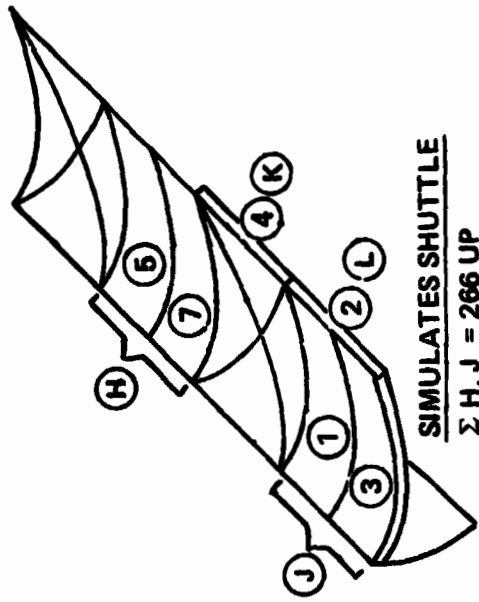
$\Sigma (1 \rightarrow 8) = 8 \times 72 = 576 \text{ FT}^2$

SIMULATES SHUTTLE

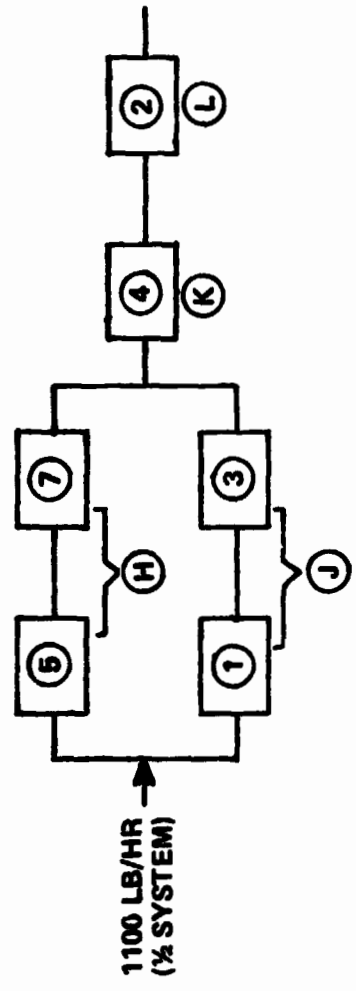
$\Sigma (G \rightarrow J) = 4 \times 133 = 532 \text{ FT}^2$

DATA FOR POINTS Δ AND ∇ WILL BE USED AS INLET TEMPERATURES IN OTHER TESTS

FIGURE 8
FLOW LOOP β



SIMULATES SHUTTLE
 Σ H, J = 266 UP
 Σ K, L = 186 DOWN
452 TOTAL

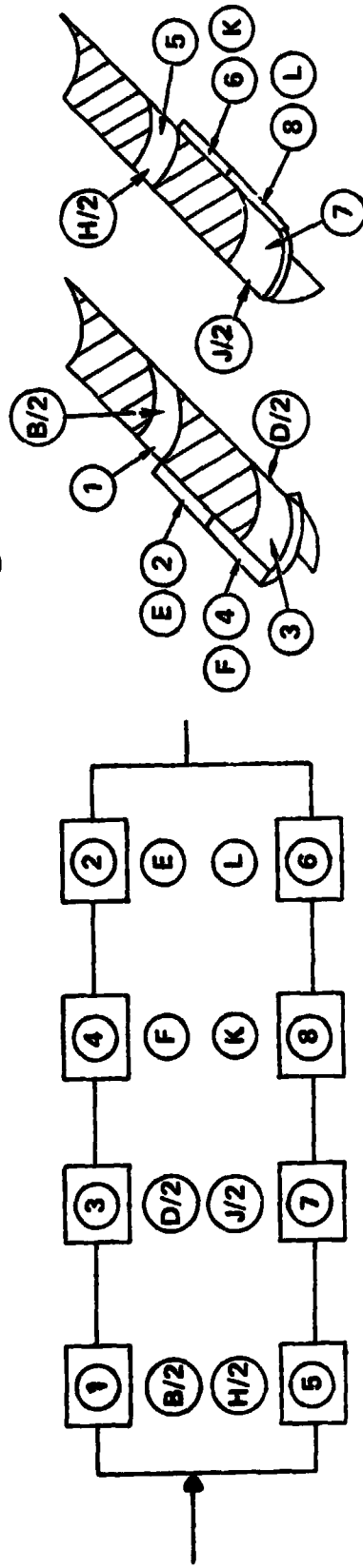


1100 LB/HR
 (1/2 SYSTEM)

TEST
 Σ 5, 7, 6, 8 = 288 UP
 Σ 4, 2 = 144 DOWN
432 TOTAL

FIGURE 9.

FLOW LOOP $\alpha 3$



SIMULATES SHUTTLE

Σ B/2, D/2, H/2, J/2 = 266 UP
 Σ E, F, K, L = 372 DOWN
 638

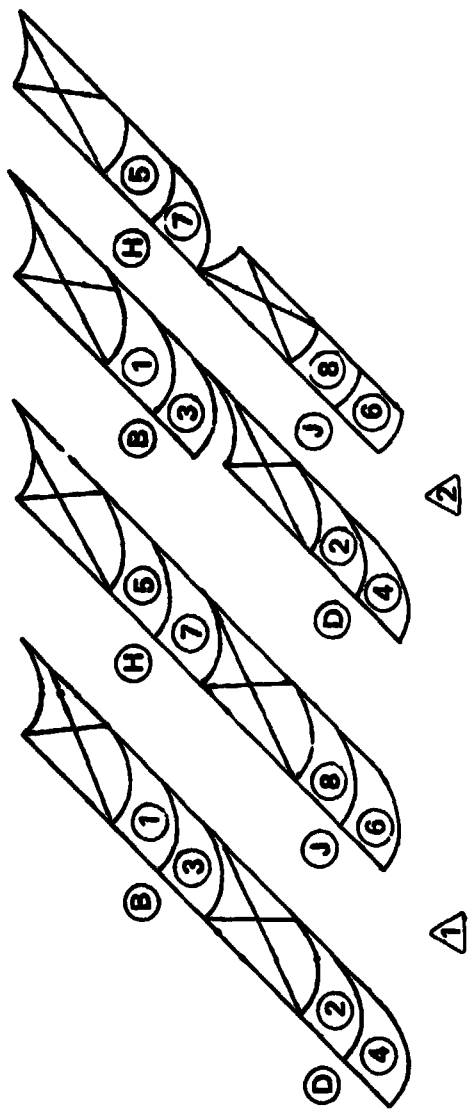
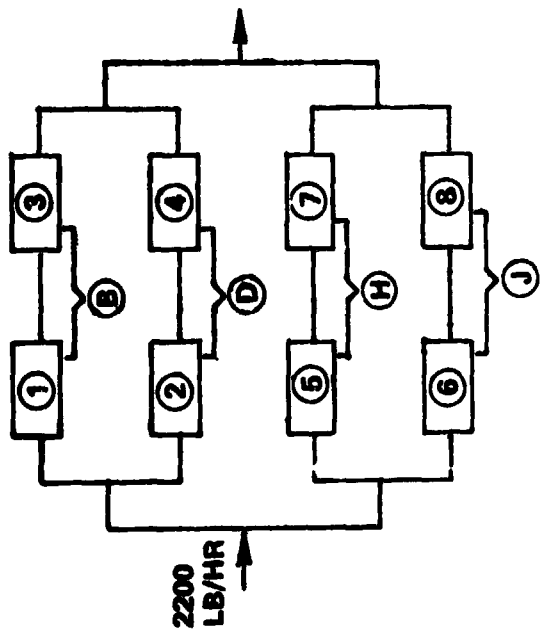
EFFECTIVE AREAS:

TEST

Σ 1, 3, 5, 7 = 288 UP
 Σ 2, 4, 6, 8 = 288 DOWN
 576

FIGURE 10

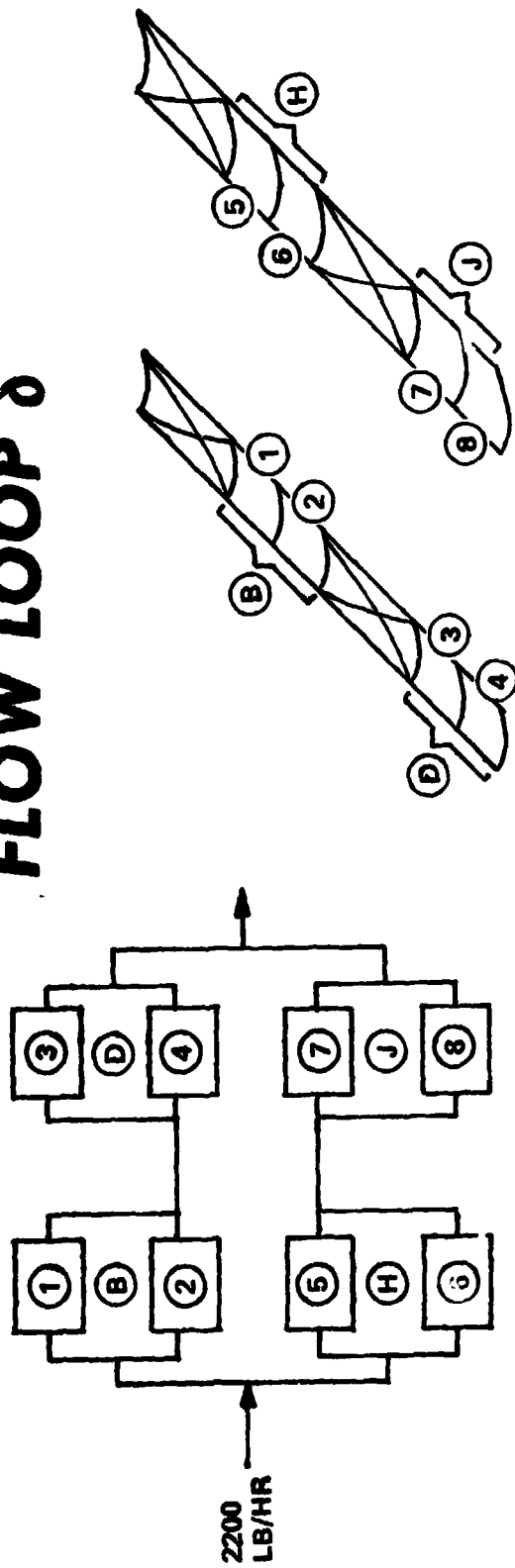
FLOW LOOP Y



TEST SIMULATES SHUTTLE
 $\Sigma (1 \rightarrow 8) = 8 \times 72 = 576 \text{ FT}^2$ $\Sigma B, D, H, J = 4 \times 133 = 532 \text{ FT}^2$

EFFECTIVE AREAS

FIGURE 11
FLOW LOOP δ



EFFECTIVE AREAS:

$$\frac{\text{TEST}}{\Sigma \textcircled{1} \rightarrow \textcircled{8}} = 576 \text{ FT}^2$$

$$\frac{\text{SIMULATED SHUTTLE}}{\Sigma \textcircled{B}, \textcircled{D}, \textcircled{H}, \textcircled{J}} = 532 \text{ FT}^2$$

FIGURE 12

FLOW LOOP €

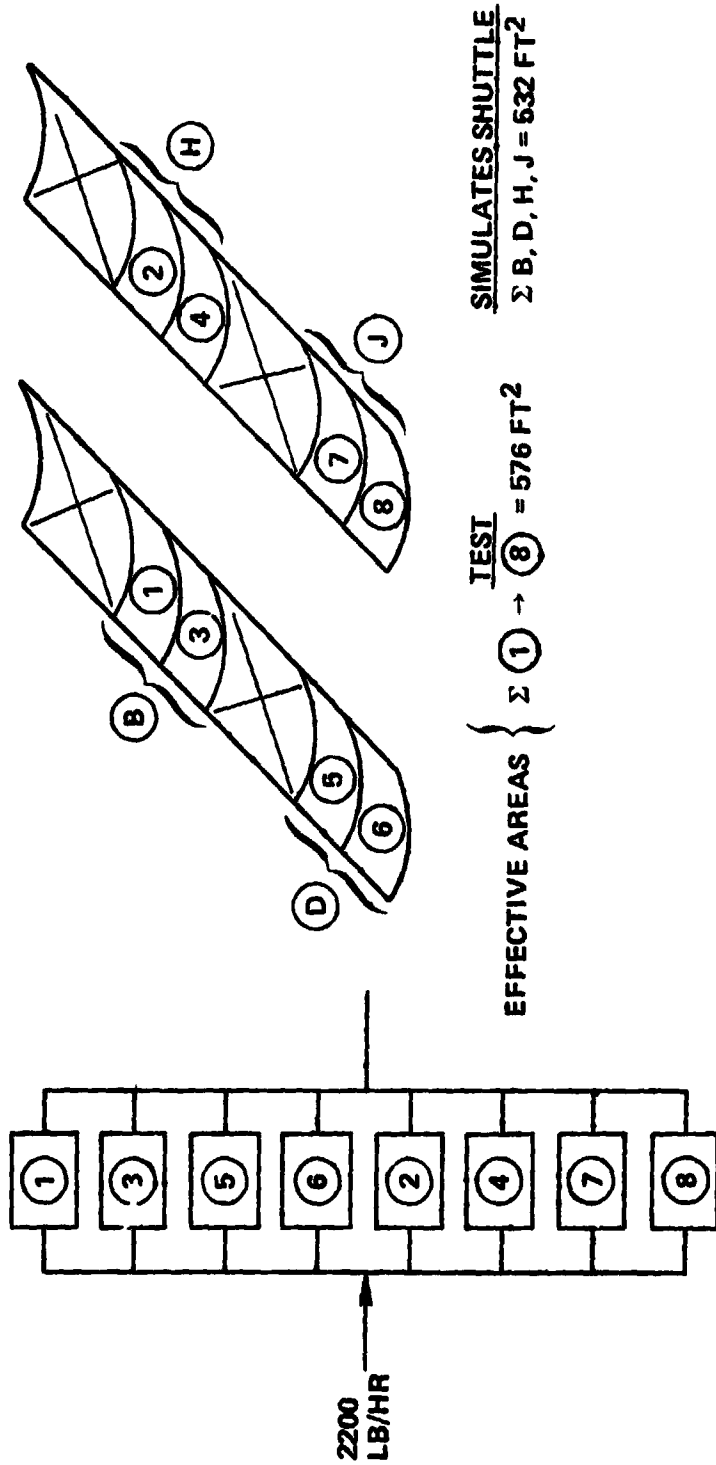


FIGURE 13

INFLUENCE OF ENVIRONMENT ON PERFORMANCE
 COMPARISON OF TEST POINTS 5 AND 8

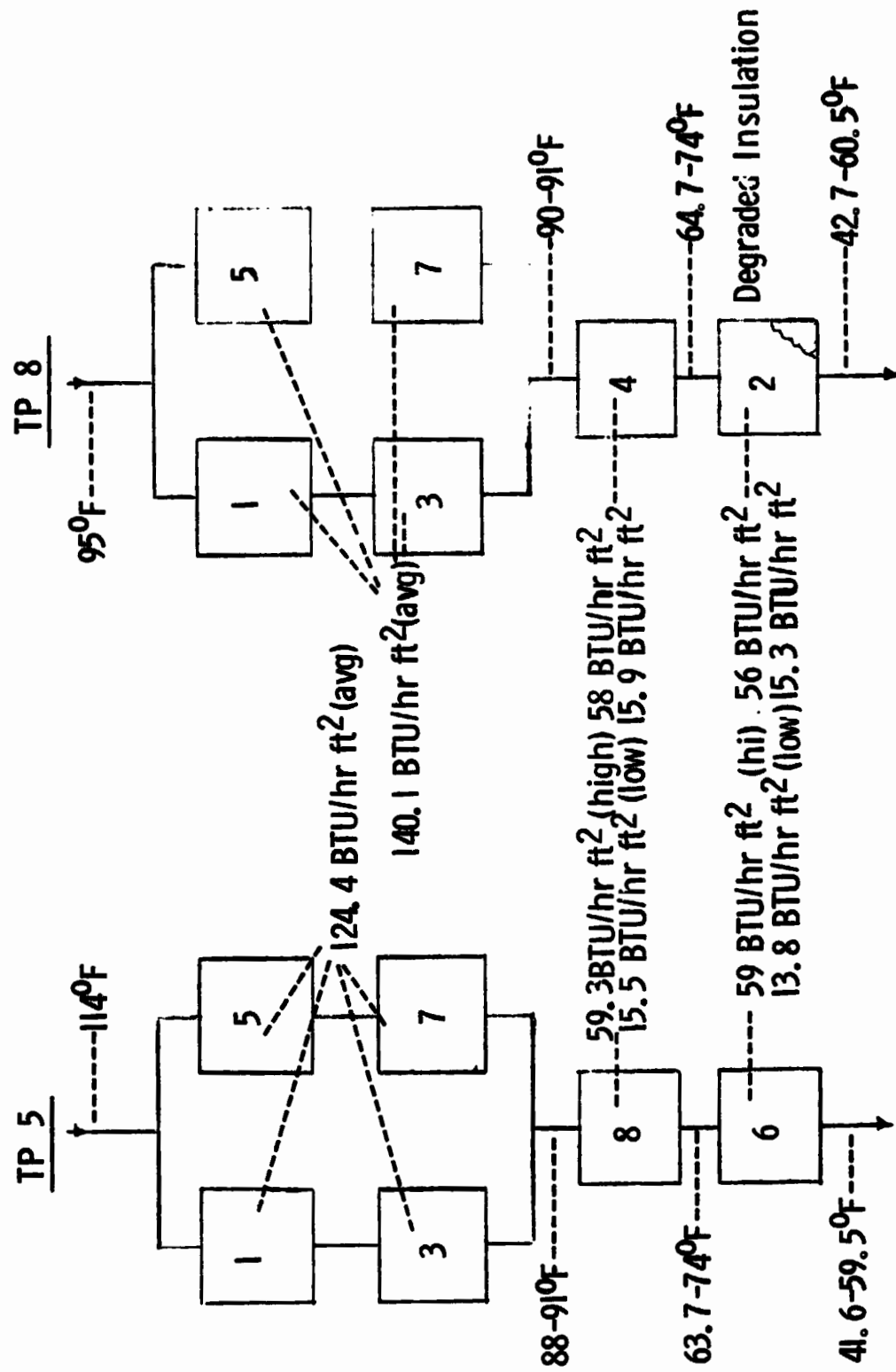


FIGURE 14

TEST GROUP 2.8 - RESPONSE TO SET POINT CHANGES

HIGH LOAD ($T_{in} = 163^{\circ}\text{F}$) SKEMED ENVIRONMENT

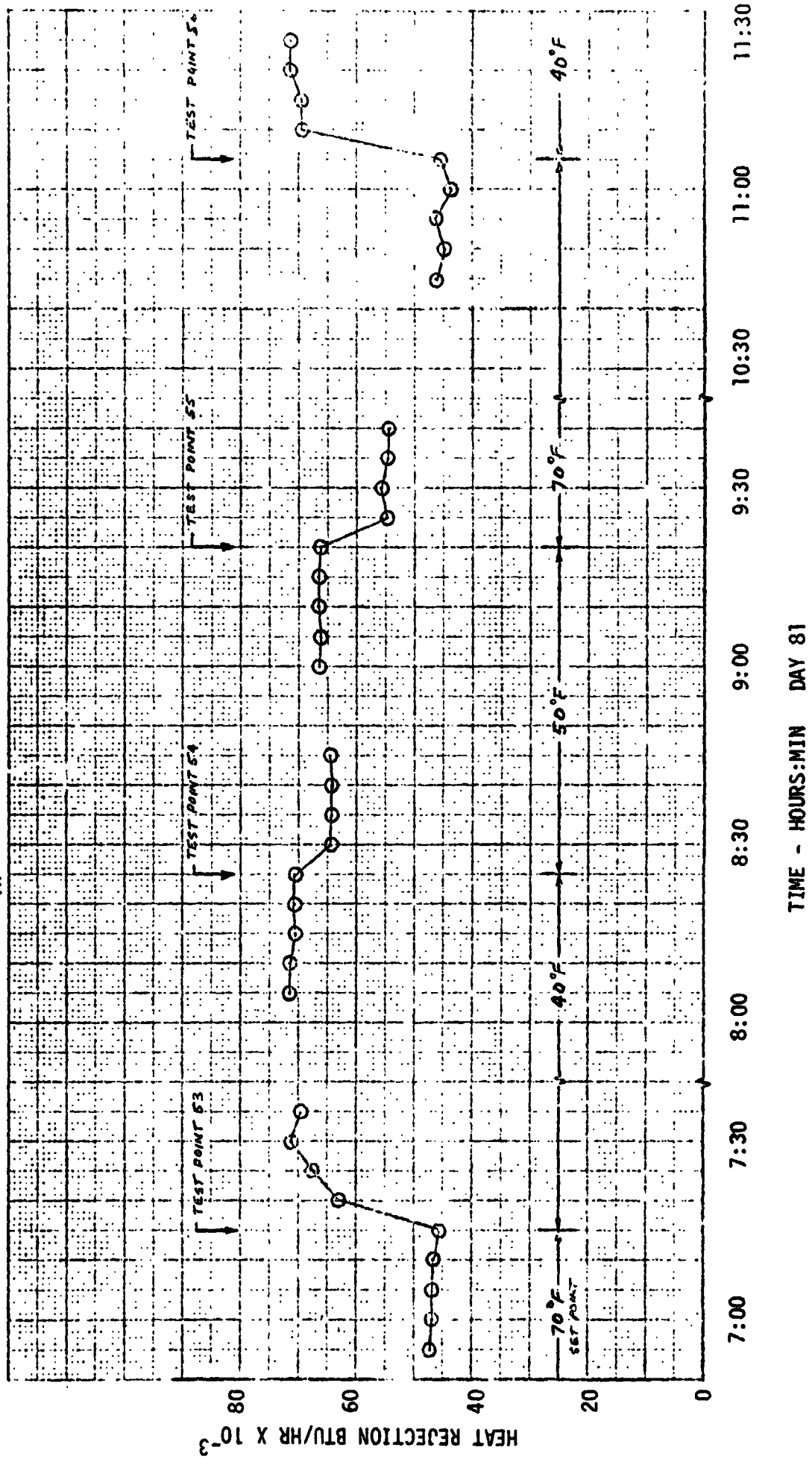


FIGURE 15

COMPARISON OF PLUMBING ARRANGEMENTS

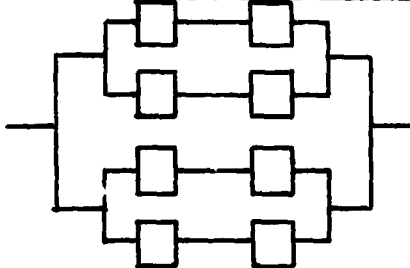
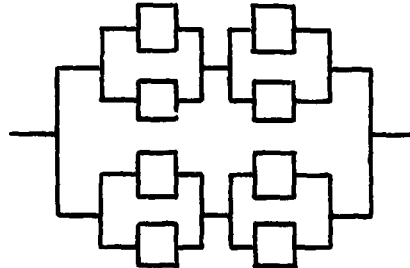
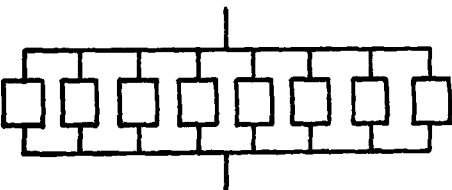
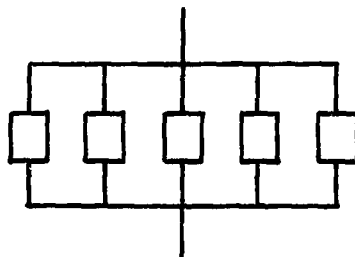
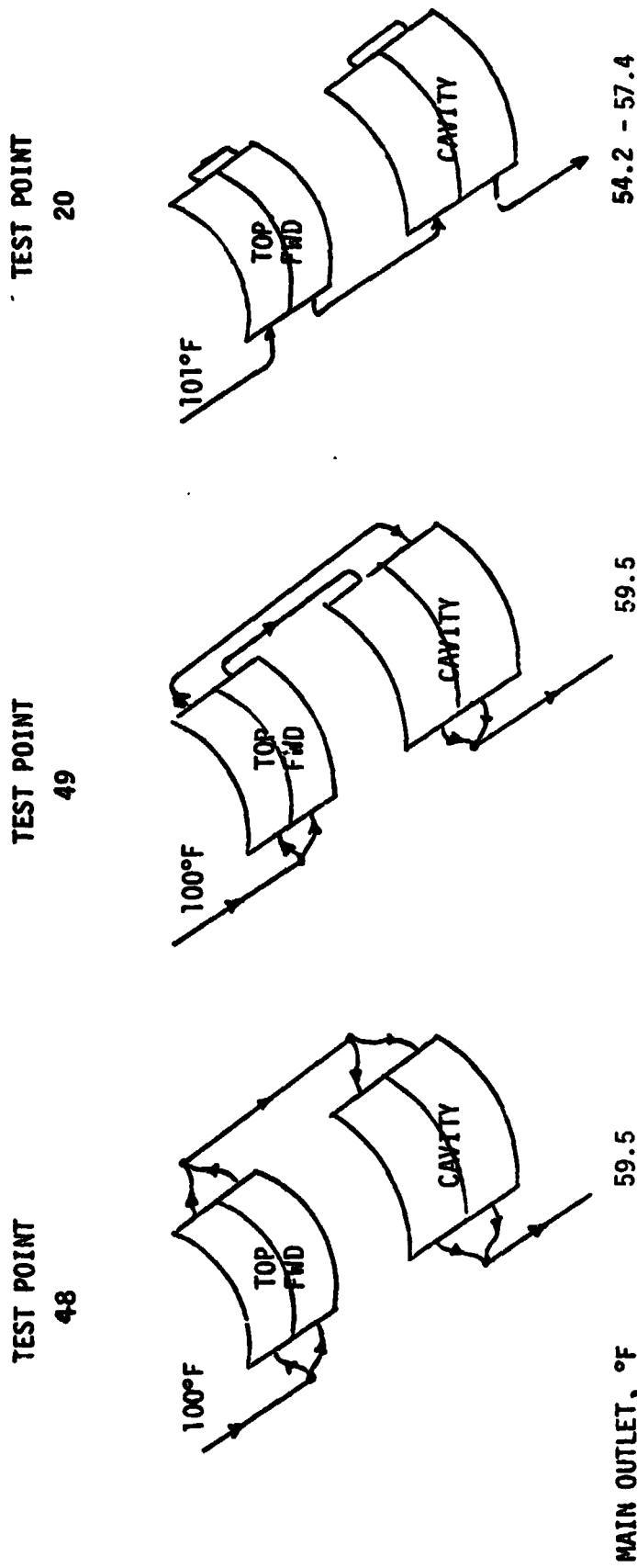
CONFIGURATION	TEST POINT	AVG ENV. BTU/HR FT ²	INLET TEMP °F	OUTLET TEMP °F	HEAT REJECTION BTU/HR	Q/A BTU/HR FT ²
	32	129.8	165.2	111.0	31,909	55.4
	33	129.6	164.1	110.0	30,679	53.4
	45	128.8	161.1	112.	29,408	51.0
	46	129.8	162.7	123.8	22,492	62.5

FIGURE 16
COMPARISON OF PLUMBING ARRANGEMENTS



	TEST POINT 48	TEST POINT 49	TEST POINT 20
MAIN OUTLET, °F	59.5	59.5	54.2 - 57.4
TOTAL HEAT REJECTED, BTU/HR	23,258	22,437	24,307-26,165
TOTAL MAIN FLOW, LB/HR	2136	2161	2124-2136
AVG. ENVIRONMENT			
TOP	129.1	128.5	124.3
CAVITY	29.6-81.1 (Steady)	29.5-76.6 (Steady)	35.7-56.4 (Cyclic)

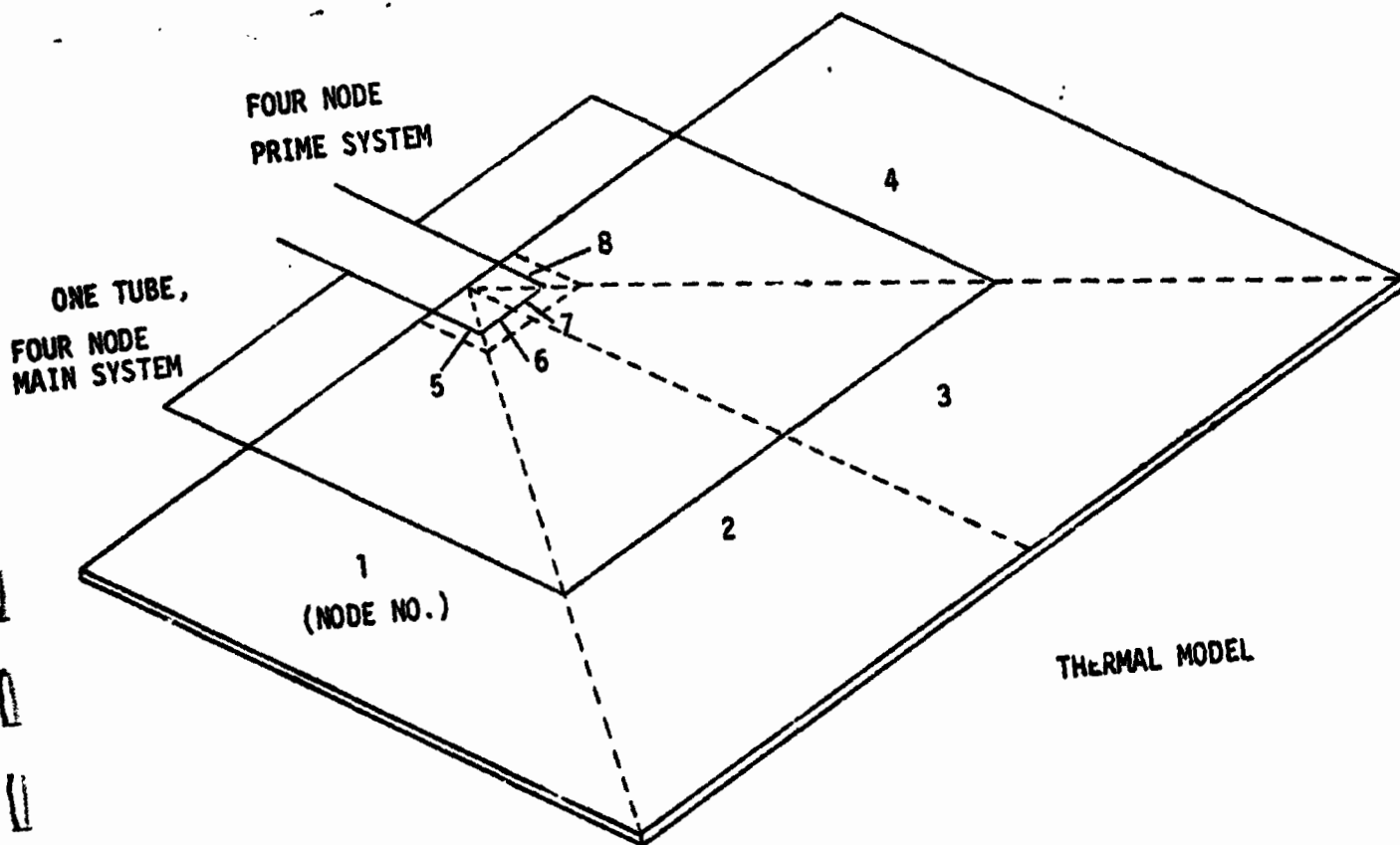
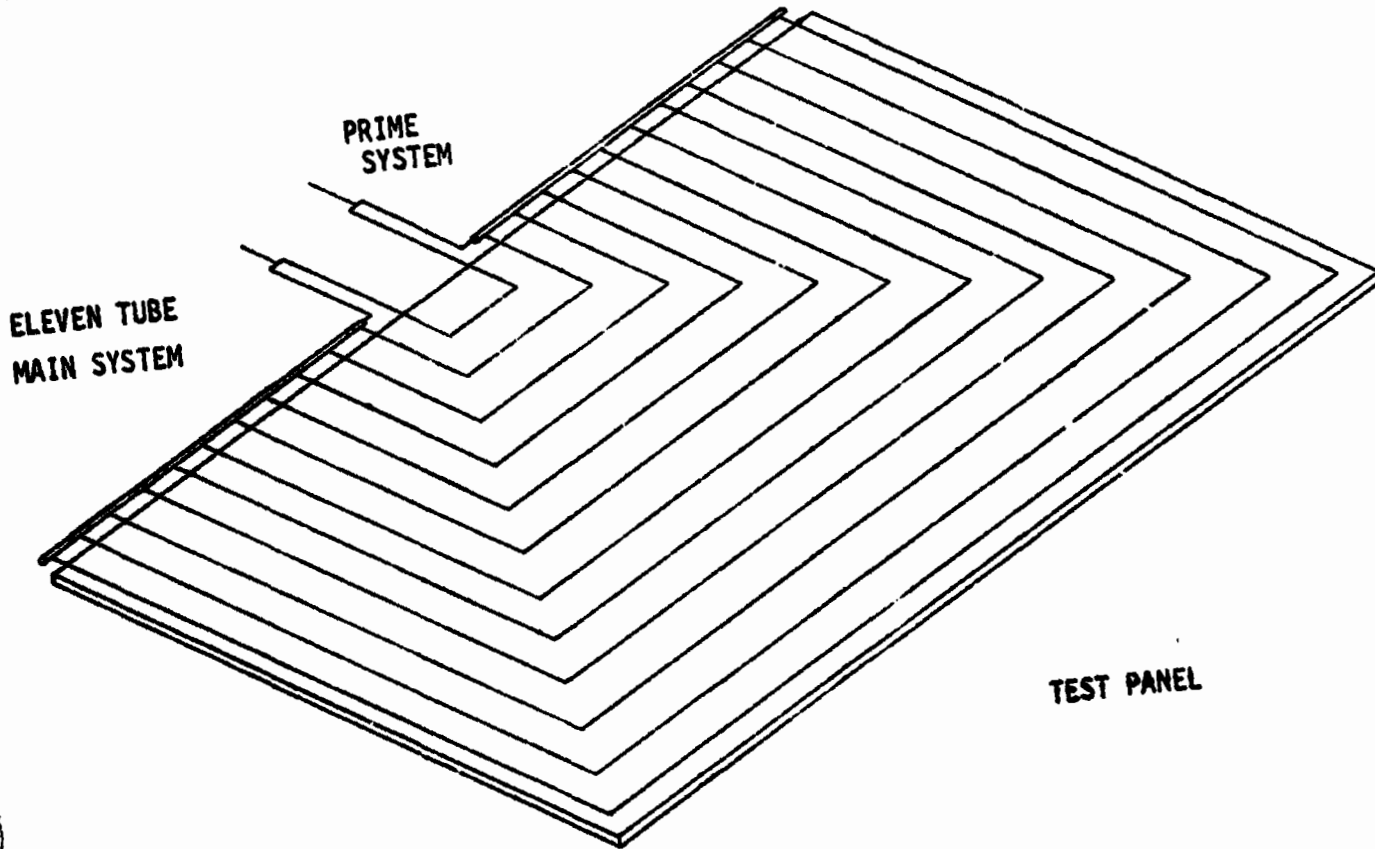
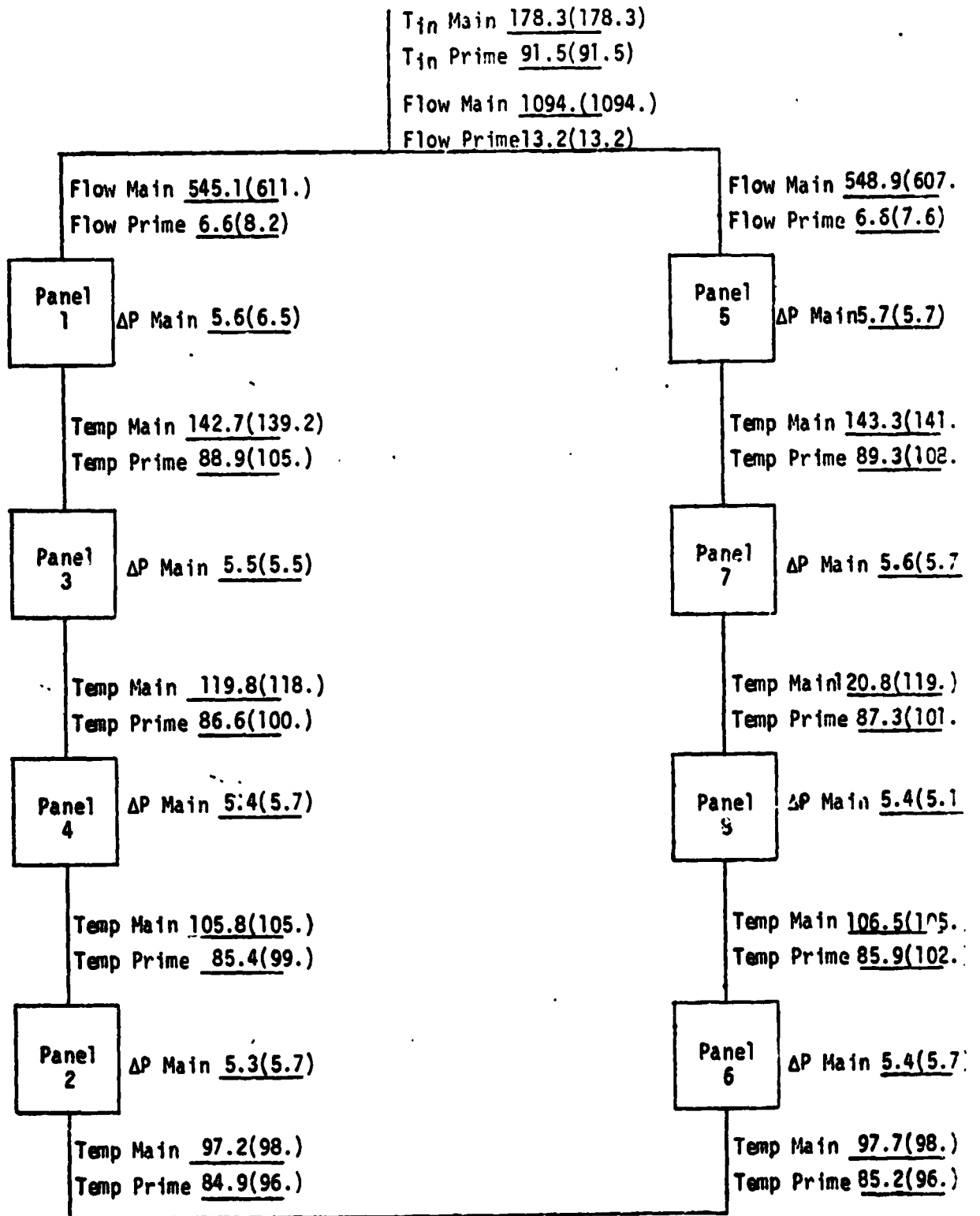


FIGURE 17 PANEL THERMAL MODEL

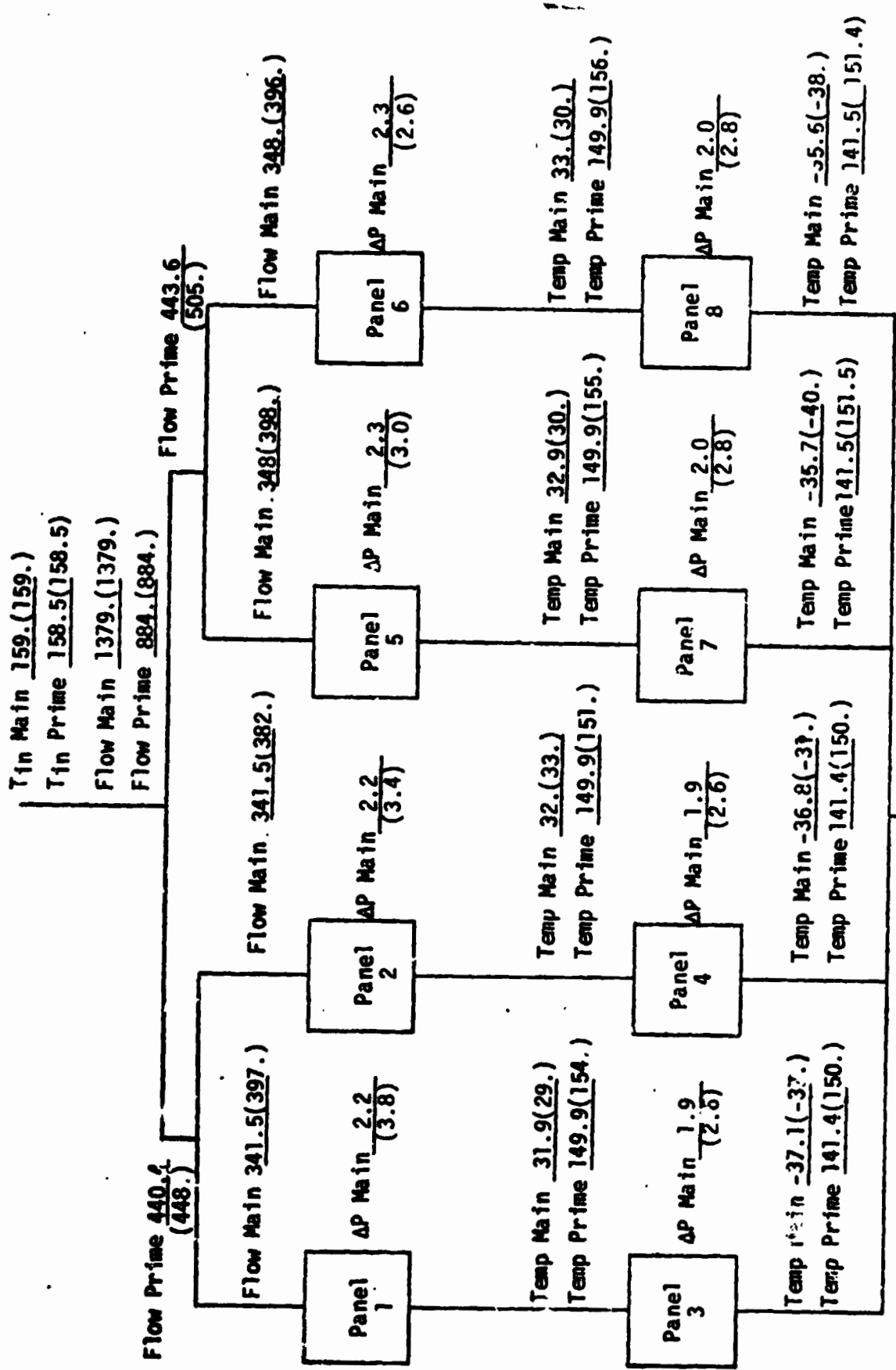
CONFIGURATION α
 FIGURE 18 TEST POINT 1A CORRELATION



Numbers in parenthesis are test values
 Numbers not in parenthesis are predicted values

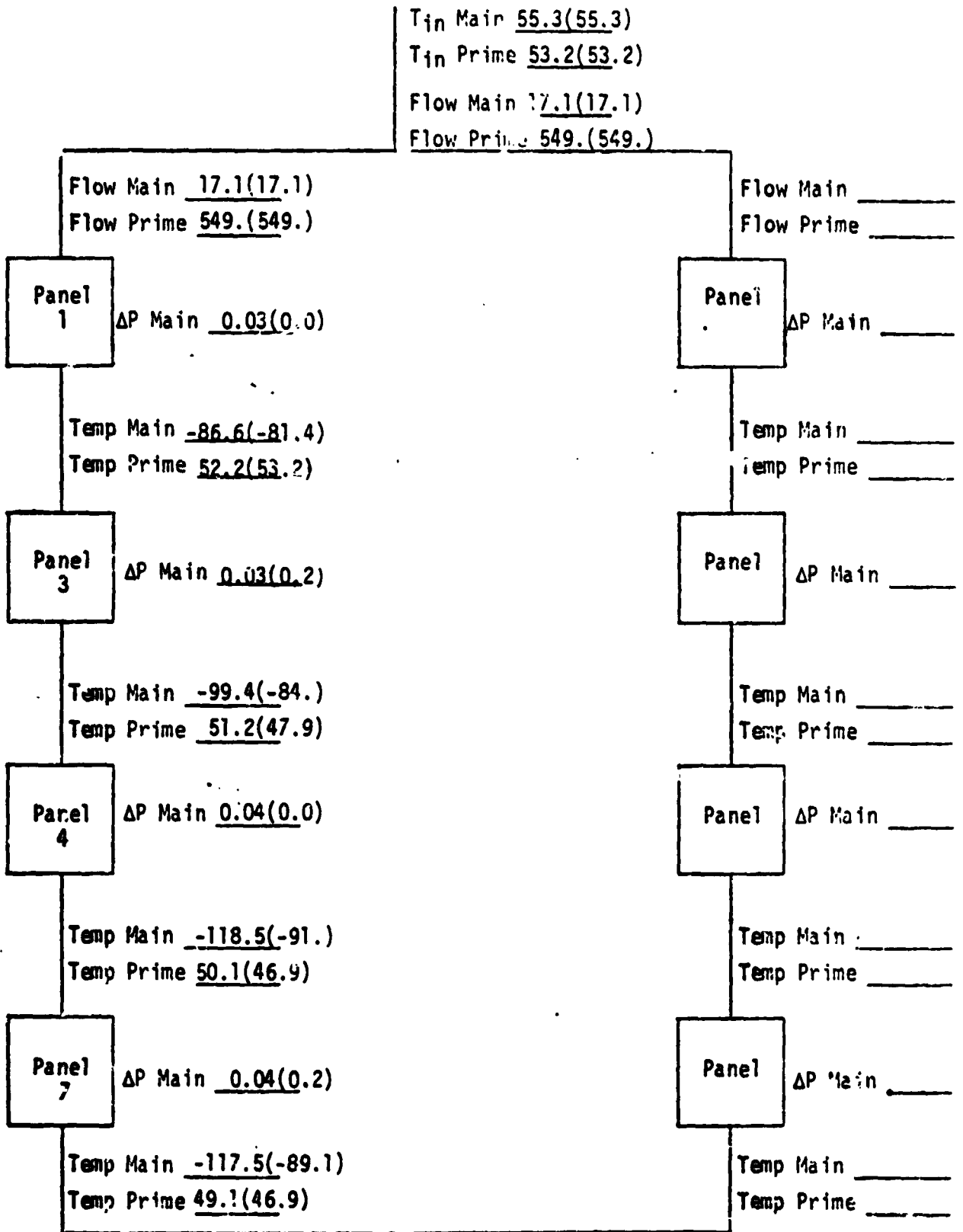
T_{out} Main 97.4(97.)
 T_{out} Prime 85.2(80.)
 Temp Mixed Prime and Main 97.3(96.)

CONFIGURATION Y
 FIGURE 19 TEST POINT 51 CORRELATION



Numbers in parenthesis are test values
 Numbers not in parenthesis are predicted values

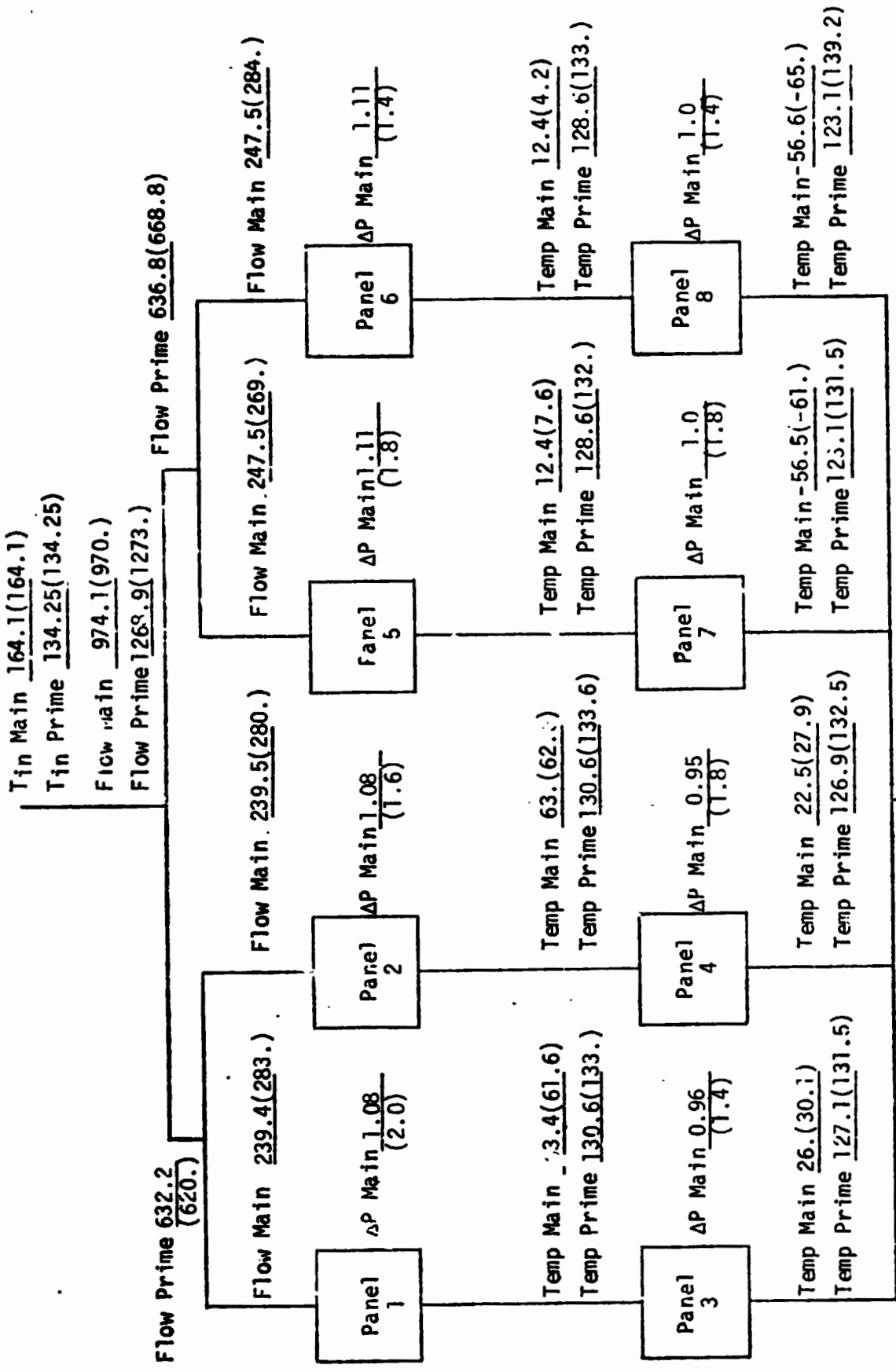
CONFIGURATION a
 FIGURE 20 TEST POINT 17 CORRELATION



Numbers in parenthesis are test values
 Numbers not in parenthesis are predicted values

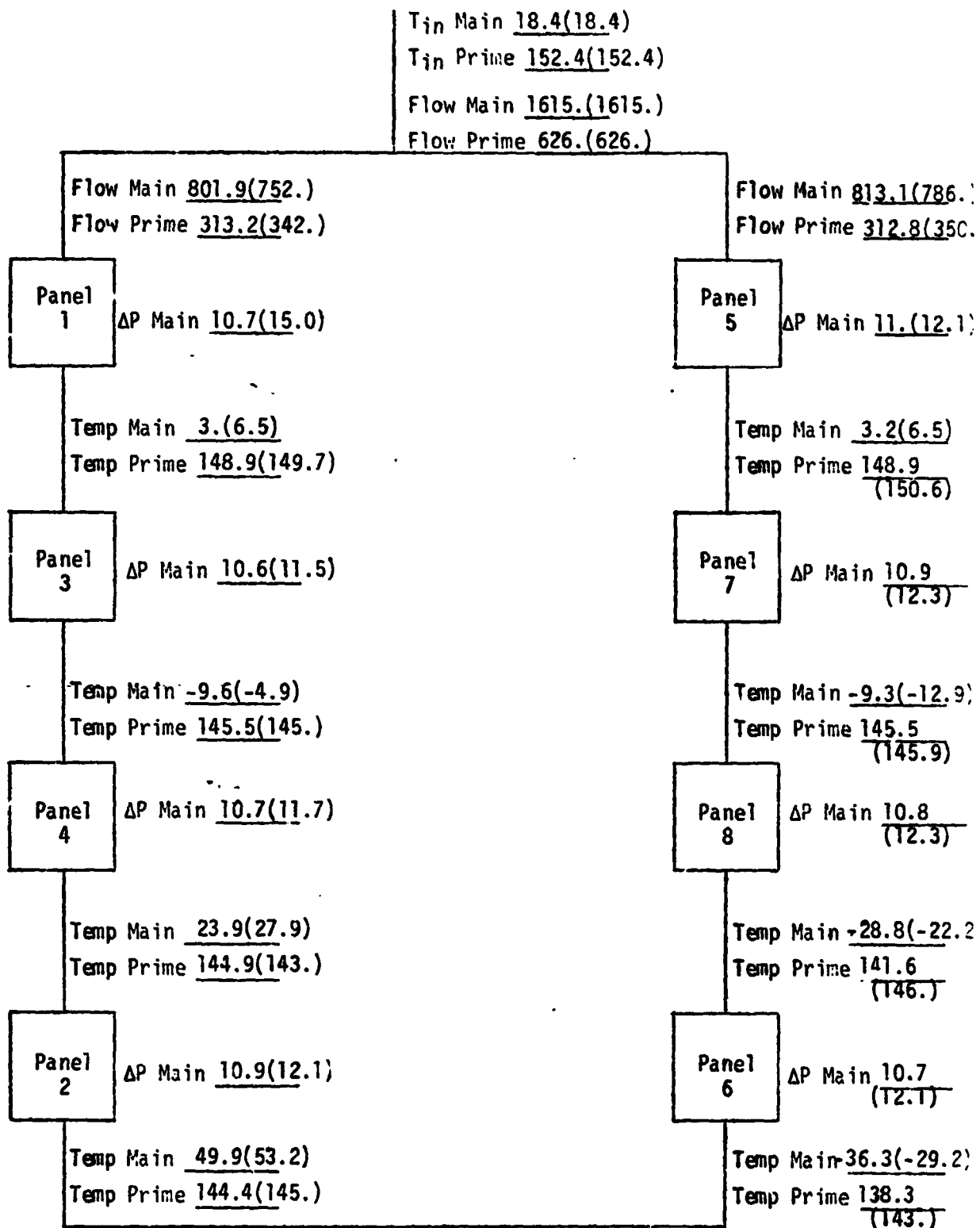
CONFIGURATION Y

FIGURE 21 TEST POINT 53 CORRELATION



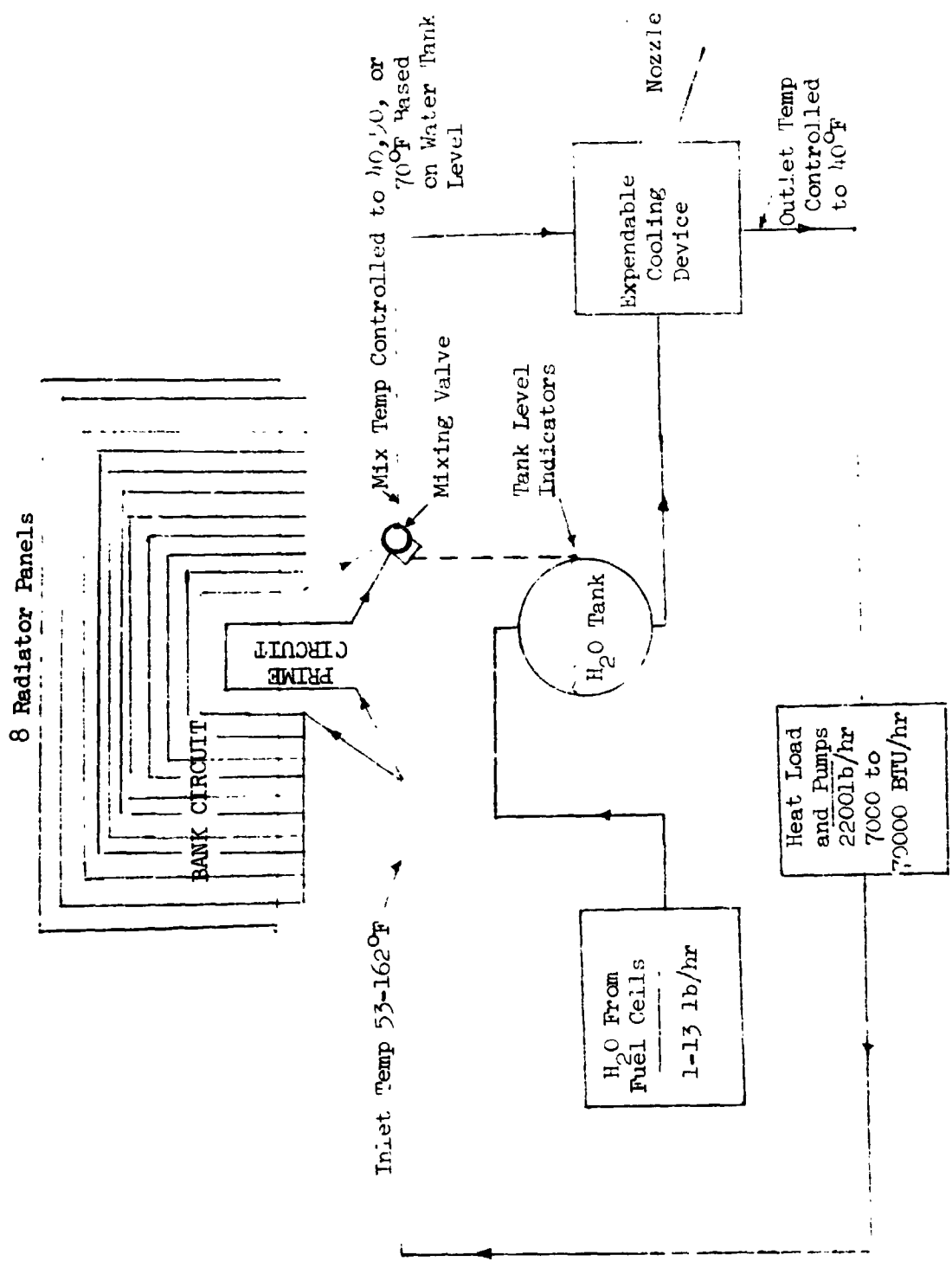
Numbers in parenthesis are test values
 Numbers not in parenthesis are predicted values

CONFIGURATION α
 FIGURE 22 TEST POINT 14 CORRELATION



Numbers in parenthesis are test values
 Numbers not in parenthesis are predicted values

FIGURE 23 INTEGRATED RADIATOR/EXPENDABLE COOLING SYSTEM SCHEMATIC



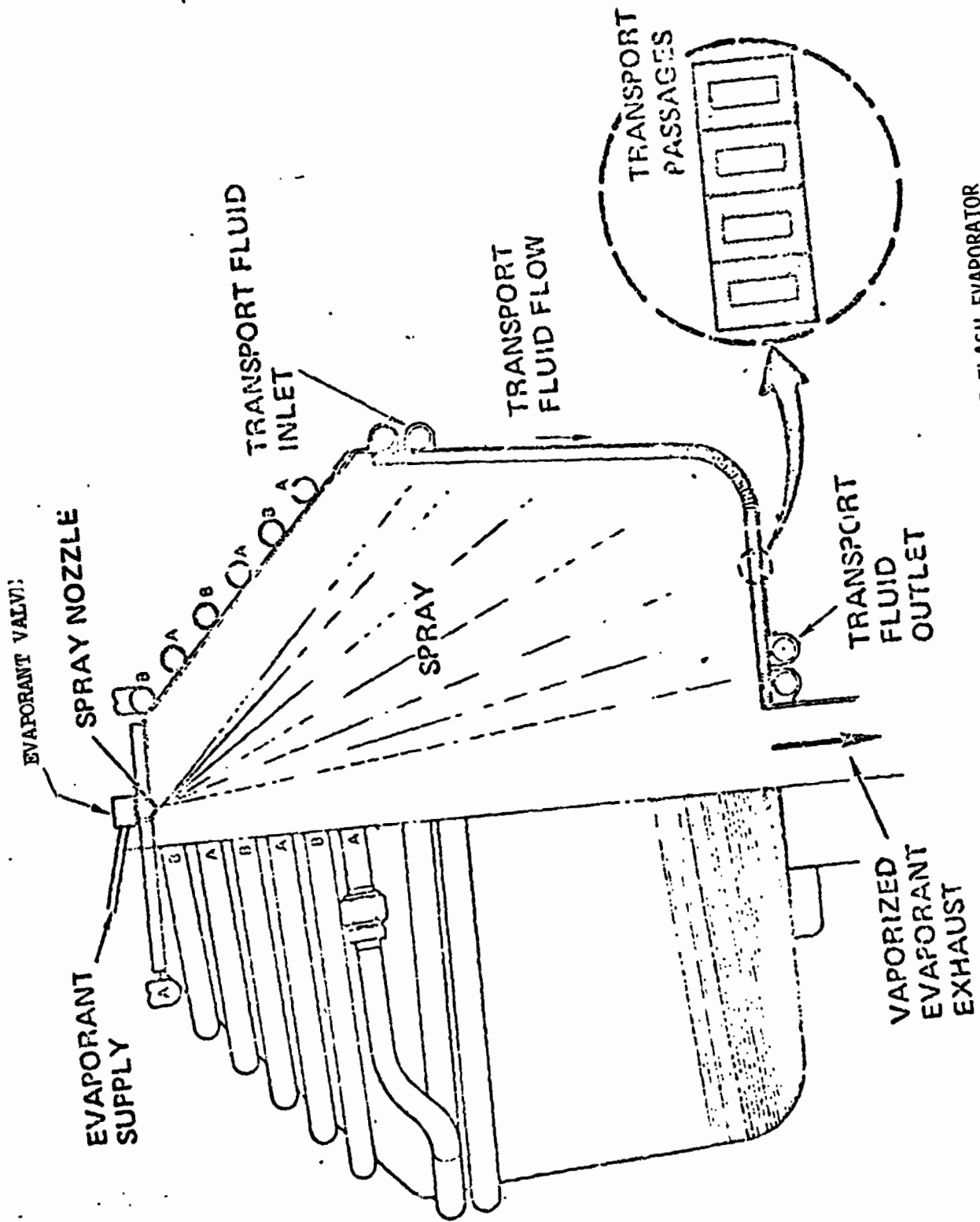


FIGURE 24 CUTAWAY DRAWING OF THE FLASH EVAPORATOR

FIGURE 25 DUCT AND NOZZLE DIMENSIONS

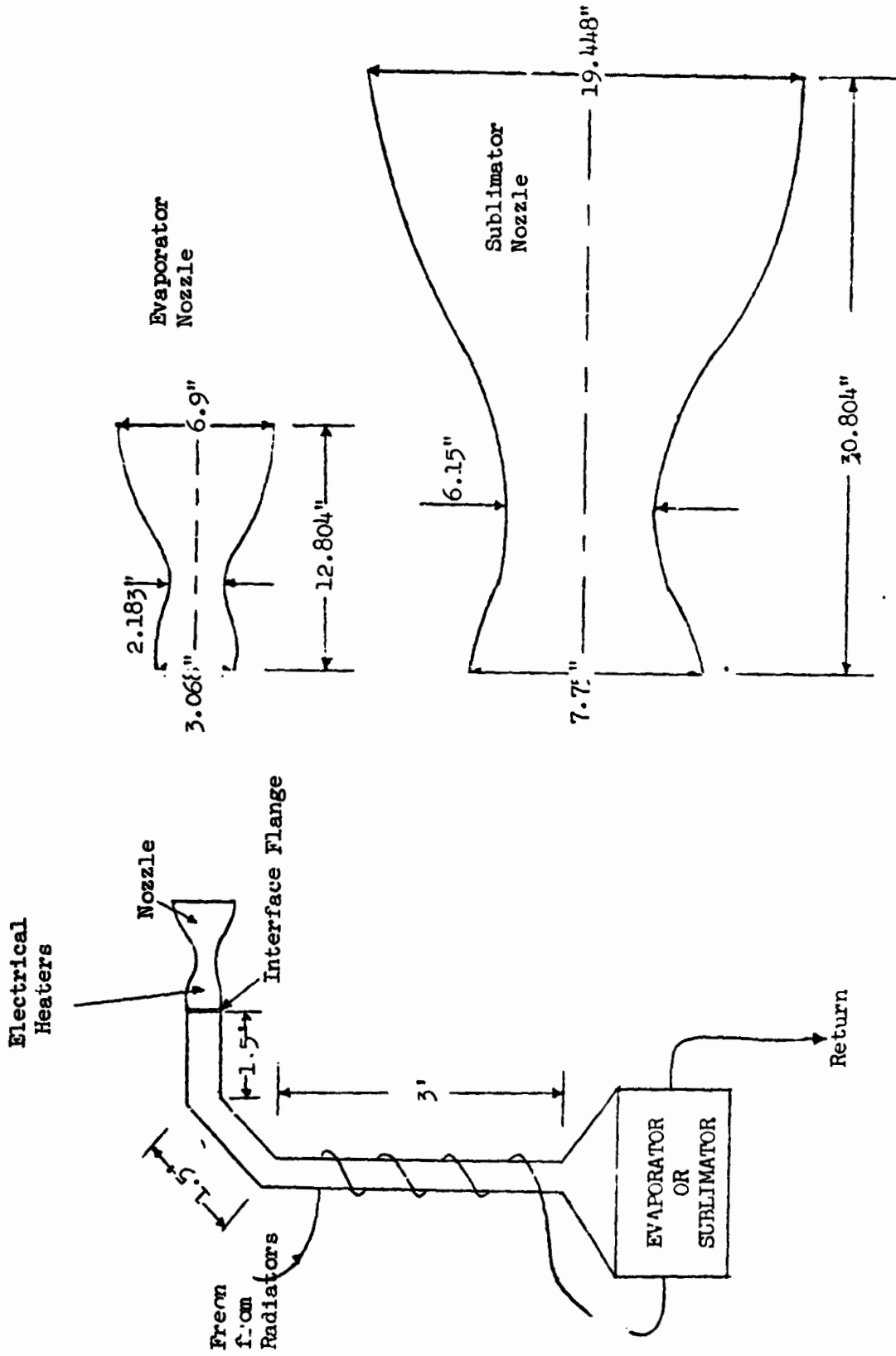


FIGURE 26: MIXED OUTLET TEMP RESPONSE DURING SET POINT CHANGES

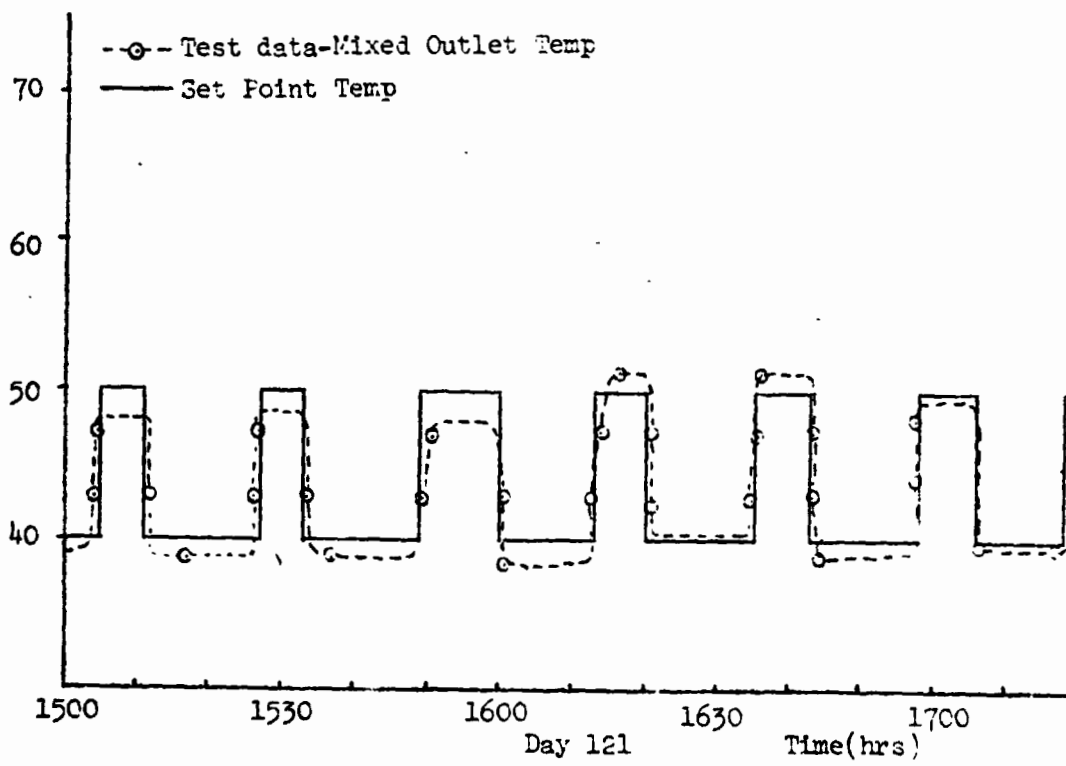
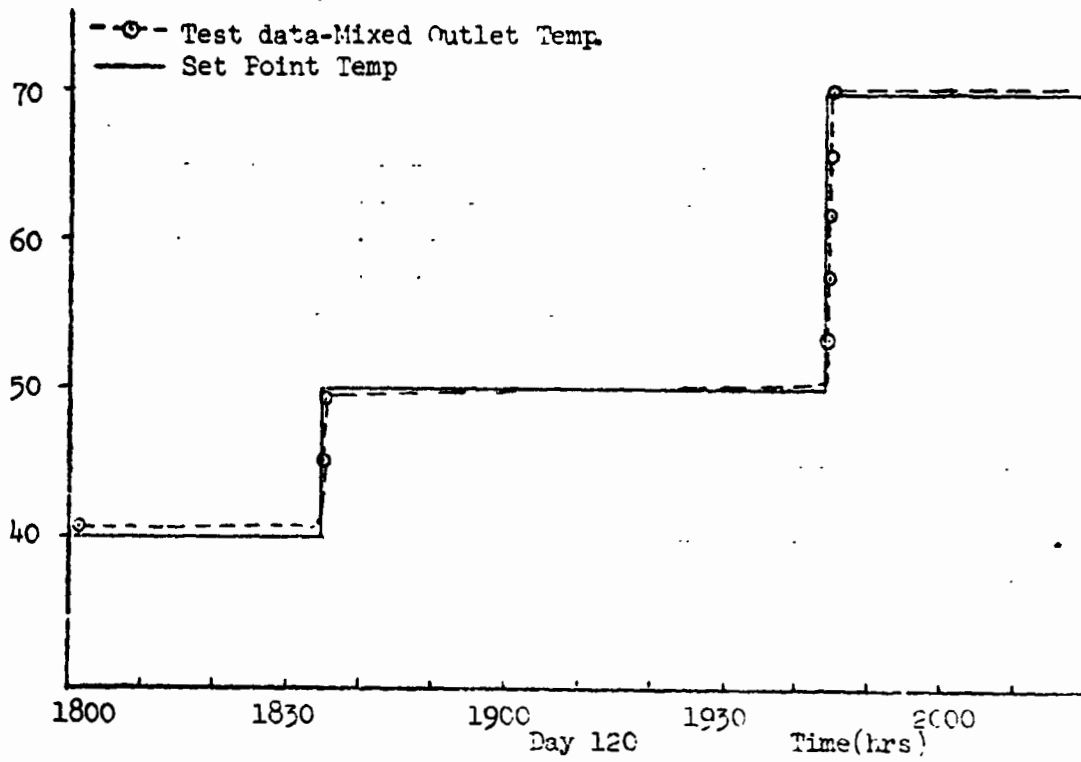


FIGURE 27: FLASH EVAPORATOR INLET AND OUTLET FRESH TEMPERATURES

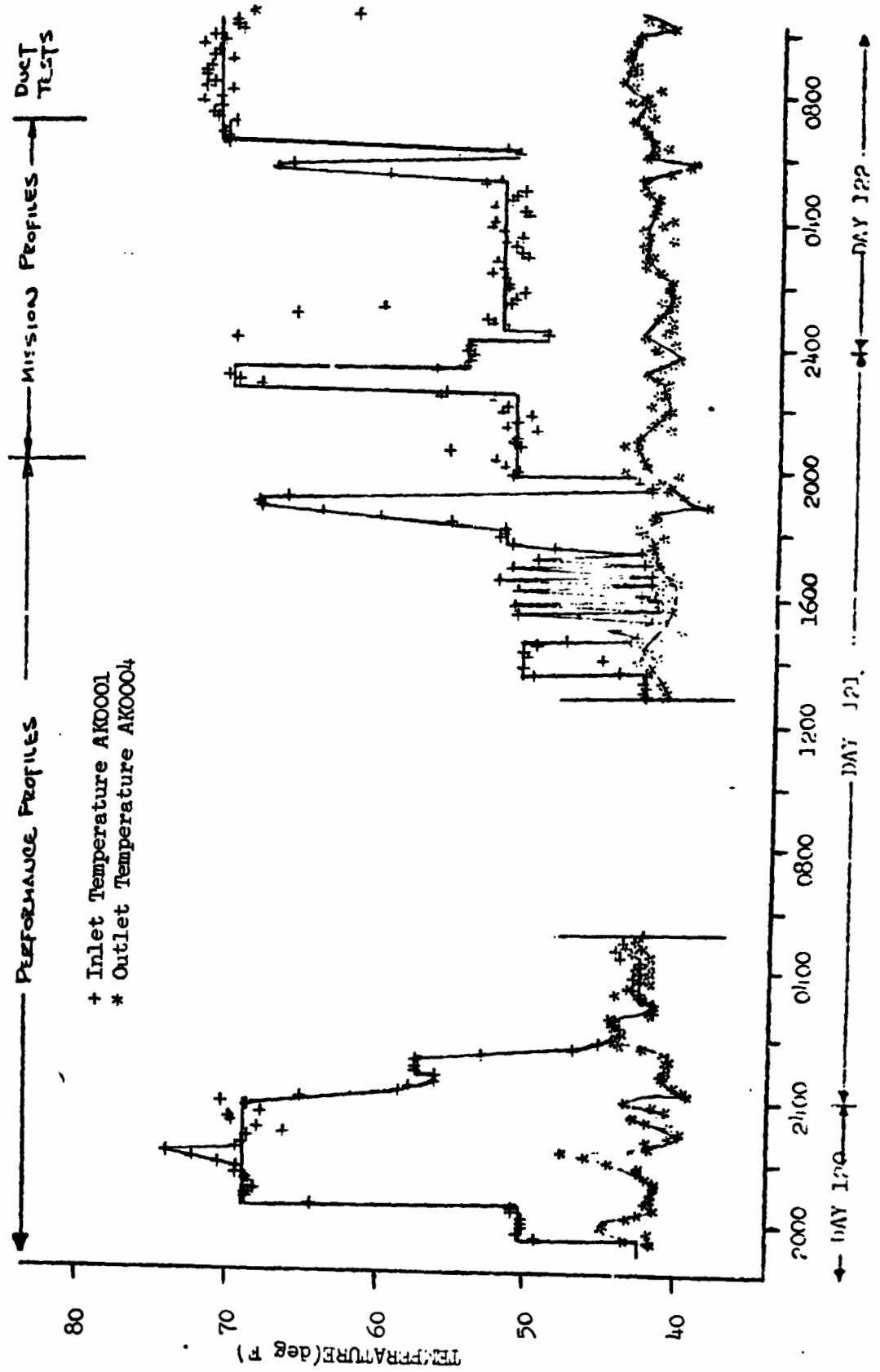


FIGURE 28

CALCULATED HEAT REJECTION FOR RADIATORS AND FLASH EVAPORATOR

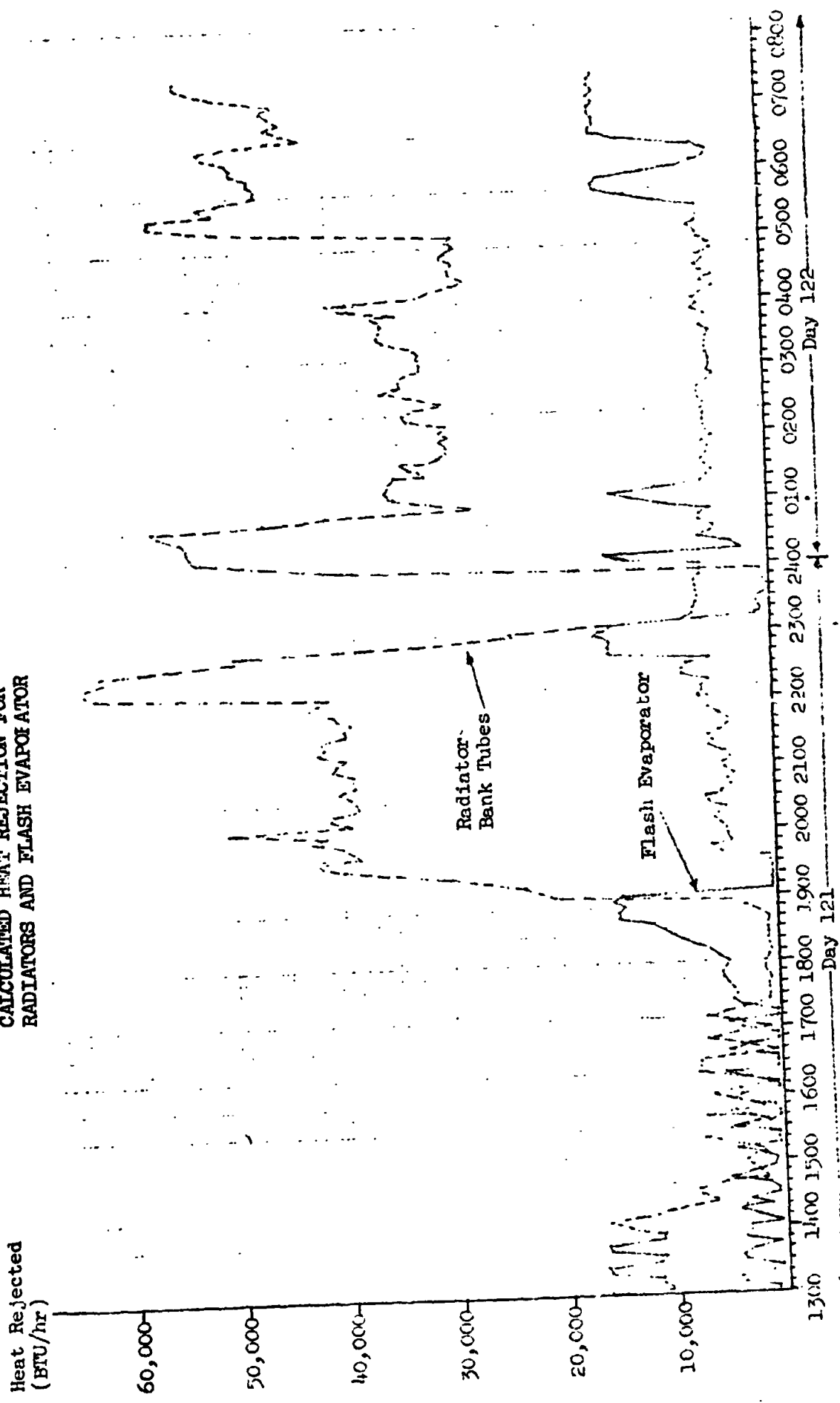


FIGURE 29

EVAPORATOR PERFORMANCE DURING DUCT AND NOZZLE HEATER TESTS

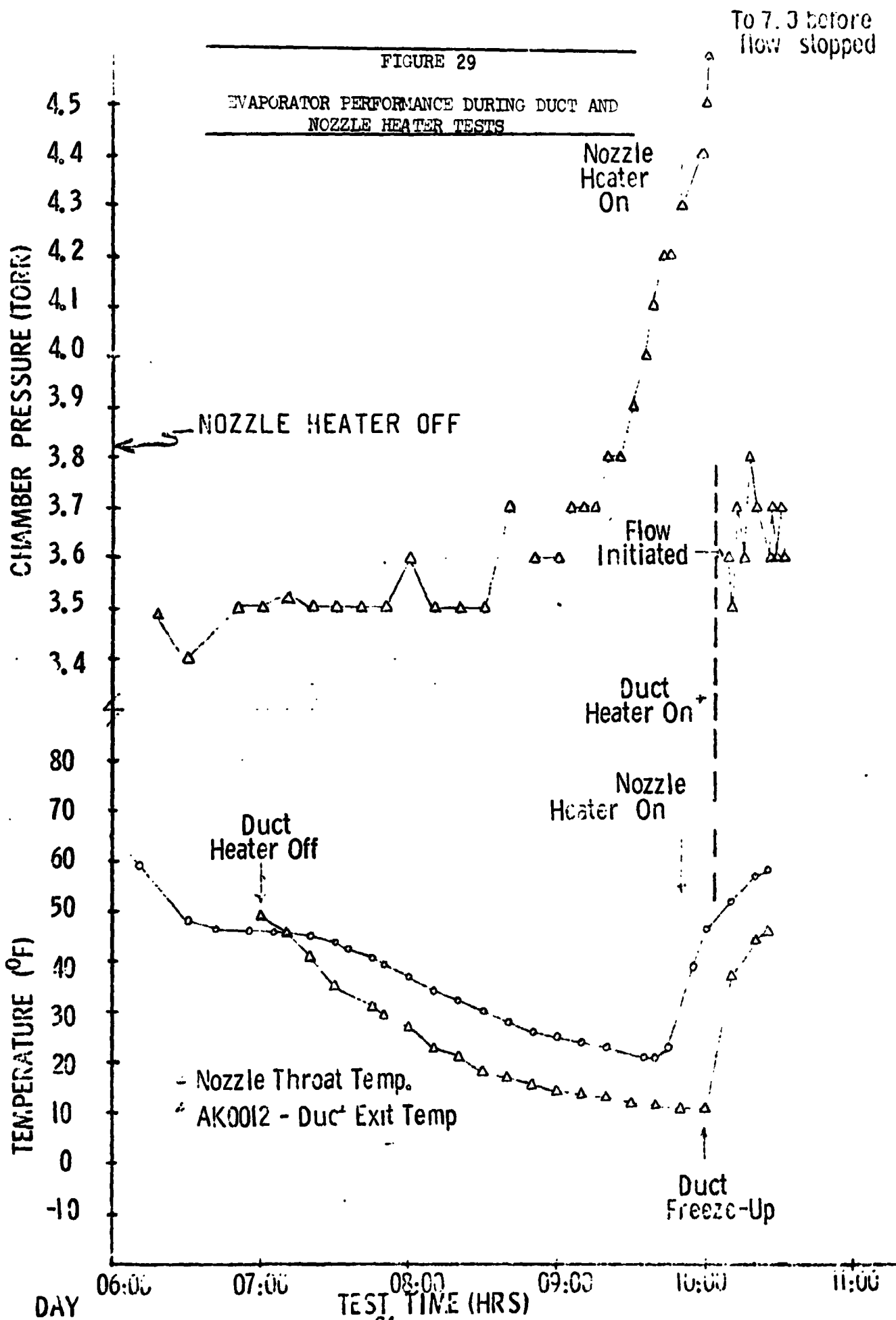


FIGURE 30

SUBLIMATOR INLET AND OUTLET TEMPERATURES

PHASE 2
SUBLIMATOR INLET (+) AND OUTLET (*)
FREON TEMPERATURES (°F)

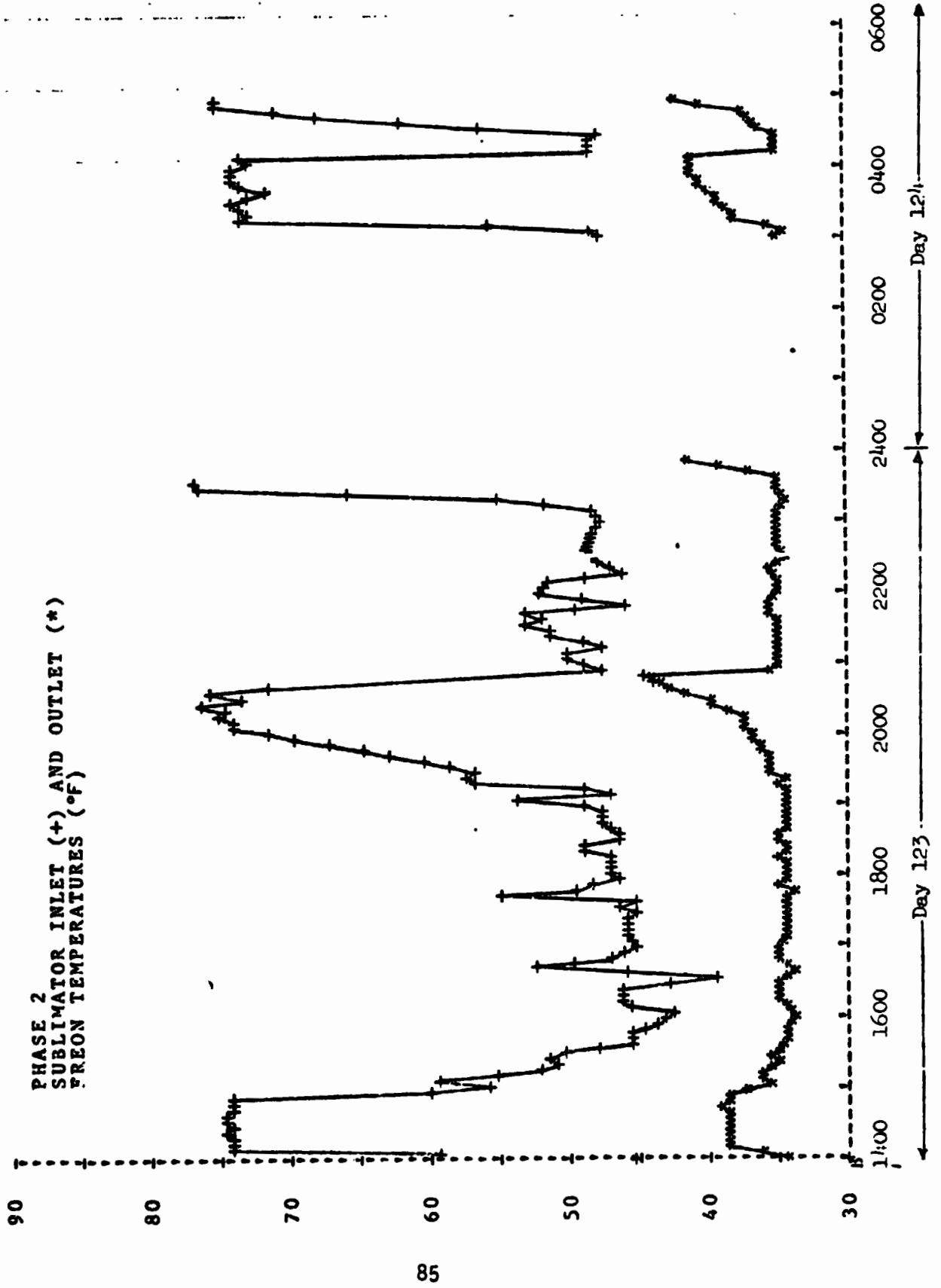


FIGURE 31
 IMPACT PRESSURE DATA - EVAPORATOR WITH NO NOZZLE

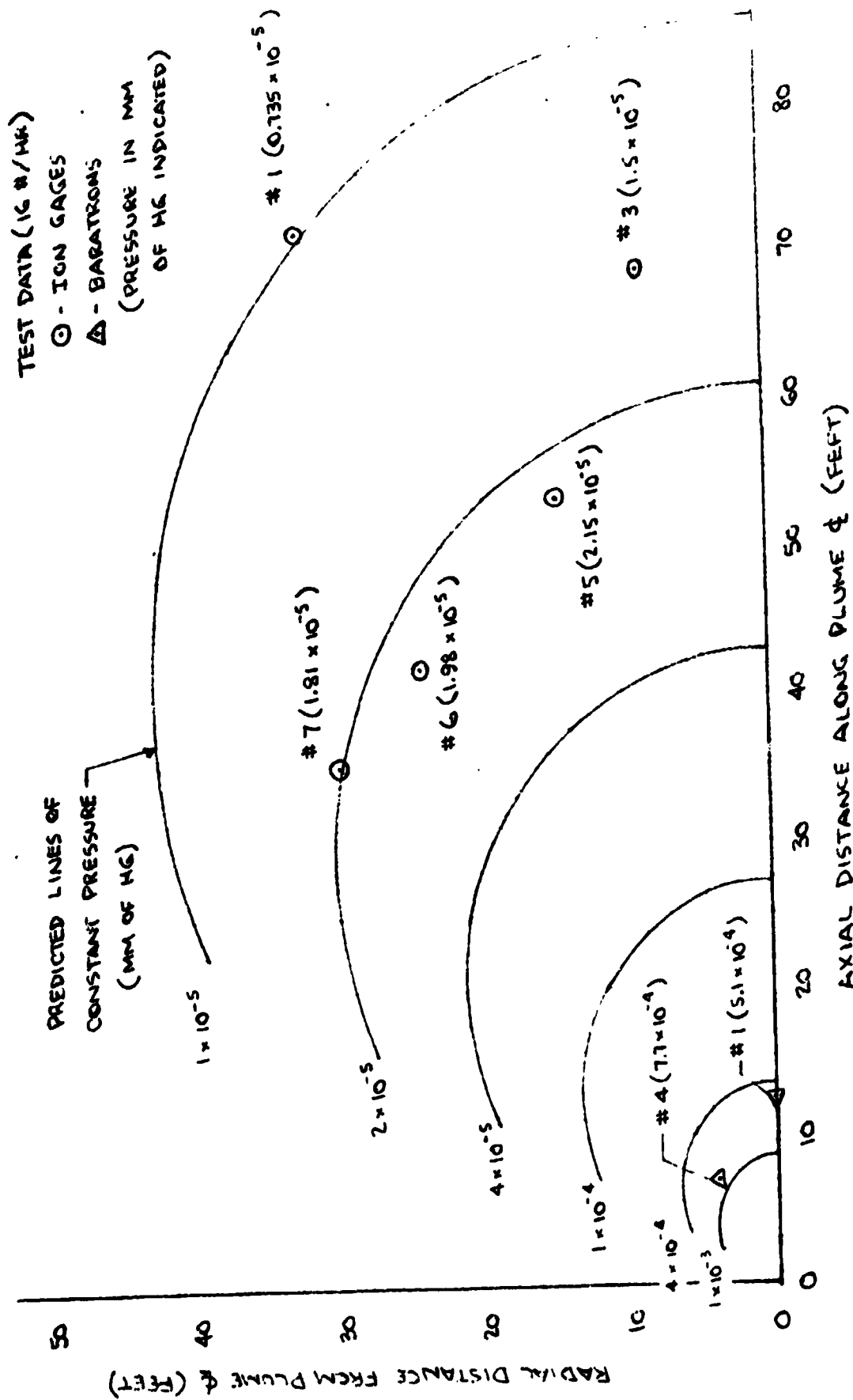


FIGURE 32
 IMPACT PRESSURE DATA - SUBLIMATOR WITH SUPERSONIC NOZZLE

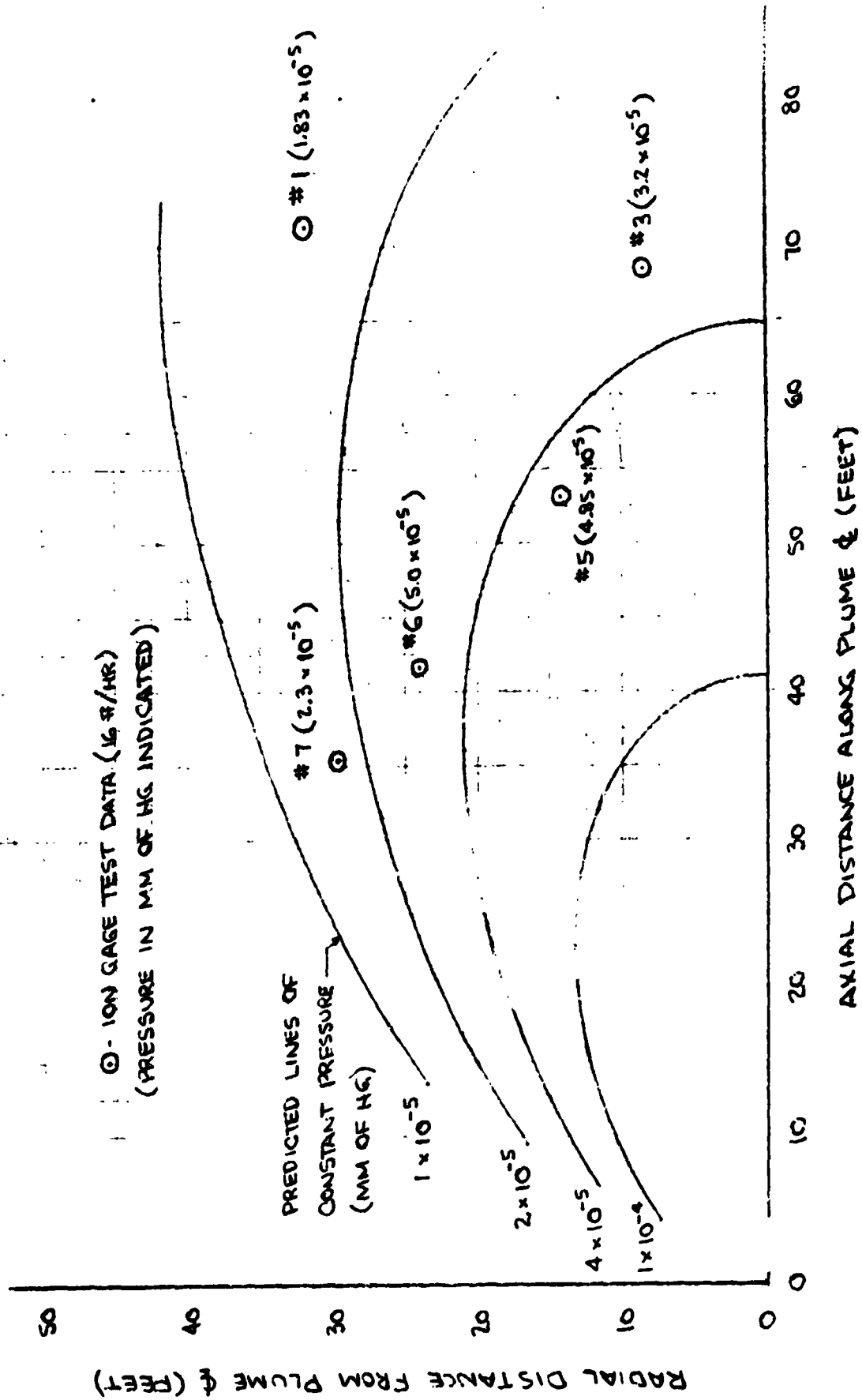


FIGURE 1A
 MASS FLUX DATA - PHASE III TEST - QCM # 9

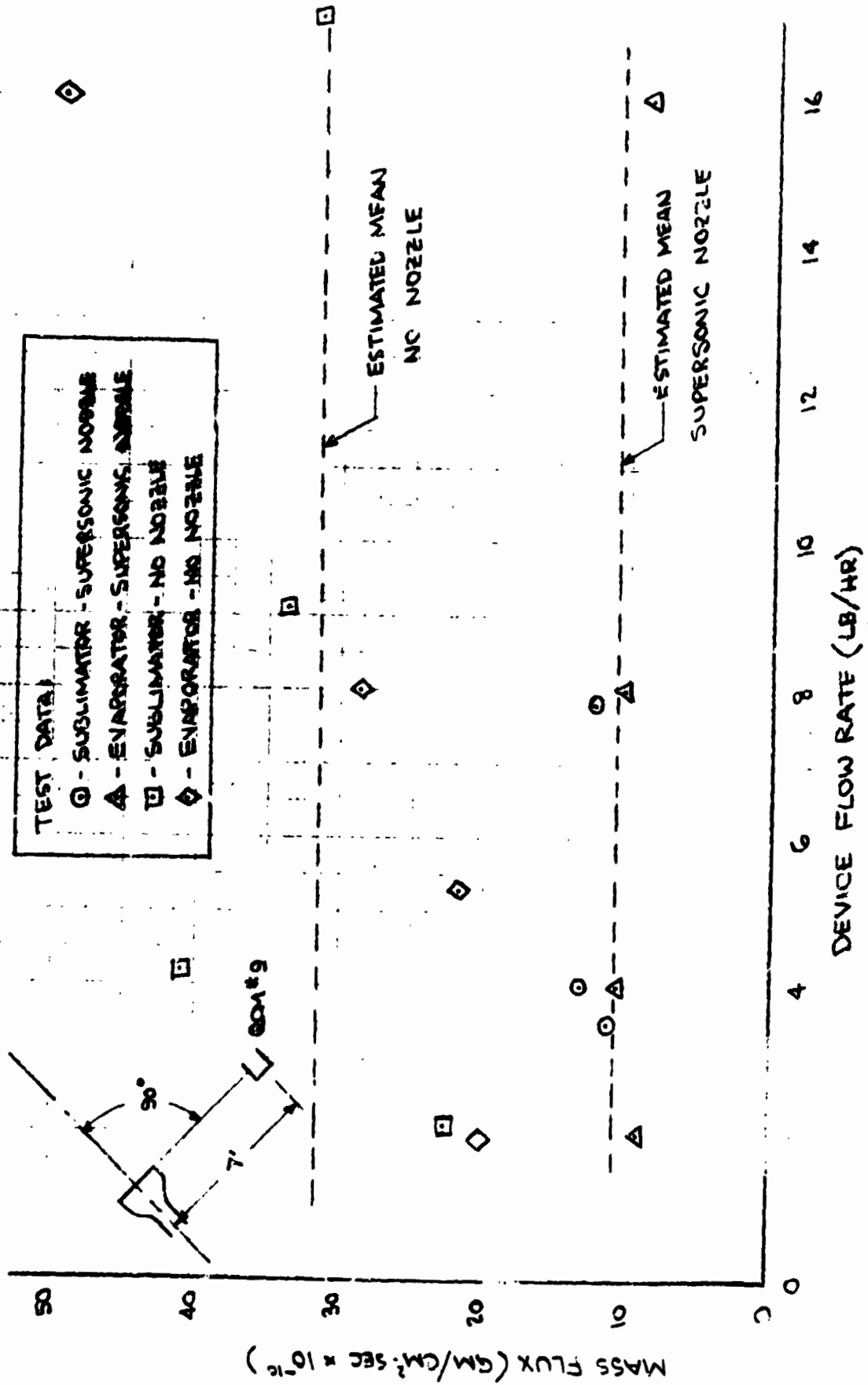


FIGURE 34
 MASS FLUX DATA - PHASE IIIA TEST - QCM # 9

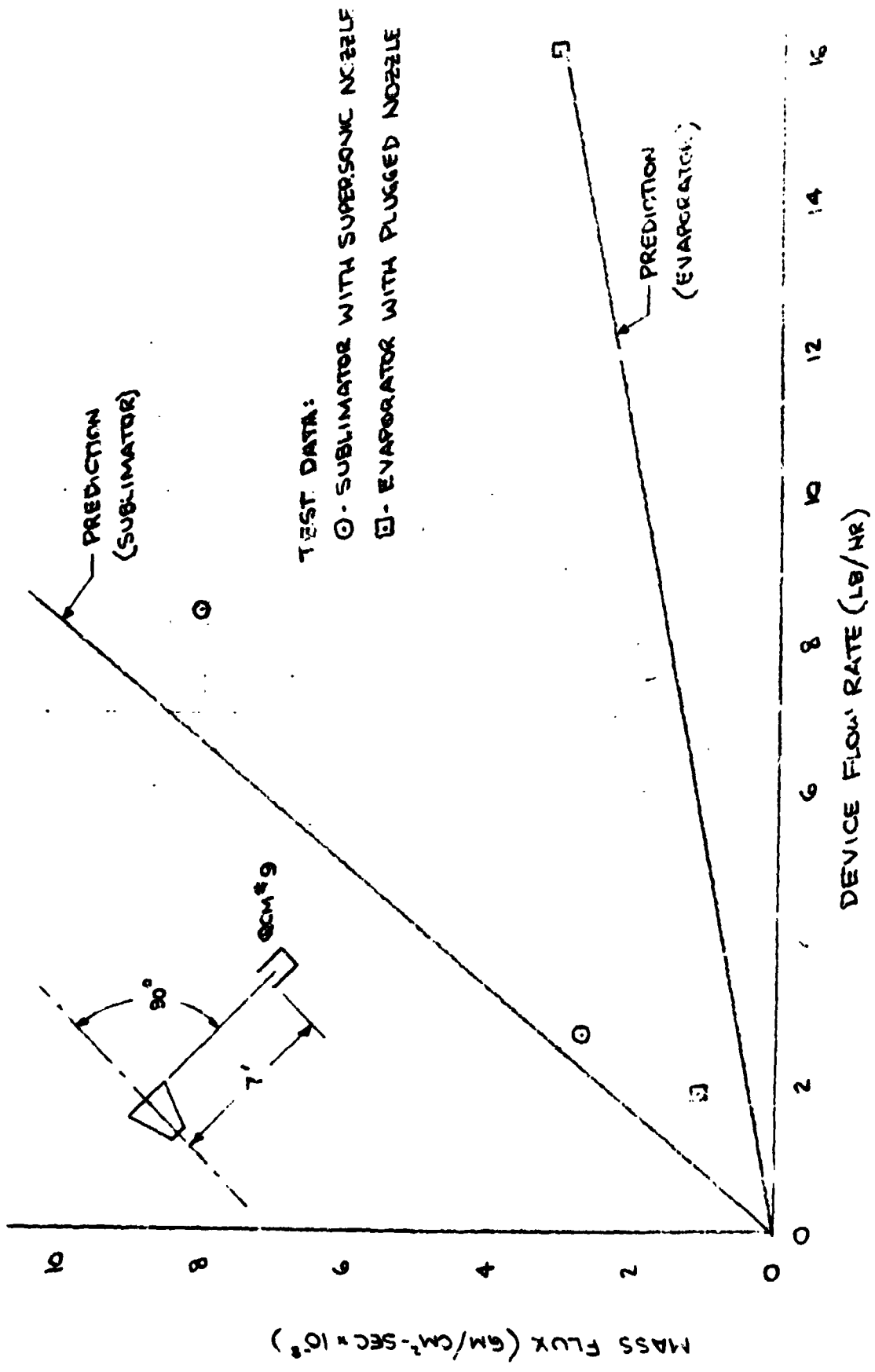
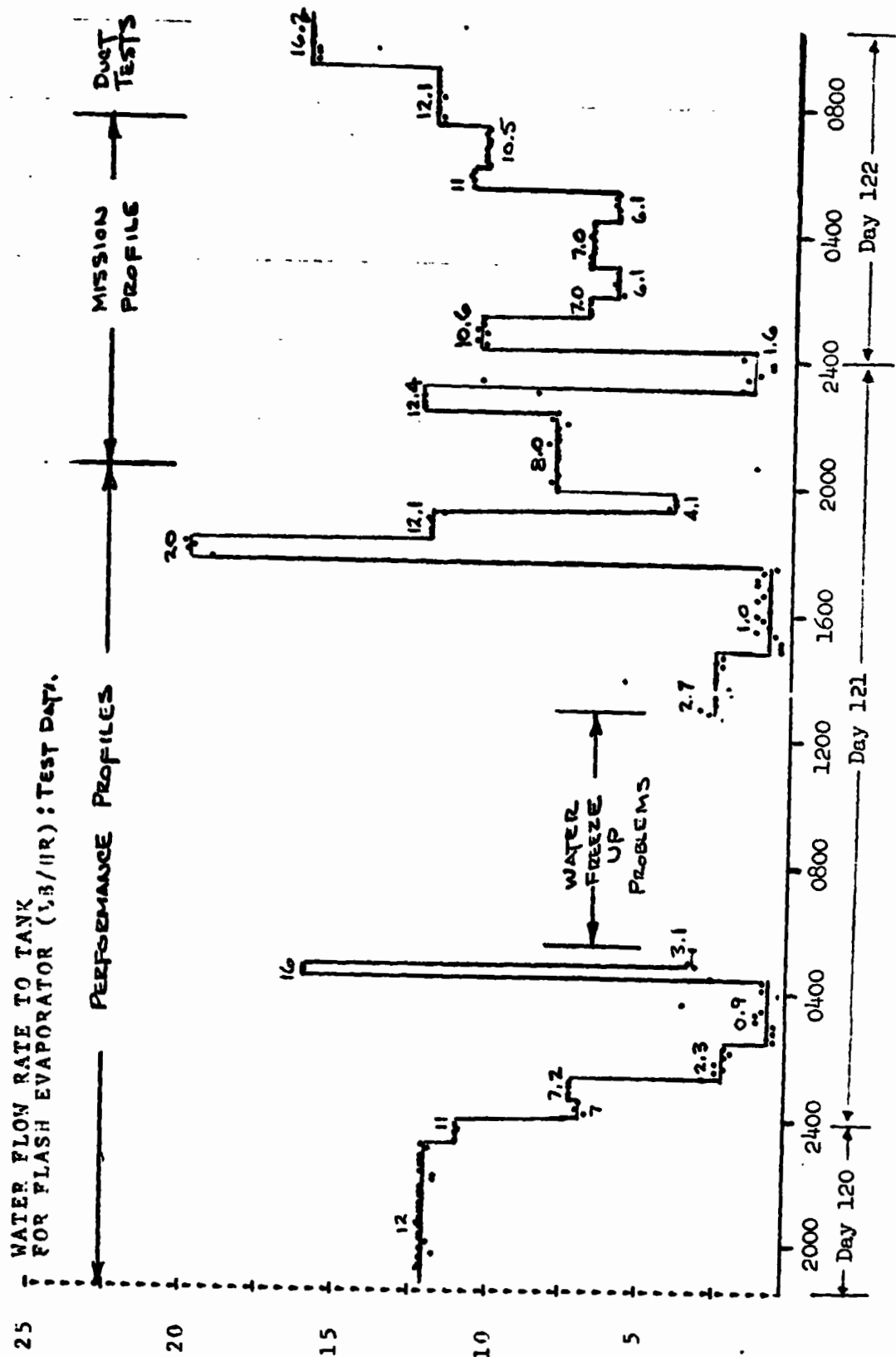


FIGURE 35

WATER FLOW TO TANK DURING FLASH EVAPORATOR TESTING



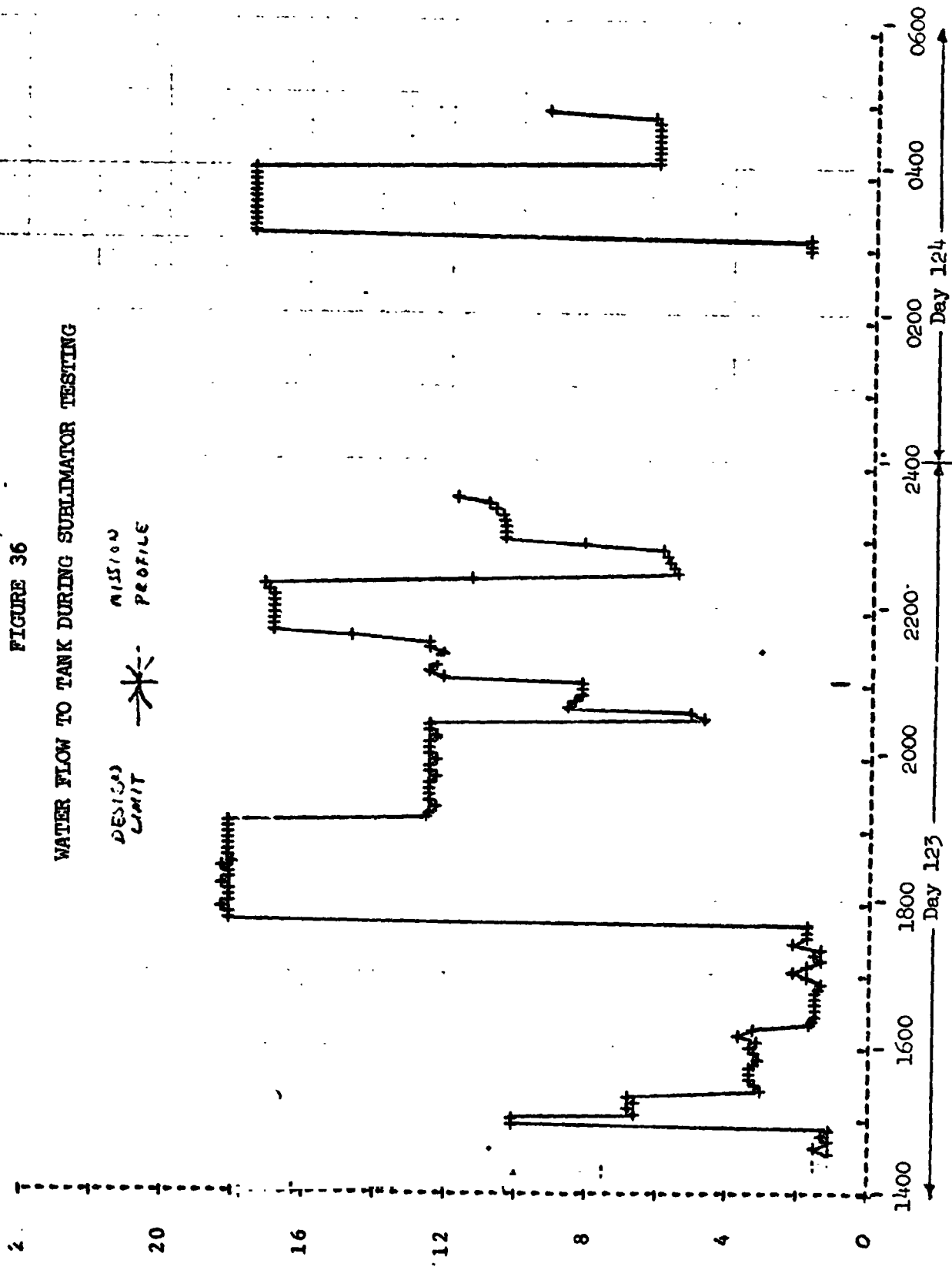


FIGURE 37

WATER QUANTITY DURING MAXIMUM FLUX AND HEAT LOAD TEST POINT

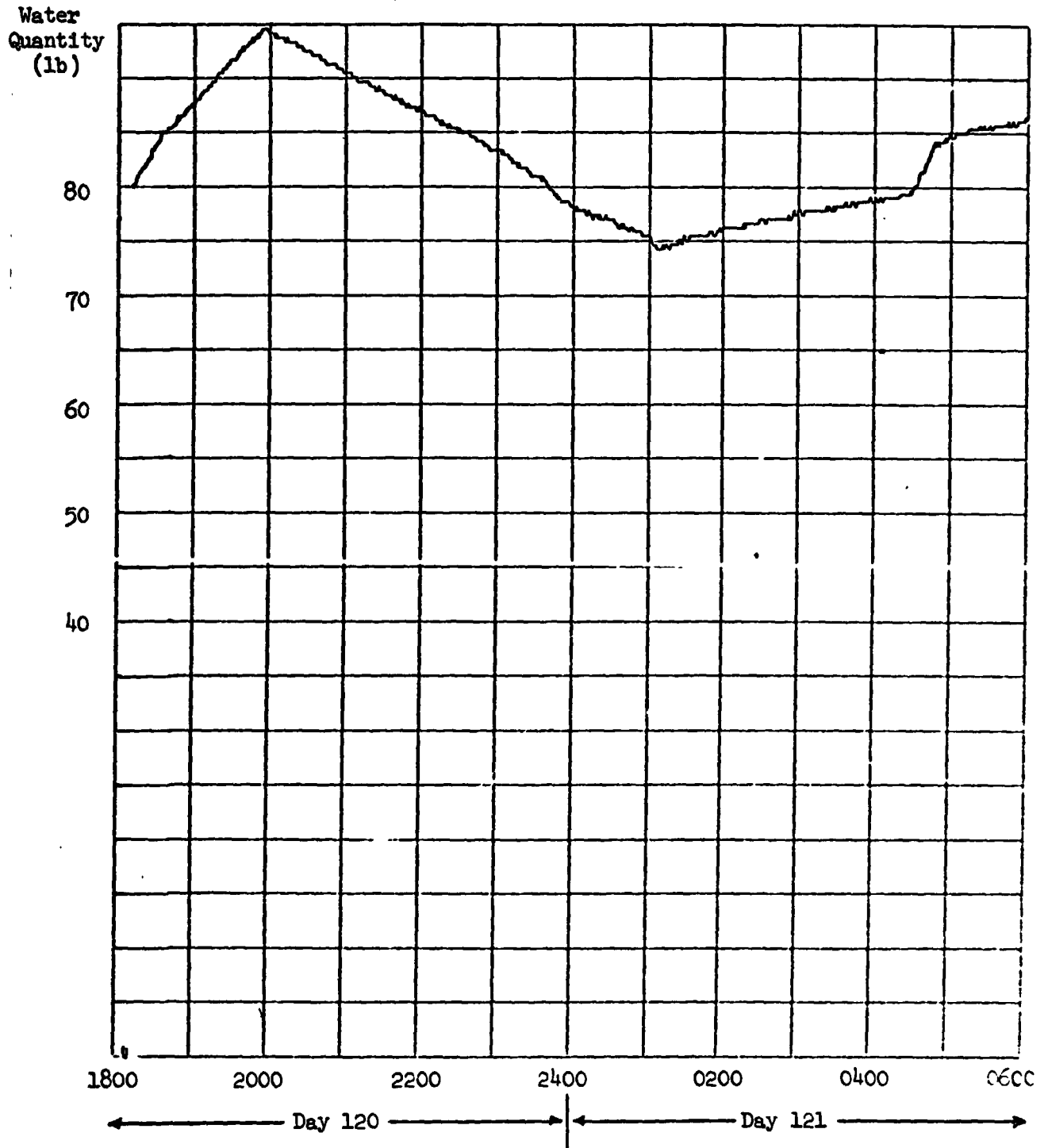


FIGURE 38 :

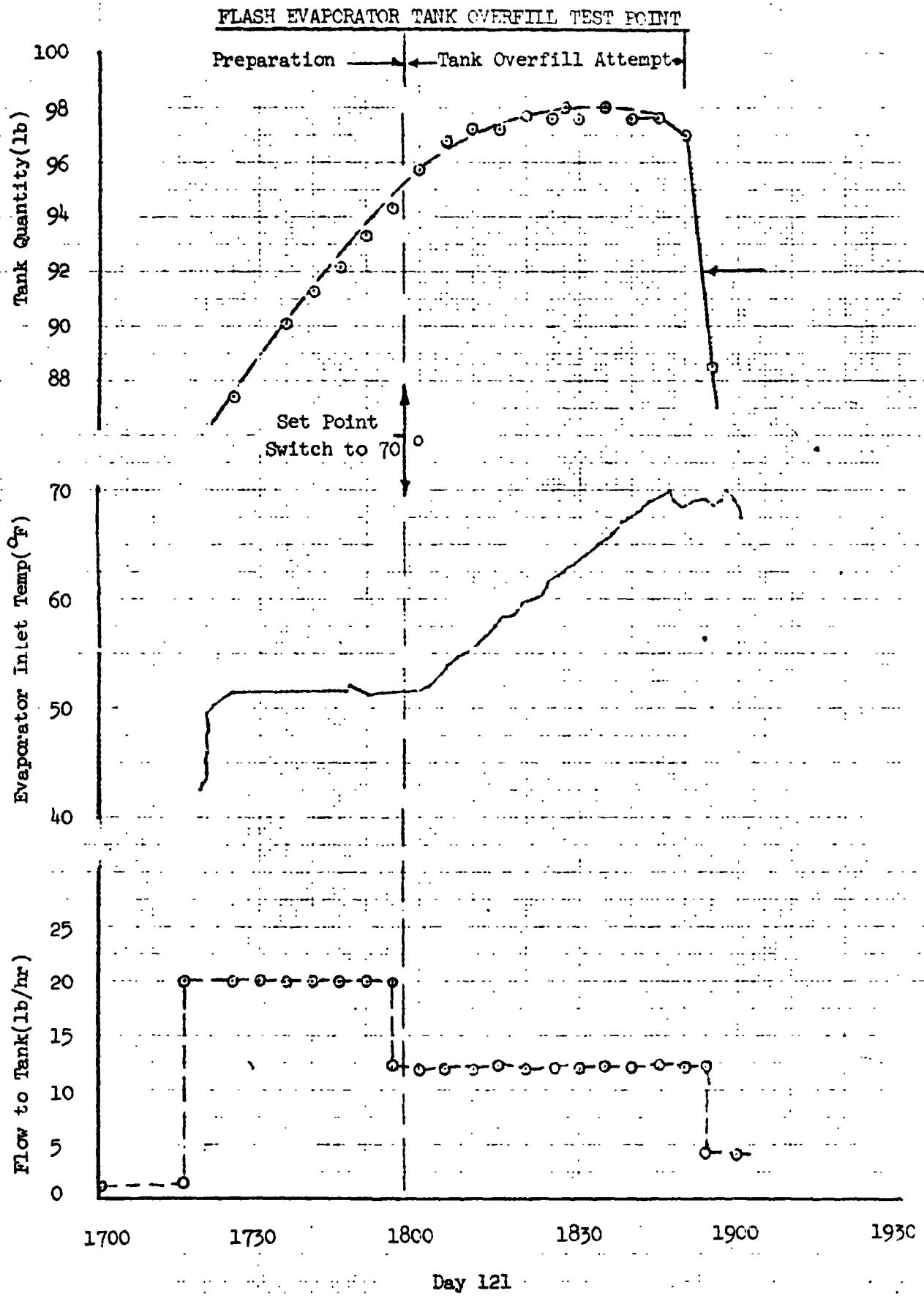
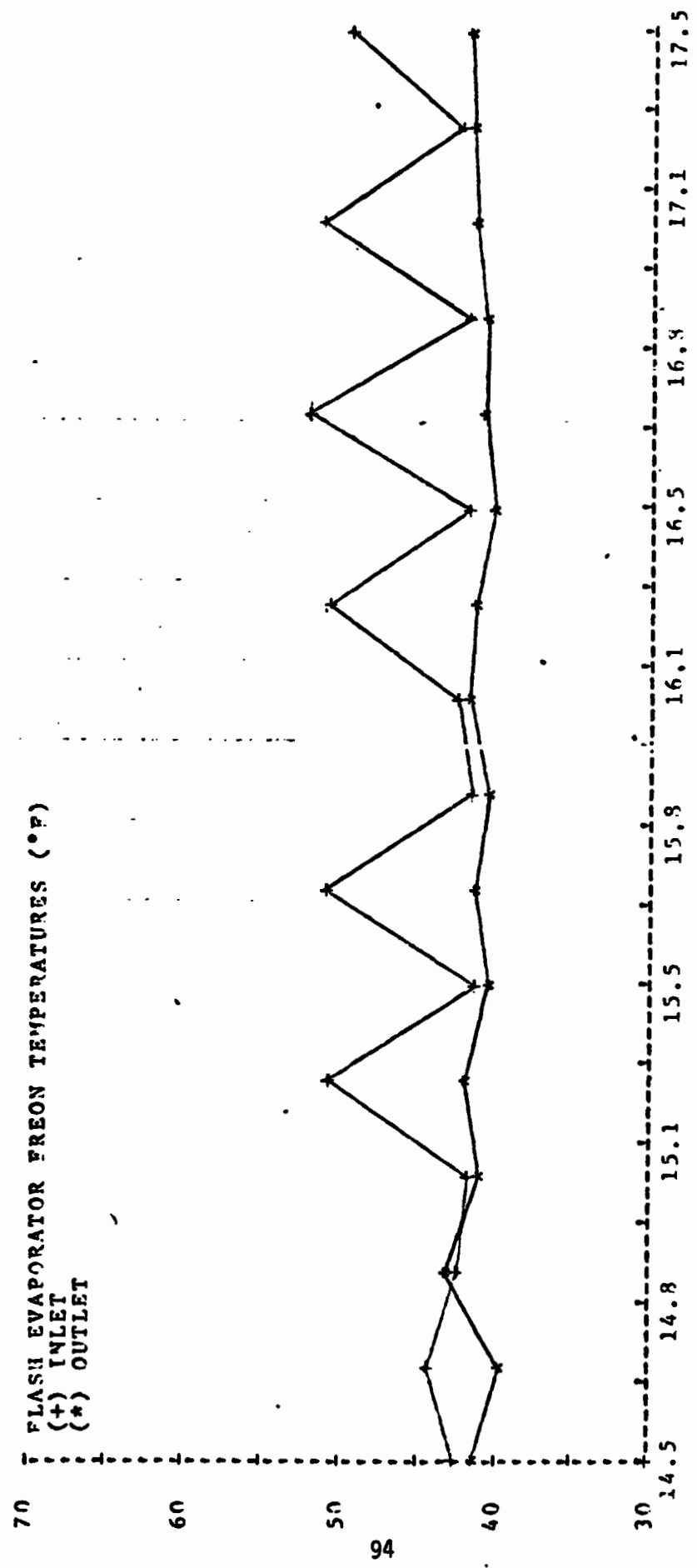


FIGURE 39
 FLASH EVAPORATOR: OUTLET TEMPERATURE
 RESPONSE TO CYCLIC SET POINT CHANGES



TEST TIME ON DAY 121 (HOURS)

REPRODUCIBILITY OF THE
ORIGINAL PAGE IS POOR

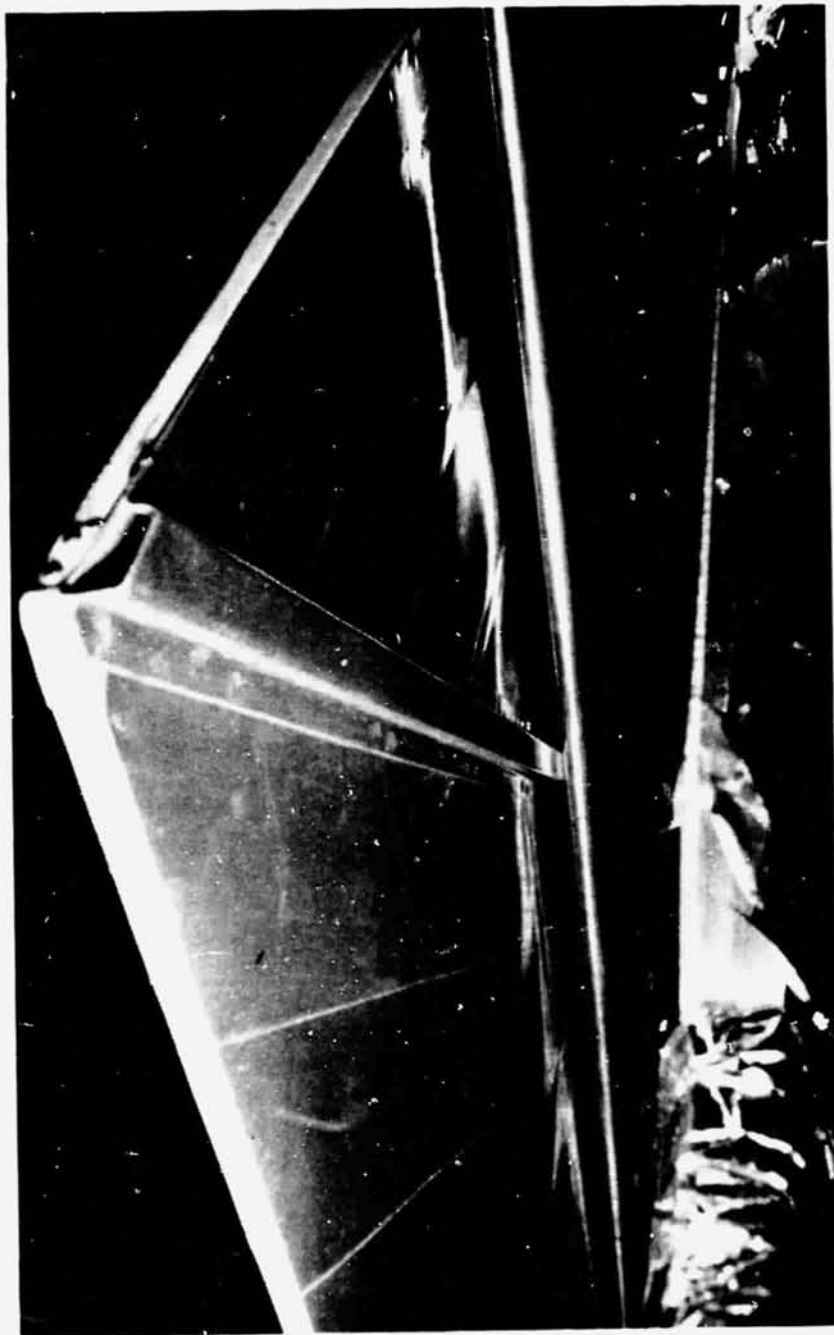
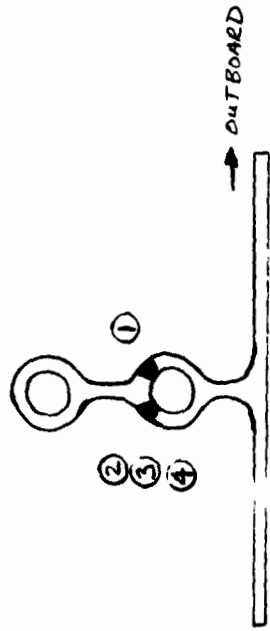
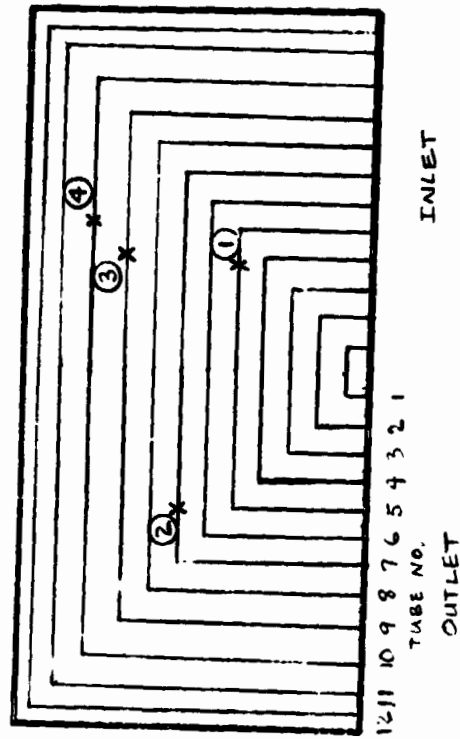


FIGURE 40 MRS PANEL INSTALLATION FOR COATINGS TEST

FIGURE 41
ANOMALY DESCRIPTION

0 4 TUBES RUPTURED ON 3 DIFFERENT PANELS DURING RAPID WARM-UP FROM A COLD SOAK CONDITION



PANEL	TUBE	LOCATION
6	5	1
5	7 & 9	2 & 3
3	10	4

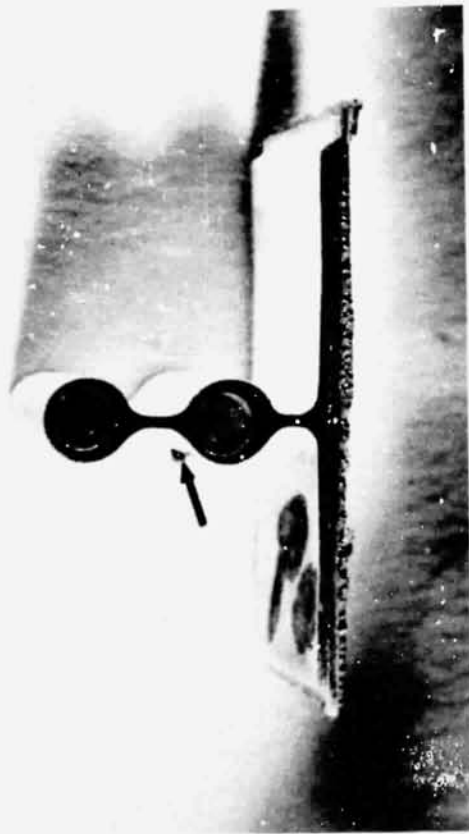
REPRODUCIBILITY OF THE
ORIGINAL PAGE IS POOR



2000X

FIGURE 42

SEM FRACTOGRAPH SHOWING DIMPLE TENSION FAILURE
SCAN FROM INSIDE DIAMETER OF BULGED AREA OF TUBE 5



APPROXIMATELY 2X

FIGURE 43

PHOTOMICROGRAPH OF EXTRUDED COOLANT TUBE WITH YIELDED THIN WALL ADJACENT TO FAILURE SITE, ARROW, OF TUBE 5

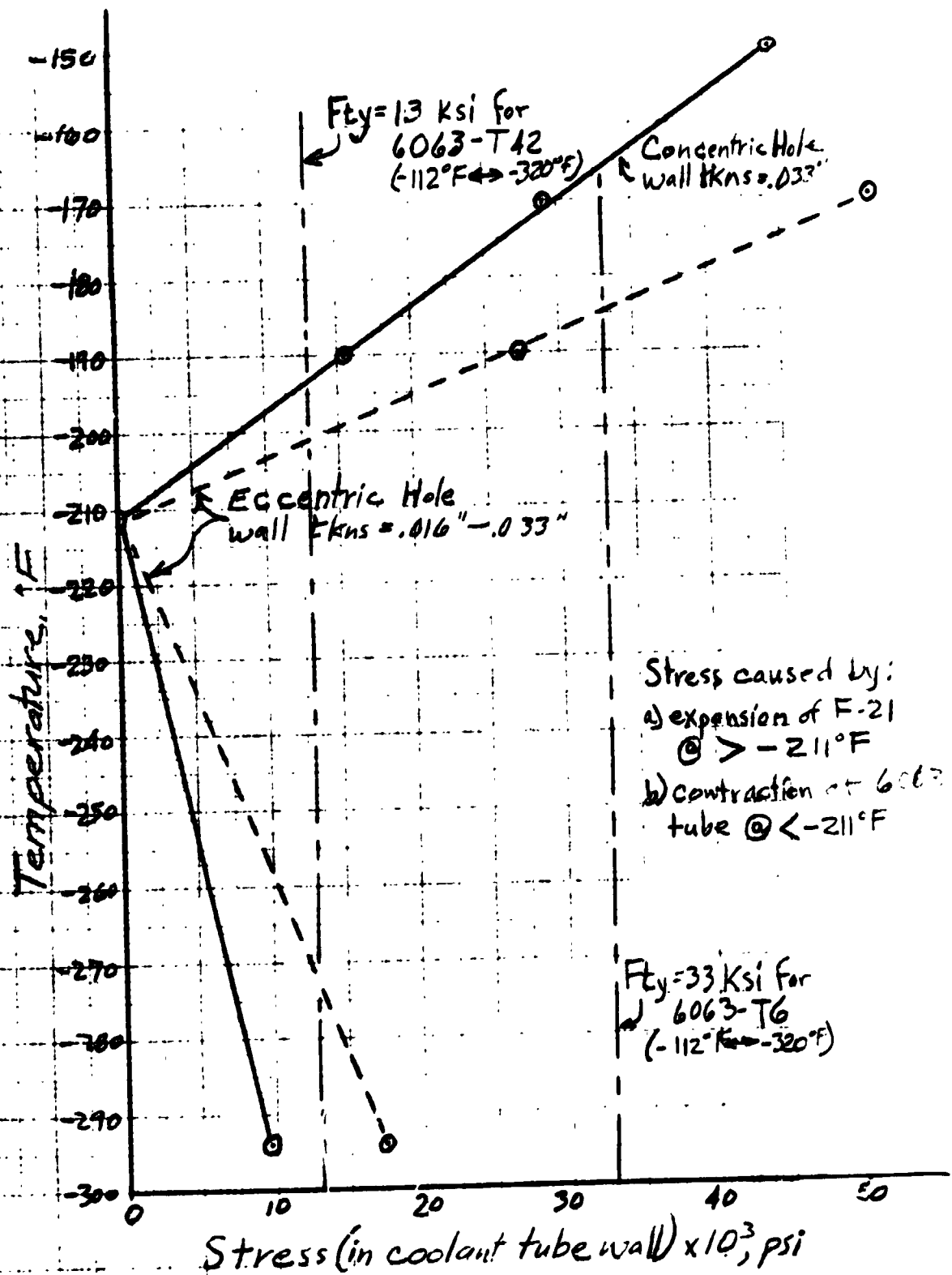


FIGURE 44

STRESS IN COOLANT TUBES VS TEMPERATURE

